
Chapter 3
Development of
Formulation for
Cilostazol

3.1 Analytical Method Development for Cilostazol.

Cilostazol and several of its metabolites are cAMP PDE III inhibitors, inhibiting phosphodiesterase activity and suppressing cAMP degradation with a resultant increase in cAMP in platelets and blood vessels, leading to inhibition of platelet aggregation and vasodilation¹⁻². There are also used as an antithrombotic agent. Chemically, Cilostazol is a 6-[4-(1-cyclohexyl-1*H*-tetrazol-5-yl) butoxy]-3, 4-dihydro-2 (1*H*)-quinolinone, and is not yet official in any Pharmacopoeia. In the market only tablet formulation of Cilostazol is available (50 mg or 100 mg) So far only liquid phase extraction-liquid chromatography and solid-phase extraction-liquid chromatography-tandem mass spectrometry methods were available for the estimation of Cilostazol³⁻¹³. But these methods are comparatively more time consuming and expensive. So it was decided to develop simple, rapid and cost-effective analytical methods based on spectrophotometry and HPLC for the determination of Cilostazol in bulk drug and in its various dosage forms.

3.1.1. Estimation of Cilostazol by Spectrophotometry.

A simple, sensitive and accurate UV method for estimation of the actual amount of Cilostazol from its formulation (microemulsion and Inclusion complexes) was developed.

3.1.1.1. Methodology :

3.1.1.1.1. Reagents :

Cilostazol working standard was obtained as a gift sample from Cadila Pharmaceutical Ltd., Ahmedabad. Methanol analytical grade reagent was purchased from Qualigen and was used to prepare the primary stock solution and subsequent dilutions for the estimation of Cilostazol.

3.1.1.1.2. Instrument :

UV-Visible double beam spectrophotometer (Shimadzu UV-1601, Japan) having ultraviolet rays as light source (1 mm width) was used for spectral measurement through out the study.

3.1.1.1.3. Preparation of working stock solution :

Cilostazol was weighed (approx. 100 mg) and transferred to 100 mL volumetric flask. About 70 mL of the methanol was added to volumetric flask. The solution was sonicated for 2 min at ambient temperature. The final dilution was made to 100 mL using methanol to obtain standard stock solution (i.e. 1000 µg/mL). An aliquot (5 mL) of standard stock solution of Cilostazol was further diluted with 10 mL of methanol to get working stock

solution (i.e. 500 µg/mL) of Cilostazol. The working stock solution was stored at 2°C to 8°C till assayed.

3.1.1.1.4. Preparation of Standard solution :

Suitable aliquots of the working stock solutions of Cilostazol ranging from (0.1, 0.2, 0.3, 0.4, 0.5, 0.6, 0.7, 0.8, 0.9 and 1.0 mL) were transferred into a 10mL volumetric flask and volume were made up to 10 mL using methanol to obtain a series of final concentrations of (5 - 50 µg/mL).

3.1.1.1.5. Determination of analytical wavelength for Cilostazol :

Cilostazol test solution having concentration 50 µg/mL was scanned for determination of absorbance maxima (λ_{\max}). The scanning was carried out in a range of 200-400 nm and the absorbance maxima (λ_{\max}) was found to be a 257 nm.

3.1.1.1.6. Calibration Curve of Cilostazol :

Six different sets of working stock solutions (i.e. 500 µg/mL) of Cilostazol were prepared and suitable aliquots from each working stock solutions ranging from (0.1, 0.2, 0.3, 0.4, 0.5, 0.6, 0.7, 0.8, 0.9 and 1.0 mL) were further diluted with 10 mL methanol to get standard solutions in the range of 5 – 50 µg/ mL. The absorbance of samples was measured at λ_{\max} 257 nm. Methanol was used as a blank. The solutions were stored at 2°C to 8°C till assayed. The results are recorded in Table 3.1.1.1. Calibration curve was obtained by plotting mean absorbance vs. concentration (Figure 3.1.1.1).

Table 3.1.1.1. Calibration curve of Cilostazol in methanol at 257 nm.

Sr. No.	Concentration (µg/mL)	Absorbance \pm SD (n=6)
1	0	0.000 \pm 0.0005
2	5	0.035 \pm 0.013
3	10	0.067 \pm 0.012
4	15	0.097 \pm 0.013
5	20	0.134 \pm 0.014
6	25	0.166 \pm 0.013
7	30	0.203 \pm 0.016
8	35	0.233 \pm 0.035
9	40	0.269 \pm 0.022
10	45	0.300 \pm 0.012

11	50	0.337 ± 0.040
----	----	-------------------

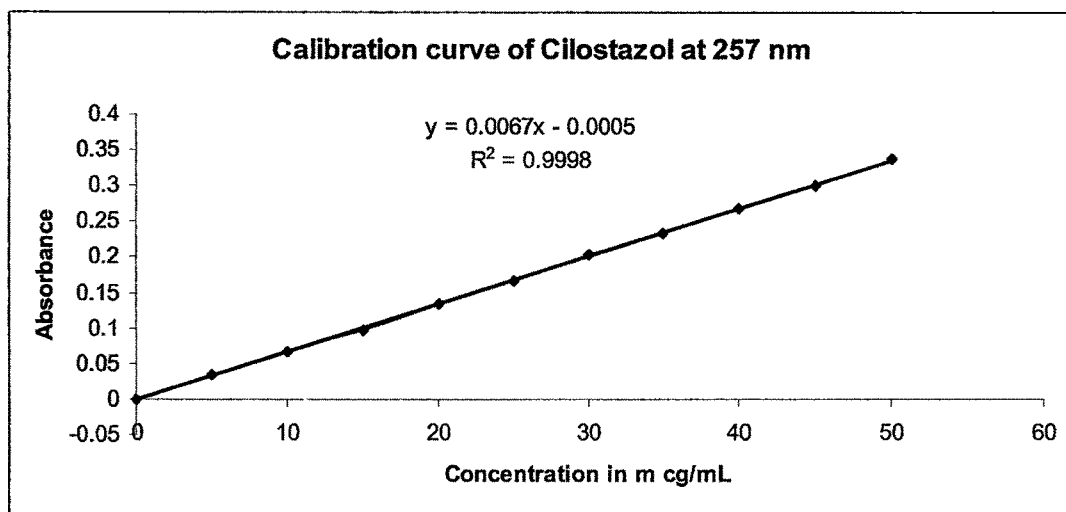


Figure 3.1.1.1 Calibration curve of Cilostazol in methanol at 257.0 nm

3.1.1.2 Method Validation :

3.1.1.2.1 Linearity :

The linearity of an analytical method is its ability to elicit, test results that are directly, or by well-defined mathematical transformation proportional to the concentration of the analyte in samples within a given range. The linearity of the assay was determined by diluting the working stock solution using methanol to obtain final concentrations in the range of 5 – 50 $\mu\text{g/mL}$. Six different sets of working stock solutions were prepared and final dilution was made using methanol. The absorbances of samples were measured on three consecutive days at λ_{max} 257 nm. Methanol was used as a blank. Calibration curves were obtained by plotting mean absorbance vs. concentration. Linear least-square regression analyses of the calibration graphs were performed and the values are noted in Table 3.1.1.2

Table 3.1.1.2. Calibration curves of Cilostazol in methanol at 257 nm on different days.

Day	Number of Runs (n)	Slope	Intercept	Linear Least Square Regression (r^2)
1	6	0.067	0.0005	0.9998
2	6	0.068	0.0005	0.9997
3	6	0.067	0.0005	0.9998

3.1.1.2.2 Accuracy :

The accuracy of an analytical method is the closeness of test results obtained by that method to the true value (The United States Pharmacopoeia 27 NF 22, 2004). The intra-day and inter-day accuracies were determined by replicate analysis of the solutions of known concentrations of Cilostazol at three quality control concentration (low – LQC, medium – MQC, and high – HQC) levels. The observed concentrations of the drug were then back calculated (from absorbance) using the equation of standard calibration curve and compared with the actual concentrations. The % relative error was calculated using the formula,

$$\% \text{ Relative error} = \frac{\text{Observed value} - \text{True value}}{\text{True value}} \times 100 \quad (\text{Equation 3.1})$$

Intra-day Accuracy of the Assay :

The aliquots of working stock solutions (0.1mL, 0.5mL and 1.0mL) were appropriately diluted using methanol to obtain final concentrations of 5 (LQC), 25 (MQC) and 50 µg/mL (HQC). Six different sets of working stock solutions were prepared and diluted in the similar manner. The absorbance of samples was measured at λ_{max} 257 nm for three times on the same day. The solutions were prepared freshly each time. Methanol was used as a blank. The % relative error was calculated and the results are recorded in Table 3.1.1.3.

Inter-day Accuracy of the Assay :

Working stock solutions were appropriately diluted using methanol to obtain final concentrations of 5 (LQC), 25 (MQC) and 50 µg/mL (HQC). Six different sets of working stock solutions were prepared and diluted in the similar manner. The absorbance of samples was measured at λ_{max} 257 nm on three consecutive days. The solutions were prepared freshly on each day. Methanol was used as a blank. The % relative error was calculated and the results are recorded in Table 3.1.1.4.

3.1.1.2.3 Precision :

The precision of an analytical method is the degree of agreement among individual test results when the procedure is applied repeatedly to multiple sampling of homogenous sample (The United States Pharmacopoeia 27 NF 22, 2004). The precision of an analytical method is usually expressed as the Standard Deviation (SD) or Relative Standard Deviation (RSD). The standard deviation is calculated from following formula given in equation below,

$$SD = \sqrt{\sum (X_i - X)^2 / (N - 1)} \quad (\text{Equation 3.2})$$

Where X_i is an individual measurement in a set

X is the arithmetic mean of the set and

N is the total number of replicated measurement taken in the set

Precision between different samples can be compared with RSD as follows:

$$\%RSD = \frac{SD}{Mean} \times 100 \text{ (Equation 3.3)}$$

The intra- and inter day precisions of the assay were calculated by replicate analysis of the solutions of known concentrations of Cilostazol at three quality control concentration (LQC, MQC, and HQC) levels. The observed concentrations of the drug were then back calculated (from absorbance) using the equation of standard calibration curve. The variations between the observed concentrations were determined by calculating the % RSD using equation 3.3.

Intra-day Precision of the Assay :

Working stock solutions were appropriately diluted using methanol to obtain final concentrations of 5 (LQC), 25 (MQC) and 50 $\mu\text{g/mL}$ (HQC). Six different sets of working stock solutions were prepared and diluted in the similar manner. The absorbance of samples was measured at λ_{max} 257 nm for three times on the same day. The solutions were prepared freshly on each time. Methanol was used as a blank. The % relative error was calculated and the results are recorded in Table 3.1.1.3.

Inter-day Precision of the Assay :

Working stock solutions were appropriately diluted using methanol to obtain final concentrations of 5 (LQC), 25 (MQC) and 50 $\mu\text{g/mL}$ (HQC). Six different sets of working stock solutions were prepared and diluted in the similar manner. The absorbance of samples was measured at λ_{max} 257 nm on three consecutive days. The solutions were prepared freshly on each day. Methanol was used as a blank. The % relative error was calculated and the results are recorded in Table 3.1.1.4.

Table 3.1.1.3. Intra day accuracy and precision for Cilostazol determination.

Run#	Cilostazol Concentration					
	Low QC, 5 µg/mL		Medium QC, 25 µg/mL		High QC, 50 µg/mL	
	Observed concentration	% Relative Error	Observed concentration	% Relative Error	Observed concentration	% Relative Error
Set I						
Run #1	4.98	-0.94	25.12	1.23	50.30	1.48
Run #2	5.04	2.20	25.25	2.49	49.89	-0.57
Run #3	4.97	-1.73	24.86	-1.45	49.54	-2.30
Run #4	5.03	1.42	25.11	1.07	49.60	-1.98
Run #5	5.04	2.20	25.17	1.70	49.78	-1.12
Run #6	4.97	-1.73	24.89	-1.13	49.67	-1.67
Mean	5.005		25.056		49.79	
SD	0.111		0.159		0.301	
Precision as % RSD	1.91		1.58		1.39	
Accuracy (%)	100.1		100.22		99.58	
Set II						
Run #1	5.04	2.20	25.25	2.49	50.39	1.95
Run #2	5.04	2.20	25.17	1.70	49.70	-1.51
Run #3	4.98	-0.94	25.22	2.17	49.51	-2.46
Run #4	4.97	-1.73	24.84	-1.61	49.81	-0.96
Run #5	5.03	1.42	25.19	1.86	50.30	1.48
Run #6	5.01	0.63	24.92	-0.82	49.48	-2.61
Mean	5.011		25.08		49.89	
SD	0.034		0.167		0.437	
Precision as % RSD	1.64		1.71		1.98	
Accuracy (%)	100.22		100.32		99.78	
Set III						
Run #1	5.04	2.20	25.08	0.76	50.22	1.09
Run #2	5.03	1.42	25.28	2.80	49.62	-1.91
Run #3	4.95	-2.52	24.87	-1.29	49.76	-1.20
Run #4	5.00	-0.16	25.23	2.33	49.49	-2.54
Run #5	5.01	0.63	24.81	-1.92	50.23	1.17
Run #6	5.06	2.99	25.08	0.76	49.71	-1.43
Mean	5.015		25.058		49.838	
SD	0.0350		0.209		0.343	
Precision as % RSD	1.94		1.88		1.58	
Accuracy (%)	100.3		100.32		99.67	

Table 3.1.1.4. Inter day accuracy and precision for Cilostazol determination.

Run#	Cilostazol Concentration					
	Low QC, 5 µg/mL		Medium QC, 25 µg/mL		High QC, 50 µg/MI	
	Observed concentration	% Relative Error	Observed concentration	% Relative Error	Observed concentration	% Relative Error
Day 1						
Run #1	5.06	2.99	25.22	2.17	50.52	2.58
Run #2	5.03	1.42	25.15	1.54	49.57	-2.14
Run #3	5.00	-0.16	25.23	2.33	49.70	-1.51
Run #4	4.98	-0.94	24.79	-2.08	49.60	-1.98
Run #5	5.01	0.63	25.28	2.80	50.26	1.32
Run #6	5.03	1.42	24.95	-0.50	49.76	-1.20
Mean	5.018		25.10		49.90	
SD	0.030		0.197		0.432	
Precision as % RSD	1.37		1.90		1.97	
Accuracy (%)	100.36		100.4		99.80	
Day 2						
Run #1	5.97	-1.73	25.17	1.70	50.25	1.24
Run #2	5.04	2.20	25.22	2.17	49.54	-2.30
Run #3	4.95	-2.52	25.17	1.70	49.82	-0.88
Run #4	5.00	-0.16	24.86	-1.45	49.70	-1.51
Run #5	5.01	0.63	25.12	1.23	50.36	1.80
Run #6	5.03	1.42	24.89	-1.13	49.79	-1.04
Mean	5.166		25.07		49.91	
SD	0.435		0.143		0.355	
Precision as % RSD	1.82		1.57		1.62	
Accuracy (%)	103.32		100.28		99.80	
Day 3						
Run #1	5.00	-0.16	24.92	-0.82	50.47	2.35
Run #2	5.03	1.42	25.17	1.70	49.46	-2.69
Run #3	5.06	2.99	25.19	1.86	49.95	-0.25
Run #4	5.01	0.63	24.76	-2.39	49.60	-1.98
Run #5	4.98	-0.94	24.90	-0.98	50.23	1.17
Run #6	5.06	2.99	25.06	0.60	50.03	0.14
Mean	5.02		25.00		49.956	
SD	0.0304		0.183		0.421	
Precision as % RSD	1.61		1.68		1.89	
Accuracy (%)	100.4		100.00		99.91	

3.1.1.2.4 Limit of Detection and Limit of Quantification :

The Limit of Detection (LoD) is a quantitative parameter. It is the lowest concentration of the analyte in a sample that can be detected with acceptable precision and accuracy under stated experimental conditions, but not necessarily quantities as an exact value (The United States Pharmacopoeia 27 NF 22, 2004). It is expressed as the concentration of analyte in the sample. The limit is usually expressed in terms of $\mu\text{g/mL}$, ng/mL , pg/mL , etc. LoD values are always specific for a particular set of experimental conditions. Anything that changes the sensitivity of a method, including instrument, sample preparation etc will change detection limits.

Limit of Quantification (LoQ) is the lowest concentration of analyte in a sample that may be measured in a sample matrix using the proposed method. The value of LoQ is almost 10 times higher than that of the blank.

Six random readings (absorbance) for analytical blank signal after "Auto Zero" were as follows 0.002, 0.001, 0.001, 0.001, 0.002 and 0.001.

LoD and LoQ were determined using the following equation.

$$LoD(or)LoQ = \frac{k \cdot S_B}{S} \text{ (Equation 3.4)}$$

Where,

k = a constant (3 for LoD and 10 for LoQ)

S_B = the standard deviation of the analytical blank signal

S = the slope of the concentration/response graph

3.1.1.3. Result and Discussion :

The calibration curves of Cilostazol were constructed by plotting the absorbance of standard Cilostazol (Y) against concentration of Cilostazol (X) (Table 3.1.1.1). The correlation coefficient and linear regression equation are shown in Fig. 3.1.1.1. Intraday and interday accuracy was carried out by determine the calculated values of % relative error and it was -2.61 – 2.99 and -2.69 – 2.99 respectively (Table 3.1.1.3 and 3.1.1.4). The developed method was validated for its intraday and interday precision in the ranges of 5 - 50 $\mu\text{g/ml}$. The intraday and interday (3 days, $n = 3$) precision were expressed as relative standard deviation in range of 1.39 – 1.98 % and 1.37 – 1.97 % respectively (Table 3.1.1.3 and 3.1.1.4).

The proposed method was rapid, economical, accurate and precise for the determination of Cilostazol. This method was later used for estimation of Cilostazol in bulk drug, and its pharmaceutical formulation.

3.1.1.4 Estimation of Cilostazol (Formulation/ Diffusion/Dissolution Medium)

Developed UV spectroscopic method was adopted for the estimation of Cilostazol in newly developed formulations (Microemulsions and CDs Complexes). In which different calibration curves were prepared in Distilled water and acidic/basic buffers for estimation of Cilostazol from solution and its formulations. For CDs complexes, different calibration curves were prepared for dissolution measurement study, inclusion efficiency measurement study and phase solubility measurement study. For microemulsions, the calibration curves were prepared for diffusion measurement study, excipients interference identification study and drug entrapment efficiency measurement study. This method was also applicable for estimation of Cilostazol for retention of drug from accelerated and stress study.

3.1.1.4.1. Preparation of working stock solution of Cilostazol :

Procedure used for preparation of working stock solution of Cilostazol was similar to that described in section 3.1.1.1.3.

3.1.1.4.2 Calibration curve of Cilostazol for inclusion efficiency measurement :

Aliquots of the working stock solution ranging from (0.50, 1.0, 1.5, 2.0 and 2.5 ml) were taken into 10 mL volumetric flask and volumes were made up with methanol to prepare a series of standard solutions (5-20 $\mu\text{g/mL}$) for calibration curve. The absorbance of the resulting solutions was measured at λ_{max} 257.0 nm against methanol as blank solution. The concentrations of Cilostazol were then back calculated (from absorbance) using the equation of standard calibration curve.

3.1.1.4.3 Calibration curve of Cilostazol for phase solubility measurement :

Aliquots of working stock solution of Cilostazol ranging from 0.50, 1.0, 1.5, 2.0 and 2.5 ml were transferred into a series of 10 ml volumetric flasks and volume was made up to the mark with distilled water to prepare a series of standard solutions (5-20 $\mu\text{g/mL}$) for calibration curve. The absorbance of the resulting solutions was measured at λ_{max} 257.5 nm against distilled water as blank solution. The concentrations of Cilostazol were then back calculated (from absorbance) using the equation of standard calibration curve (Fig. 3.1.1.2).

Table 3.1.1.5 Calibration data for Cilostazol in distilled water

Concentration ($\mu\text{g/ml}$)	Mean (n=5)	% RSD
0.00	0.00 \pm 0.0013	1.75
5.0	0.030 \pm 0.0041	2.06

10.0	0.059 ± 0.0043	1.13
15.0	0.091 ± 0.0052	0.92
20.0	0.123 ± 0.0049	0.63
25.0	0.0.163 ± 0.0074	0.77

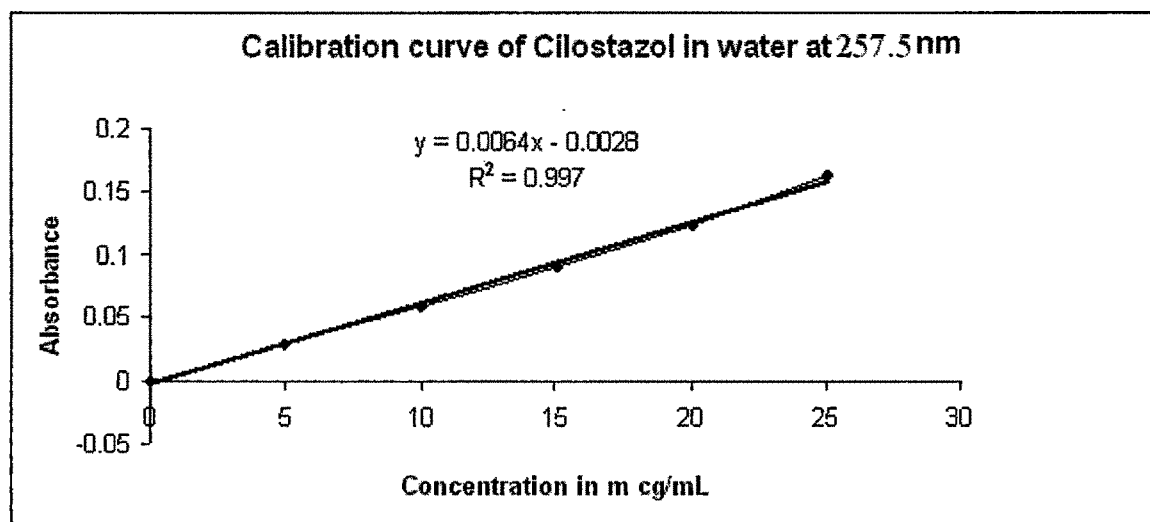


Figure 3.1.1.2. Calibration curve of Cilostazol in water at 257.5 nm.

3.1.1.4.4 Calibration curve of Cilostazol for dissolution measurement :

Suitable aliquots of working stock solution of Cilostazol ranging from 0.50, 1.0, 1.5, 2.0 and 2.5 ml were transferred into a series of 10 ml volumetric flasks and volume was made up to the mark with phosphate buffer (pH 6.8) to prepare a series of standard solutions (5-20 $\mu\text{g/mL}$) for calibration curve. The absorbance of the resulting solutions was measured at λ_{max} 257.8 nm against phosphate buffer (pH 6.8) as blank solution (Table 3.1.1.6). The concentrations of Cilostazol were then back calculated (from absorbance) using the equation of standard calibration curve. (Figure 3.1.1.3).

Table 3.1.1.6 Calibration data for Cilostazol in phosphate buffer (pH 6.8)

Concentration ($\mu\text{g/ml}$)	Mean \pm S.D.	%RSD
0.0	0.000 \pm 0.0014	1.90
5.0	0.037 \pm 0.0030	1.49
10.0	0.067 \pm 0.0064	1.69
15.0	0.097 \pm 0.0043	0.75
20.0	0.134 \pm 0.0068	0.88

25.0	0.166 ± 0.0074	0.77
------	--------------------	------

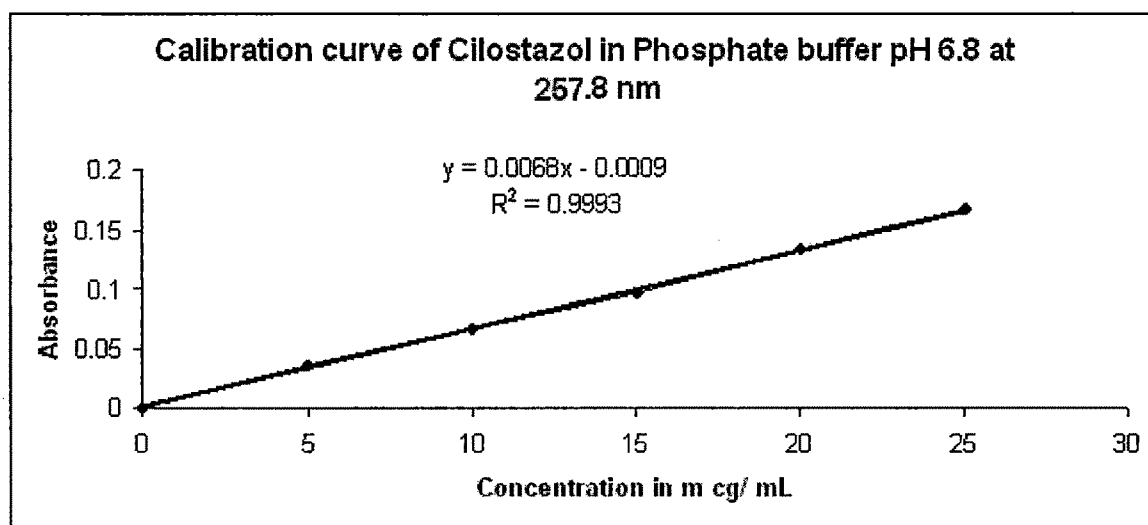


Figure 3.1.1.3. Calibration curve of Cilostazol in phosphate buffer pH 6.8 at 257.8 nm.

3.1.1.4.5 Estimation of Cilostazol from its formulation :

Cilostazol formulation (microemulsion -0.10 mL) was taken in a 10 mL volumetric flask. The formulation was diluted up to 10 mL using methanol (AR grade) and sonicated for 2 min at ambient temperature. The diluted solution (0.50 mL) was transferred in to 10 mL volumetric flask and volume was made up to 10 mL using methanol (AR grade) and analyzed at λ_{\max} 257.0 nm for estimation of drug substance. The concentrations of the active ingredient (Cilostazol) were then back calculated (from absorbance) using the equation of standard calibration curve (Figure 3.1.1.1).

3.1.1.4.6. Calibration curve of Cilostazol for diffusion measurement :

Cilostazol microemulsion containing diffusion medium (0.20 mL) was taken in a 10 mL volumetric flask. Then it was diluted up to 10 mL using methanol (AR grade) and sonicated for 2 min at ambient temperature. The diluted solutions were analyzed at λ_{\max} 257.0 nm for estimation of drug substance. The concentrations of Cilostazol were then back calculated (from absorbance) using the equation of standard calibration curve (Figure 3.1.1.1).

3.1.1.4.7. Estimation of Cilostazol (Drug Retention at Stress and Accelerated Conditions) :

The procedure was similar to that described in section 3.1.1.4.5.

3.1.1.4.8. Interference of the excipients used :

Certain excipients may interfere with the estimation of drug(s). Hence, Interference of the excipients used in the formulation has been evaluated at highest concentration by measuring their absorbance at the λ_{max} of the Cilostazol i.e. 257 nm and the results are summarized in Table 3.1.1.7.

Table 3.1.1.7. Interference of excipients observed during estimation of drug.

Sr. No	Name of Excipient	Quantity Taken (% w/w)	Observation
1	Labrafil M 2125 CS [®]	60	No interference observed
2	Labrafil M 1944 CS [®]	10 – 20	No interference observed
3	Labrafac PG [®]	10 – 20	No interference observed
4	Cremophor RH 40 [®]	20 – 50	No interference observed
5	Cremophor EL [®]	20 – 50	No interference observed
6	Cotton seed oil	10 – 20	No interference observed
7	Peanut oil	10 – 20	No interference observed
8	Plurol	10 – 20	No interference observed
9	Transcutol P [®]	10 – 30	No interference observed
10	Capmul MCM C10 [®]	10 – 20	No interference observed
11	Capmul MCM C8 [®]	10 – 20	No interference observed
12	Tween 20	10 – 30	No interference observed
13	Tween 40	10 – 30	No interference observed
14	Tween 60	10 – 30	No interference observed
15	Tween 80	10 – 30	No interference observed
16	Captex 1000	10 – 20	No interference observed
17	Captex 200P	10 – 20	No interference observed
18	Captex 355EP/NF	10 – 20	No interference observed

3.1.2. Estimation of Cilostazol by HPLC method.

3.1.2.1. Introduction :

The HPLC and LC-MS-MS methods for pharmaceutical formulation and matrix (plasma/urine) have been reported in literature⁴⁻¹⁴. The availability of an HPLC method with high sensitivity and selectivity was desirable for the estimation of Cilostazol in pharmaceutical dosage forms.

3.1.2.2. Methodology :

3.1.2.2.1. Materials and reagents :

Cilostazol working standard was obtained as a gift sample from Cadila Pharmaceutical Ltd., Ahmedabad. Methanol and acetonitrile (HPLC grade, Spectrochem Ltd, Bombay, India), and triple distilled water were used in the study. Commercially available Cilostazol tablets were procured from the local market.

3.1.2.2.2. Apparatus :

Quantitative HPLC was performed on an isocratic high pressure liquid chromatograph (Shimadzu Prominence HPLC) with LC-20AT pumps, a multi wavelength UV/VIS detector (SPD-20A) and Phenomenex Luna column (250 mm × 4.6 mm i.d., particle size 5 μ). The HPLC system was equipped with the software "Spinchrom CFR" version (Shimadzu).

3.1.2.2.3. Preparation of working stock solutions :

A primary stock solution of Cilostazol (1000 μg/ml) was prepared by dissolving 100 mg of Cilostazol in a 100 ml of volumetric flask containing 50 ml of methanol, sonicated for about 15 min at ambient temperature and diluted it up to the mark with methanol. Working stock solution of Cilostazol (100μg/ml) was prepared by taken a 5 mL aliquot of primary stock solution transferred it into a 50 ml volumetric flasks and volume was made up to the mark with the mobile phase. All stock solution were protected from light and kept at -20°C. They are stable for at least 6 months.

3.1.2.2.4. Chromatographic conditions :

The mobile phase was prepared by mixing acetonitrile and water in the ratio of 60:40 v/v. The mobile phase was filtered through a 0.45 μm membrane filter, degassed by ultra sonication for 15 min and pumped from the solvent reservoir to the column at a flow rate of 0.400 ml/min. The run time was set at 15 min. The volume of injection loop was 20 μl. Prior to injection of the drug solutions; the column was equilibrated for at least 30 min with the mobile phase flowing through the systems. The eluents were monitored at 254 nm and the

data were acquired, stored and analyzed with the software Spinchrom CFR version (Shimadzu).

3.1.2.2.5. Preparation of calibration curve :

Different aliquots (0.10, 0.50, 1.00, 2.00, 3.00, 4.00 and 5.00 ml) of working stock solution were taken in 10 ml volumetric flasks and diluted it up to the mark with mobile phase to get concentrations of 1.00, 5.00, 10.00, 20.00, 30.00, 40.00 and 50.00 µg/ml. Each of these drug solutions (20 µl) was injected three times into the column and the peak area and retention times were recorded.

3.1.2.2.6. Procedure for pharmaceutical formulations :

Twenty tablets were weighed to obtain the average tablet weight and powdered. A sample of the powdered tablets, equivalent to 25 mg of the Cilostazol was taken in a 25 ml volumetric flask containing 10 ml of methanol, sonicated it for 15 min at ambient temperature and diluted it up to the mark with methanol. The solution was filtered through a 0.45 µm membrane filter. An aliquot of solution (1.0 ml) was transferred to a 10 ml volumetric flask and diluted with mobile phase to get a concentration of 100µg/ml. From this, an aliquot (2.0 ml) was transferred to a 10 ml volumetric flask and diluted to the mark with mobile phase to obtain 20 µg/ml of test concentration. The resulting solution (20µl) was injected to HPLC system. All determinations were performed in triplicate.

3.1.2.3. Result and Discussion :

The HPLC method for the analysis of Cilostazol was developed by using the most commonly employed Phenomenex Luna column (250X4.6 mm, 5µ) with UV detection (254 nm).The chromatographic procedure was optimized for various parameters and these parameters are shown in Table 3.1.2.1. The retention time (*t*_R) of Cilostazol was found to be 12.1-12.3 min. (Fig. 3.1.2.1). The calibration curve of Cilostazol was constructed by plotting the peak area of Cilostazol standard (*Y*) against concentration of Cilostazol (*X*) (Table 3.1.2.2). It was found to be linear with a correlation coefficient of 0.9998, the representative linear regression equation being $Y = 68.211X - 18.244$ (Fig. 3.1.2.2).

The relative standard deviations based on the peak area for triplicate injections were found to be 0.27-2.00 % for calibration curve. The developed method was validated for its intraday and interday precision in the range of 1.00-50.00 µg/ml. The intraday and interday (3 days, *n* = 3) precision were expressed as relative standard deviation in range of 0.65-1.39 % and 0.72-1.61 %, respectively (Table 3.1.2.3).

Robustness studies were performed for wavelength (+ 2 nm), flow rate (+ 0.01 unit) and analyst to analyst variations. The results of robustness studies are shown in Table 3.1.2.4. The HPLC method developed in the present study was used to quantify Cilostazol in tablet dosage forms. Cilostazol tablets (50 mg, and 100 mg) were analyzed. The obtained results are given in Table 3.1.2.4. The drug content was found to be 99.70–100.31 % of the labeled amount. No interfering peaks were found in the chromatogram, indicating that the tablet excipients did not interfere with the estimation of the drug by the proposed HPLC method. In the system suitability study, six replicate injections of freshly prepared working stock solution of Cilostazol (30 µg/mL) were injected to the HPLC system, and the % relative standard deviation (%RSD) of peak areas, tailing factors, and theoretical plates were determined in Table 3.1.2.5. The results obtained from the system suitability study were in agreement with the USP requirements and the variation in the retention time among six replicate injections of Cilostazol working solutions was very low, rendering a R.S.D. of 1.4 %.

Also, when a known amount of the drug solution was added to a powdered sample of the tablet dosage form and subjected to an estimation of the drug by the proposed method, there was a high recovery of Cilostazol (99.73–100.17%, Table 3.1.2.7.), indicating that the proposed procedure for the estimation of Cilostazol in the tablet dosage forms is accurate. The results of the study showed that the developed RP-HPLC method was simple, rapid, precise and accurate and could be used for the determination of Cilostazol in its new pharmaceutical dosage forms. Summary of method validation parameters is shown in Table 3.1.2.8.

Developed HPLC method was further adopted for the estimation of Cilostazol in newly developed formulations (Microemulsions and CDs Complexes) and it could be used for estimation of Cilostazol from matrix (Plasma/Urine), required for pharmacokinetic study to estimate the actual amount of drug absorbed from G.I. Tract.

Table 3.1.2.1. Chromatographic parameters

HPLC parameters	
Column	Phenomenex Luna (Torrance U.S.A.), C ₁₈ ODS (250 mm × 4.6 ID, 5μ) preceded with ODS guard column (10 mm × 5 mm ID)
Mobile Phase	Acetonitrile : Water (60 : 40)
Injection Volume	20 μl
Flow Rate	0.4 mL/min.
Analytical Wavelength (nm)	254
Retention Time (min.)	12.1 – 12.3
System	Shimadzu (Kyoto, Japan)
Detector	SPD-20A prominence UV/VIS
Pump	LC-20AT prominence solvent delivery module
Injector	A manual rheodyne injector with 20 μl fixed loop
Software	Spynchrom chromatographic station CFR version-2.4.0.193 (Spinchrom Pvt. Ltd., Chennai, India).
Temperature	Ambient

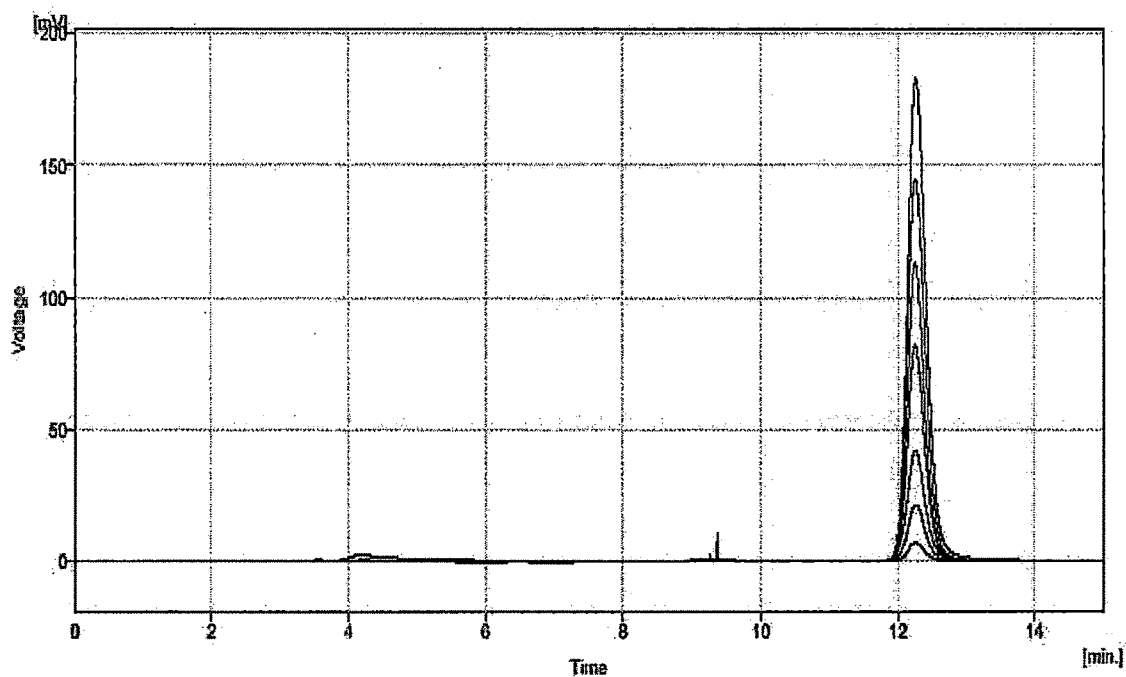
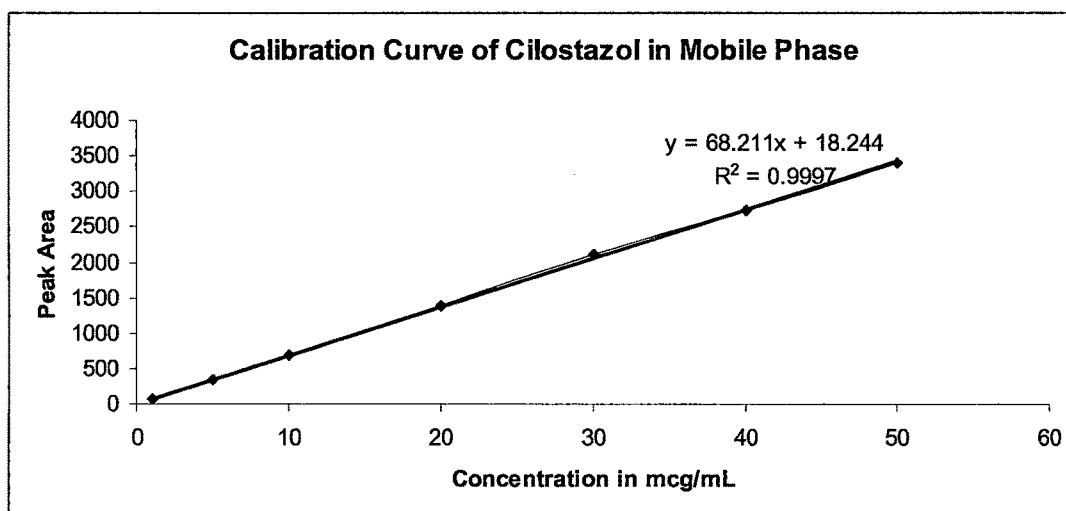
**Fig. 3.1.2.1. The overlay chromatograms of standard Cilostazol from 1.0 to 50.0μg/ml in mobile phase**

Table 3.1.2.2. Calibration data of Cilostazol by the proposed HPLC method

Concentration of Cilostazol ($\mu\text{g/ml}$)	Mean peak area in mV (n=3)	% RSD
1.00	73.38	2.0068
5.00	352.3323	0.6159
10.00	695.149	1.3468
20.00	1397.565	0.3321
30.00	2106.589	1.4233
40.00	2733.672	1.138
50.00	3409.995	0.2759

Regression equation: $Y = 68.211X - 18.244$ ($r = 0.9998$)

**Fig. 3.1.2.2. Calibration Curve of Cilostazol in Mobile phase at 254 nm.****Table 3.1.2.3. Interday and intraday precision of proposed HPLC method**

Concentration of Cilostazol ($\mu\text{g/ml}$)	Amount of Cilostazol found ($\mu\text{g/ml}$)			
	Intraday precision		Interday precision	
	Mean Area (n = 3)	%RSD	Mean Area (n = 3)	%RSD
1.00	73.1	1.39	73.3	1.57
5.00	358.0	1.37	364.3	1.61
10.00	701.3	1.39	715.7	1.43
20.00	1377.7	1.33	1340.0	1.20
30.00	2113.3	0.84	2121.3	1.11

40.00	2701.3	0.84	2725.7	0.85
50.00	3391.7	0.65	3401.7	0.72

Table 3.1.2.4 Robustness studies of Cilostazol by proposed HPLC method

Parameters	Retention time variation (min)			Peak area variation		
	Mean area	S.D.	% RSD	Mean area	S.D.	% RSD
Wavelength (+ 2 nm)	12.27	0.06	0.47	1369.7	19.50	1.33
Flow rate (+ 0.01 unit)	11.87	0.06	0.49	1390.3	18.18	1.23
Analyst to Analyst	12.25	0.05	0.41	1372.3	23.86	1.62

Table 3.1.2.5. System suitability parameters.

Parameter	
RT(min \pm SD)	12.269 \pm 0.023
Tailing factor \pm SD	1.288 \pm 0.018
Theoretical plates \pm SD	11180.33 \pm 73.104
%RSD	1.4

Table 3.1.2.6. Analysis of marketed formulations by proposed HPLC method

Dosage Forms Code	Labeled amount (mg/tab)	Amount found* (mg/tab)	% Assay*
Tablet-1	50	49.89 \pm 0.53	99.78 \pm 1.05
Tablet-2	100	100.31 \pm 1.03	100.31 \pm 1.02
Tablet-3	100	99.70 \pm 1.34	99.70 \pm 1.35

Tablet-1 were the Pletoz(50 mg) tablet from Cipla Limited, Goa
 Tablet-2 were the Zilast (100 mg) tablet from IPCA Limited, Mumbai and
 Tablet-3 were the Pletoz(100 mg) tablet from Cipla Limited, Goa
 *Mean \pm S.D. of three determinations

Table 3.1.2.7. Recovery studies of Cilostazol tablets by proposed HPLC method

Concentration of Cilostazol ($\mu\text{g/ml}$)			Amount found [#] ($\mu\text{g/ml}$)	% Recovery [#]
Initial	Added	Total		
10	5	15	15.00 \pm 0.13	100.00 \pm 0.87
10	10	20	19.95 \pm 0.23	99.73 \pm 1.15
10	20	30	30.05 \pm 0.26	100.17 \pm 0.85

[#]Mean \pm S.D. of three determinations

Table 3.1.2.8. Summary of method validation parameters

Method validation parameters	Results
Linearity and Range	
• Linearity ($\mu\text{g/ml}$)	1.00-50.00
• Linear equation ($Y = MX + C$)	$Y = 68.211X - 18.244$
• Regression co-efficient (r)	0.9998
Precision (% RSD)	
• Interday precision	0.72-1.61
• Intraday precision	0.28-1.26
Robustness for retention time (% RSD)	
• Wavelength (+2 nm)	0.47
• Flow rate (+ 0.01 unit)	0.49
• Analyst to Analyst	0.41
Robustness for peak area ratio (% RSD)	
• Wavelength (+2 nm)	1.33
• Flow rate (+ 0.1 unit)	1.23
• Analyst to Analyst	1.62
Limit of Quantification ($\mu\text{g/ml}$)	1.00
Percentage Recovery	99.73-100.17
Percentage Assay	99.17 -100.31

3.1.3. Estimation of Cilostazol in Human Plasma by HPLC method.

3.1.3.1. Methodology :

3.1.3.1.1. Reagents :

The reagents are described in section 3.1.2.2.1.

3.1.3.1.2. Apparatus :

The apparatus are described in section 3.1.2.2.2.

3.1.3.1.3. Preparation of working stock solutions :

A working stock solution of the Cilostazol (1000 µg/ml) was prepared by dissolving 25 mg of Cilostazol in a 25 ml of volumetric flask containing 10 ml of mobile phase (acetonitrile and water in the ratio of 60:40 v/v), sonicated for about 15 min and diluted up to volume with mobile phase. A working stock solution was protected from light and kept at -20°C. They were stable for at least 6 months.

3.1.3.1.4. Plasma Calibration Standards :

Plasma calibration standards of 0.100, 0.250, 0.5, 1, 2, 4, 10, and 20 µg/ml of Cilostazol were obtained by diluting the suitable aliquots of working stock solution ranging from (0.01, 0.025, 0.05, 0.1, 0.2, 0.4, 1.0 and 2.0 mL) with up to the 100 mL of drug-free human plasma. Stability of the drug in plasma at -20 °C over 6 months was documented.

3.1.3.1.5. Sample extraction Procedure :

1.0 mL of calibration standard was mixed with 0.5 mL of drug-free human plasma in 5 mL-polypropylene centrifuge tube with flat caps and mixed for 3 minutes on vortex. To each tube 3 mL of methyl tertiary butyl ether was added, and the tube was vortexed for 30 sec. at high speed. The sample was finally shaken on a rotating shaker (50 rotations /minute) for 3 minutes. The sample was centrifuged for 20 minutes at 2000 rpm at 4°C the clear methyl tert. butyl ether layer was transferred with a calibrated pipette to a disposable glass tube and evaporated under a gentle stream of nitrogen. The dried residue was taken up with 25 µL of mobile phase, and 20 µL of this mixture were injected in the HPLC system.

3.1.3.1.6. System suitability study.

In this study, 1.0 mL of calibration standard Cilostazol (10µg/mL) was mixed with 0.5 mL of drug-free human plasma in 5 mL-polypropylene centrifuge tube with flat caps and mixed for 3 minutes on vortex. To each tube 3 mL of methyl tertiary butyl ether was added, and the tube was vortexed for 30 sec. at high speed. The sample was finally shaken on a rotating shaker (50 rotations /minute) for 3 minutes. The sample was centrifuged for 20 minutes at 2000 rpm at 4°C the clear methyl tert. butyl ether layer was transferred with a

calibrated pipette to a disposable glass tube and evaporated under a gentle stream of nitrogen. The dried residue was taken up with 25 μL of mobile phase, and 20 μL of this mixture were injected in the HPLC system. The study was repeated six times and the % relative standard deviation (%RSD) of peak areas, tailing factors, and theoretical plates were determined in Table 3.1.3.4.

3.1.3.1.7. Chromatographic conditions :

The chromatographic conditions are described in section 3.1.2.2.4. and Table 3.1.2.1.

3.1.3.2. Result and Discussion :

3.1.3.2.1. Assay Validation :

For assay validation, Cilostazol was mixed with drug-free human plasma over the concentration ranges 0.1 – 20 $\mu\text{g/ml}$. Concentration higher than 20 $\mu\text{g/ml}$ were not tested for linearity. The retention time (t_R) of Cilostazol was found to be 12.1-12.3 min. (Fig. 3.1.3.1). The calibration curve of Cilostazol was constructed by plotting the peak area of Cilostazol standard (Y) against concentration of Cilostazol (X) (Table 3.1.3.1). It was found to be linear with a correlation coefficient of 0.9989, the representative linear regression equation being $Y = 58.29x + 12.223$ (Fig. 3.1.3.2).

The relative standard deviations based on the peak area for triplicate injections were found to be 0.30-5.55 % for calibration curve. The developed method was validated for its intraday and interday precision in the range of 0.10-20.00 $\mu\text{g/ml}$. The intraday and interday (3 days, $n = 3$) precision were expressed as relative standard deviation in range of 1.32 – 5.09 % and 1.89 – 5.00 %, respectively (Table 3.1.3.2).

The limit of quantification (LoQ) was calculated using the standard deviation of the intercepts and the mean slope of the calibration curves ($\text{LoQ} = 3 \times \text{standard deviation of the intercepts} / \text{mean slope}$) and it was 0.02485 $\mu\text{g/ml}$. The limit of detection (LoD) was calculated using the standard deviation of the intercepts and the mean slope of the calibration curves ($\text{LoD} = 10 \times \text{standard deviation of the intercepts} / \text{mean slope}$) and it was 0.08454 $\mu\text{g/ml}$.

3.1.3.2.2. Extraction Yield :

Several extraction solvents were attended: diethylether, methanol, chloroform, n-hexane, di chloromethane and methyl tertiary butyl ether. Best results were obtained with methyl tertiary butyl ether. Extraction recoveries determined by comparing the peak height heights obtained by direct injection of standard Cilostazol solution with those obtained after methyl tertiary butyl ether extraction of plasma samples were not less than 83.422% over the 0.1 – 20 $\mu\text{g/ml}$ concentration range. (Table 3.1.3.1.)

3.1.3.2.3 Stability :

The amount of Cilostazol recovered over a 6-month period in plasma samples stored at -20°C did not show significant differences from the initial concentrations. (Table 3.1.3.3) and stored samples of Cilostazol with drug free human plasma was unaffected by the presence of disodium ethylene diamine tetra acetic acid or heparin in the collection tube.

3.1.3.2.4. System suitability:

The results obtained from the system suitability study (Table 3.1.3.4.) were in agreement with the USP requirements and the variation in the retention time among six replicate injections of Cilostazol working solutions was very low, rendering a R.S.D. of 0.6 %.

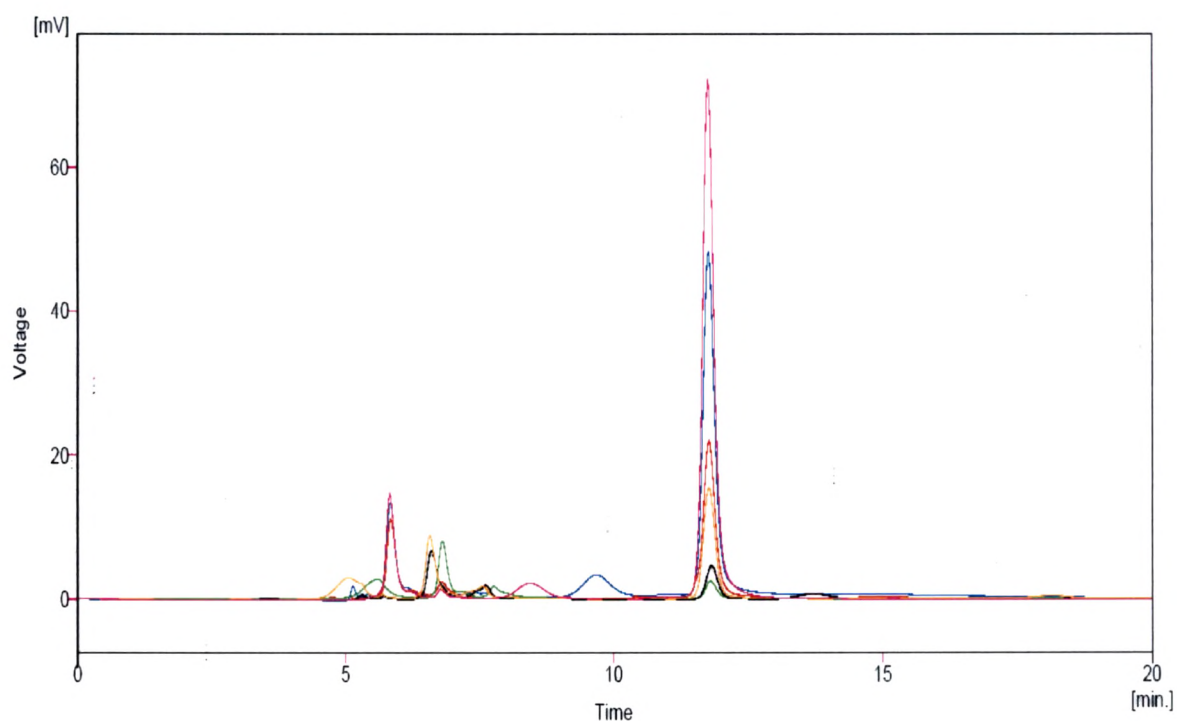


Fig. 3.1.3.1 The overlain chromatograms of standard Cilostazol from 0.5 to 20.0 $\mu\text{g}/\text{ml}$ in mobile phase

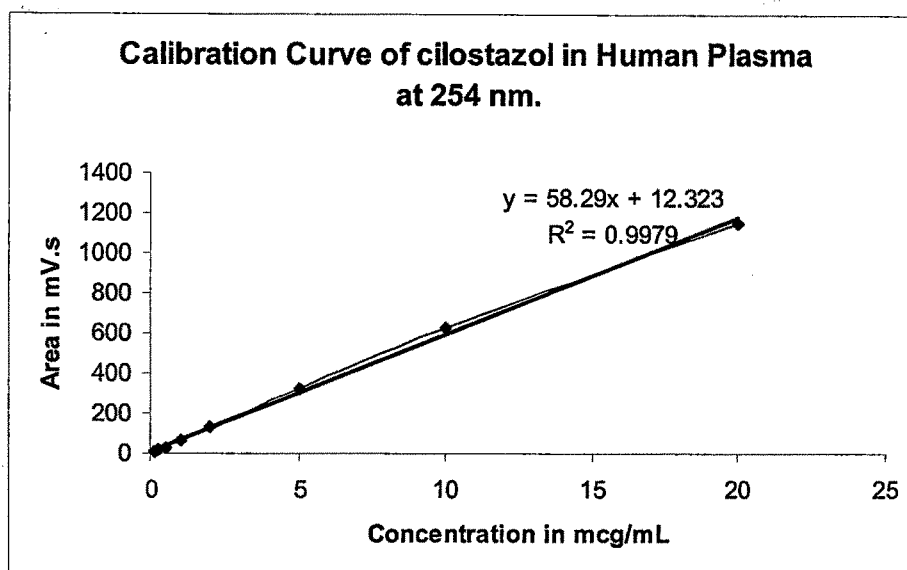


Fig. 3.1.3.2 Calibration data of Cilostazol in human plasma at 254 nm.

Table 3.1.3.1 Cilostazol recovery after extraction: Drug-free human plasma was spiked with Cilostazol at different concentrations and extraction coefficient calculated.

Concentration of Cilostazol ($\mu\text{g/ml}$)	Average Extraction Coefficient (%) (n=3 for each level)	Mean peak area in mV (n=3)	Standard Deviation
0.1	86.98262	5.505	1.161069
0.250	86.64286	15.7695	0.306177
0.5	86.83565	31.3065	3.284511
1	89.2150	65.466	3.023589
2	91.91996	133.909	5.55
5	93.01337	327.7145	5.17911
10	95.134	625.94	12.8927
20	83.42224	1156.965	3.06073

Table 3.1.3.2 Interday and intraday variability of the assay for Cilostazol in plasma (3 series)

Concentration of Cilostazol ($\mu\text{g/ml}$)	Amount of Cilostazol found ($\mu\text{g/ml}$)			
	Intraday precision		Interday precision	
	Mean Area ($n = 3$)	SD	Mean Area ($n = 3$)	SD
0.1	4.685	1.32	5.372	2.04
0.25	15.986	2.86	15.553	3.36
0.5	34.183	1.49	29.538	1.89
1	63.328	3.82	67.604	3.36
2	144.909	5.09	122.909	4.46
5	367.227	4.86	288.202	3.29
10	611.061	3.23	633.505	4.14
20	1130.052	3.55	1183.878	5

Table 3.1.3.3 Drug-free human plasma spiked with three different concentrations of Cilostazol and Stored at -20°C Over 3- Month Period.

Concentration Added ($\mu\text{g/ml}$)	Concentration Obtained in $\mu\text{g/ml}$ along with Mean Area($n = 3$)			
	Day 1	Day 30	Day 90	Day 180
0.1	0.11(5.506)	0.135(6.327)	0.10(5.126)	0.107(5.889)
2	2.09(120.07)	1.88(136.20)	2.56(185.47)	2.12(152.59)
20	18.85(1065.07)	21.51(1253.37)	19.1(1079.19)	20.44(1154.91)

Table 3.1.3.4. System suitability parameters.

Parameter	
RT(min \pm SD)	11.9396 \pm 0.0065
Tailing factor \pm SD	1.278 \pm 0.0165
Theoretical plates \pm SD	14571.33 \pm 251.8518
%RSD	0.54

3.1.4. References

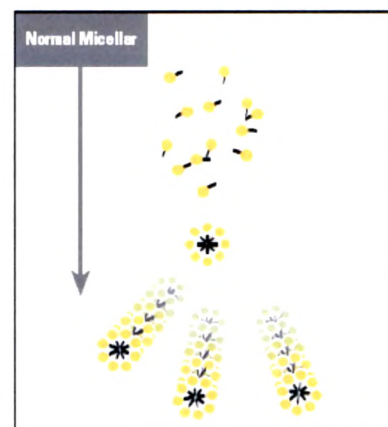
1. J. Kambayashi, Y. Liu, B. Sun, Y. Shakur, M. Yoshitake, F. Czerwiec, Cilostazol as a unique antithrombotic agent, *Curr. Pharm. Des.*, 2003,9, 2289-2302.
2. S.K. Woo, W.K. Kang, K.I. Kwon, Pharmacokinetic and pharmacodynamic modeling of the antiplatelet and cardiovascular effects of Cilostazol in healthy humans, *Clin. Pharmacol. Ther.*, 2002,71, 246-252.
3. D.L. Ardhani, P. Tini, O. Bertha, Y. Mochammad and I. Gunawan, HPLC determination of Cilostazol in tablets, and its validation, *J. Chromatogr. Rel. Tech.*, 2004,27, 2603-2612.
4. T. Shimizu, T. Osumi, K. Niimi, Physico-chemical properties and stability of Cilostazol, *Arzneimittelforschung*, 1985,35, 1117-1123.
5. H. Akiyama, S. Kudo, M. Odomi and T. Shimizu, High-performance liquid chromatography procedure for the determination of a new antithrombotic and vasodilating agent, Cilostazol, in human plasma, *J. Chromatogr.*, 1985,338, 456-459.
6. H. Akiyama, S. Kudo, T. Shimizu, The absorption, distribution and excretion of a new antithrombotic and vasodilating agent, Cilostazol, in rat, dog and man, *Arzneimittelforschung*, 1985,35, 1124-1132.
7. Kyu-Jeong Yeon, Young-Joon Park, Kyung-Mi Park, Jeong-Sook Park, Eunmi Ban, Mee-Kyung Kim, Yang-Bae Kim, Chong-Kook Kim, High performance liquid chromatographic analysis of Cilostazol in human plasma with on-line column switching, *J. Chromatogr. Rel. Tech.* 28 (2005) 109 –120.
8. P.N.V. Tata, C.H.J. Fu, S.L. Bramer, Determination of Cilostazol and its metabolites in human urine by high performance liquid chromatography, *J. Pharm. Biomed. Anal.* 24 (2001) 381-389.
10. P.N.V. Tata, C.H.J. Fu, N.J. Browder, P.C. Chow, S.L. Bramer, The quantitative determination of Cilostazol and its four metabolites in human liver microsomal incubation mixtures by high-performance liquid chromatography, *J. Pharm. Biomed. Anal.* 18 (1998) 441-451.
11. C.J. Fu, P.N.V. Tata, K. Okada, H. Akiyama, S.L. Bramer, Simultaneous quantitative determination of Cilostazol and its metabolites in human plasma by high-performance liquid chromatography, *J. Chromatogr. Biomed. Sci. Appl.* 728 (1999) 251-262.
12. R.V.S. Nirogi, V.N. Kandikere, M. Shukla, K. Mudigonda, W. Shrivasthava, P.V. Datla and A. Yerramilli, Simultaneous quantification of Cilostazol and its primary metabolite 3,4-dehydroCilostazol in human plasma by rapid liquid

chromatography/tandem mass spectrometry, **Anal. Bioanal. Chem.** 384 (2006) 780-790.

13. S.L. Bramer, P.N. Tata, S.S. Vengurlekar, J.H. Brisson, Method for the quantitative analysis of Cilostazol and its metabolites in human plasma using LC/MS/MS, **J. Pharm. Biomed. Anal.** 26 (2001) 637-650.

3.2 Microemulsion:

Microemulsions (ME) are thermodynamically stable systems which can be broadly classified into three major categories (1) oil-in-water (o/w) ME, (2) water-in-oil (w/o) ME, and (3) bicontinuous ME^{1,2}. Typical ME can be formulated which is usually constituting four phases viz. (1) aqueous phase (AQ component) which could be water (hydrous) or anhydrous in nature, (2) Oil phase (O component), (3) surfactant (S component), and (4) co-surfactant (CoS component)³. Regardless of the type of ME



systems, ME can be formulated easily by mixing the oil component with surfactant and co-surfactant components. Aqueous components can be added gradually to the mixture of oil containing surfactant and co-surfactant components. Since, the ME are thermodynamically stable systems; it undergoes spontaneous formation facilitated as a result of micelle formation without input of external energy into the system⁴.

In recent years, lipid microemulsions incorporating medium-chain glycerides have attracted much interest as oral dosage forms to improve drug dissolution and/or intestinal absorption⁵, because (1) they are stable food grade products and generally recognized as safe by the US Food and Drug Administration; (2) microemulsions incorporating these excipients can be formulated at ambient temperature over a wide range of compositions; and (3) early studies have shown that medium-chain glycerides like, C8/C10 mono/di-glyceride (Capmul MCM) and fatty acids improve intestinal absorption of many drug molecules^{6,7,8}. In the small intestine, they are hydrolyzed by intestinal lipases to generate monoglycerides and free fatty acids that can be directly absorbed through the portal route and detected in the plasma.

Microemulsion formulation techniques have been reported by many researchers⁹. These techniques mainly include (1) Titration method, and (2) pseudo-ternary phase diagram construction¹⁰.

Titration method is most commonly employed simplest approach particularly when the aim is to accurately delineate the phase boundaries. In titration method, a series of pseudo binary component systems are formed which are titrated using the third component, evaluating the mixture after each addition. Most commonly the third component is the aqueous phase however, surfactants mixture or oil phase can also be employed. Titrating binary phase with the third component will yield an optically clear system from which

usually the ratio and concentrations of individual components are derived by back calculation method. Heat and sonication are often employed tools to speed up the process. However, care must be exercised especially when the phase boundary is approached as the time taken may greatly increase for system to equilibrate. Utmost care should be taken to ensure that not only the temperature is accurately and precisely controlled but also that the optical observations for clarity are not made on metastable systems. The advantages associated with titration techniques are (1) rapid, (2) reasonably accurate and precise, and (3) economical as large number of observations can be made using limited excipients and drugs. The major disadvantage with titration technique is that it can provide true picture of the phase boundaries but the systems existing within the periphery can't be taken in isolated manner for further studies such as characterization¹¹.

Pseudo-ternary phase diagram is a very useful and important tool to study the phase behaviour. Pseudo-ternary phase diagram can be represented in a triangular format (triangle) which has three coordinates. Each coordinate represents one component of ME system. A typical pseudo-ternary phase diagram illustrating the different phases on respective coordinates is shown in Figure 3.2.1. As seen from the Figure 3.2.1., each coordinate is representing one phase present in the ME system viz. (1) Oil phase (O component), (2) Surfactant: Co-surfactant phase (S: CoS component), and (3) Aqueous phase (AQ component). Each coordinate also represents 0 to 100% concentration of each of the phases in the increment of 10%. In case where four or more components are investigated to formulate ME system, pseudo-ternary phase diagram is used wherein each corner typically represents binary mixture of two components such as surfactant/co-surfactant, water/drug, or oil/drug. Phase diagram is an imperative tool to comprehensively study the ME system and its phase behavior although constructing phase diagram is highly time consuming exercise. In addition to that, phase diagram represents 36 ME points hence, for each ratio or a ME system, a number of experiments including excipients and drug are required to extensively study the phase behavior¹¹. However, as a conservative approach, it is a traditional scientific practice to appropriately blend the titration technique with phase diagram approach together in order to save time and to make it commercially viable option. In this investigation, an approach derived on the basis of titration technique followed by construction of phase diagram was used. The experiments conducted are represented in the form of two-dimensional phase diagram. Microemulsion has four basic components; oil phase (O component), surfactant (S component), Co-surfactant (CoS component) and aqueous phase (AQ component). ME is represented by a four dimensional point.

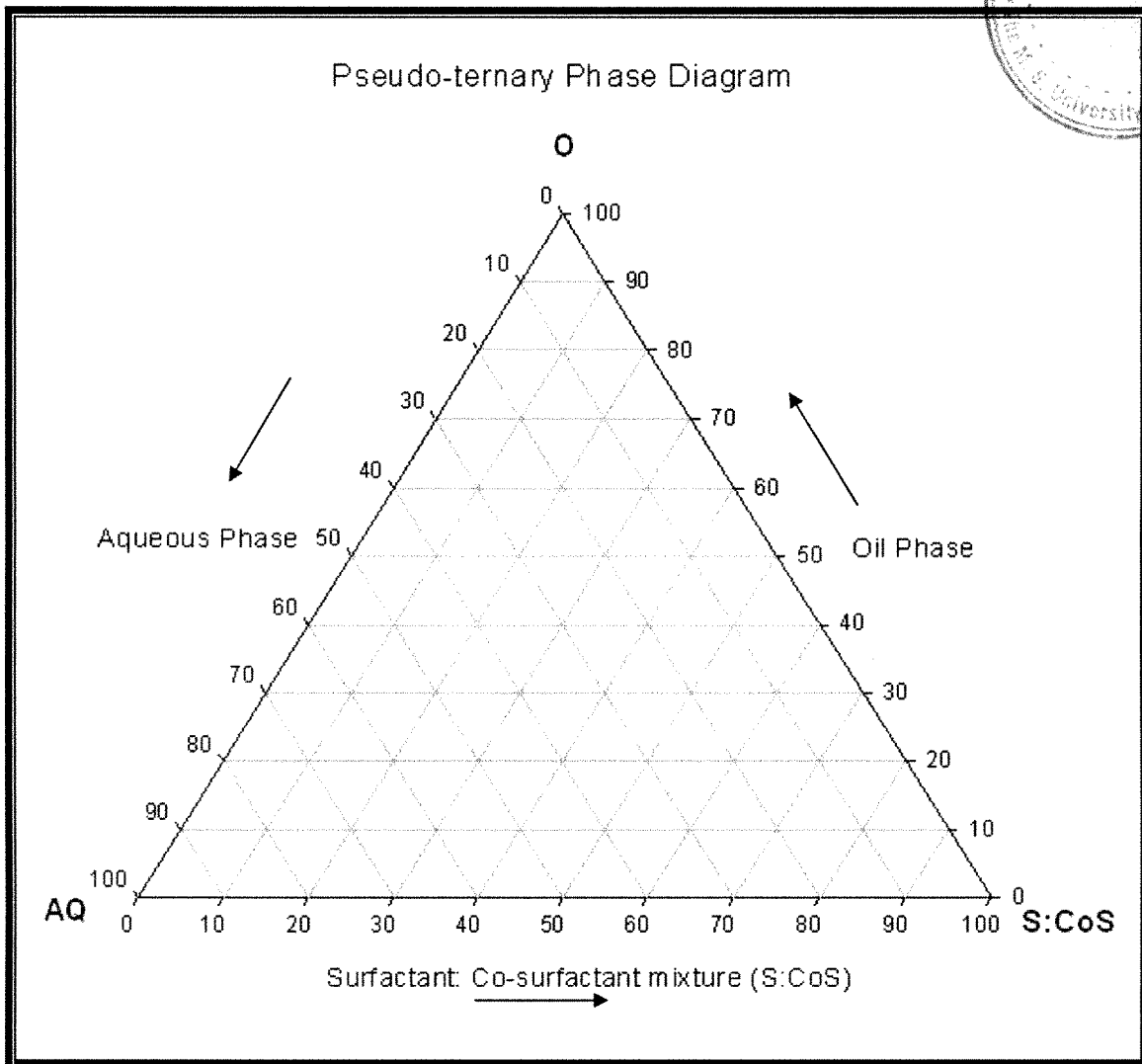
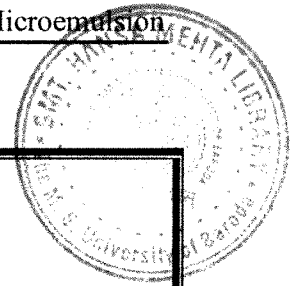


Figure 3.2.1.1. Pseudo-ternary phase diagram representing the three phases and various ME points where three phases intercept

3.2.1. Preparation of Oral Microemulsion of Cilostazol (CME)

3.2.1.1. Solubility of Cilostazol in various oils/surfactants/co-surfactants :

Solubility of Cilostazol in various oils/surfactants/co-surfactants was determined by taking a known amount of Cilostazol (5 mg) in to a dried empty 25 mL beaker. Known amount of various oil/surfactant/co-surfactant (5 mL) were added to it. The beaker was covered with aluminum foil and the solution was stirred gently for 24 hour. The resulting solution was filtered through Whatman filter paper (0.45 micron).An aliquot of 0.1 ml of this solution was taken into a 10 mL volumetric flask and diluted with suitable solvent (methanol/chloroform). The absorbance of the resulting solution was measured spectrophotometrically against pure methanol /chloroform as blank solution. The concentrations of Cilostazol were then back calculated (from absorbance) using the equation of standard calibration curve. Solubility profile of Cilostazol is summarized in Table 3.2.1.1.

Table 3.2.1.1. Solubility profile of Cilostazol in different oils/ surfactants/co-surfactants.

Sr. No.	Name of oil/surfactant/co-surfactant	Solubility of Cilostazol(mg/mL) in oil /surfactant/co-surfactant
1	Peanut oil	1.50
2	Cotton seed oil	2.8
3	Captex 355 EP/NF	0.5
4	Captex 200 P	0.63
5	Labrafac PG	1.96
6	Labrafil M 2125	2.21
7	Cremophor EL	4.65
8	Cremophor RH 40	3.26
9	Labrafil M 1944	8.55 $\sqrt{(S)}$
10	Plurol	0.15 —
11	Transcutol P	16.21 $\sqrt{(Co S)}$
12	Capmul MCM (C8)	11.6 $\sqrt{(O)}$
13	Capmul MCM (C10)	6.25
14	Captex 1000	0.8
15	Tween 80	2.0
16	Tween 20	9.14 $\sqrt{(S)}$

The solubility of Cilostazol was found to be better in Labrafil M 1944, Transcutol P, Capmul MCM (C8) and Tween 20, these were further used for the preparation of ME.

3.2.1.2. Preparation of Cilostazol Microemulsions (CME) :

CME (system 1, CME 1) were prepared by titration method using Capmul MCM C8[®] as an oil phase (O), Labrafil M 1944[®] as a surfactant (S), Transcutol P[®] as a co-surfactant (CoS) and distilled water as an aqueous phase (AQ). Cilostazol (10 mg/mL) was dissolved in oil phase containing surfactant and co-surfactant at room temperature with continuous stirring. To the resultant mixture distilled water was added gradually with continuous stirring. Similarly, another set of CME (system 2, CME 2) was prepared using Capmul MCM C8[®] as oil phase, Tween - 20[®] as surfactant, Transcutol P[®] as co-surfactant and distilled water as an aqueous phase. Cilostazol (10 mg/mL) was dissolved in oil phase containing surfactant and co-surfactant at room temperature with continuous stirring. To the resultant mixture distilled water is added gradually with continuous stirring. The excipient profile for CME system 1 and 2 is shown in Table 3.2.1.2.

Table 3.2.1.2. Excipient profiles for two different systems of Cilostazol microemulsions:

Ingredients	System 1	System 2
Cilostazol	√	√
Capmul MCM C8 (O)	√	√
Labrafil M 1994 CS [®] (S)	√	⊗
Tween 20 [®] (S)	⊗	√
Transcutol P [®] (CoS)	√	√
Water (AQ)	√	√

√ Ingredients used

⊗ Ingredients not used

For optimization of ME composition distilled water was added with stirring to the mixture of oil and surfactant / co-surfactant (at different mass ratios viz. 1:1, 2:1 and 3:1) containing Cilostazol. Visually clear and transparent MEs were considered as acceptable. The concentrations of O, S/ CoS, AQ phase and S: CoS ratios of the clear CME compositions of selected batches are recorded in Table 3.2.1.3.

Table 3.2.1.3. Composition of CME 1 and CME 2 along with different S:CoS ratios.

Foemulation	S:CoS ratio	O (%)	S (%)	CoS (%)	AQ (%)	Cilostazol (mg/mL)
CME 1	1:1	15	17.5	17.5	50	10
	2:1	15	23.33	11.66	50	10
	3:1	15	26.25	8.75	50	10
CME 2	1:1	13.8	16.24	16.24	53.72	10
	2:1	13.8	21.65	10.82	53.72	10
	3:1	13.8	24.36	8.12	53.72	10

The concentrations of various phases which yielded clear MEs were plotted as two dimensional pseudo ternary phase diagrams as shown in Figure 3.2.1.2. (CME 1) and Figure 3.2.1.3. (CME 2) respectively, to obtain ME region. Phase study indicated that, the ME region for CME 1 (3:1 S:CoS ratio) and CME 2 (1:1 S:CoS ratio) were found to be highest among all formulations and hence selected for further characterization study.

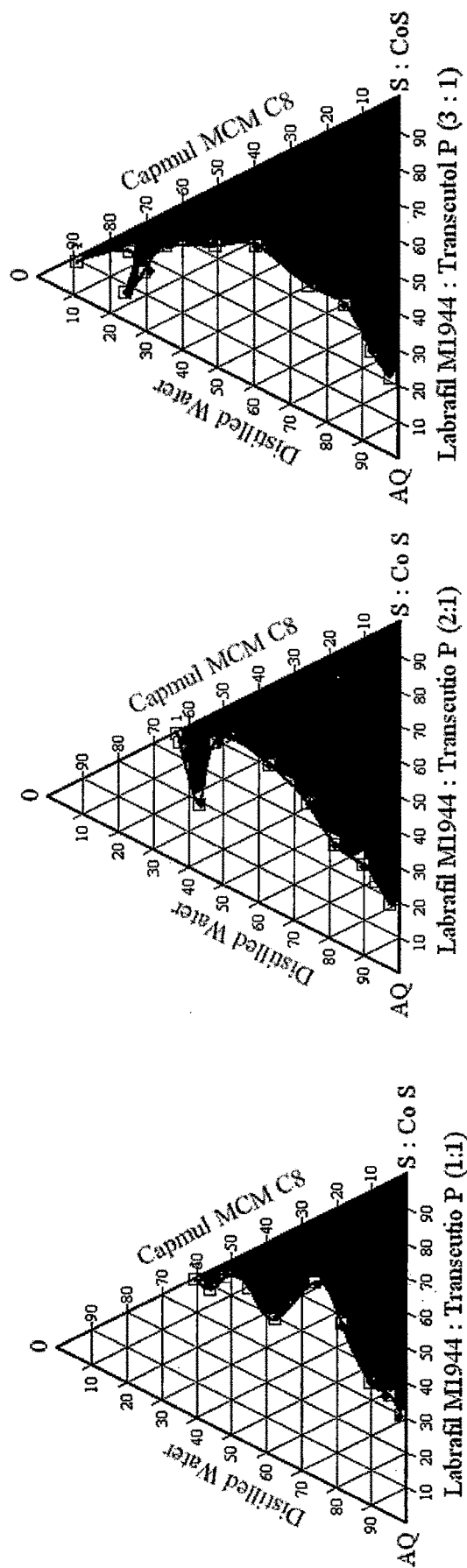


Figure 3.2.1.2. Pseudo-ternary phase diagrams for CME 1 (System 1) showing ME regions (Shaded) at S: CoS ratio 1:1, 2:1 and 3:1.

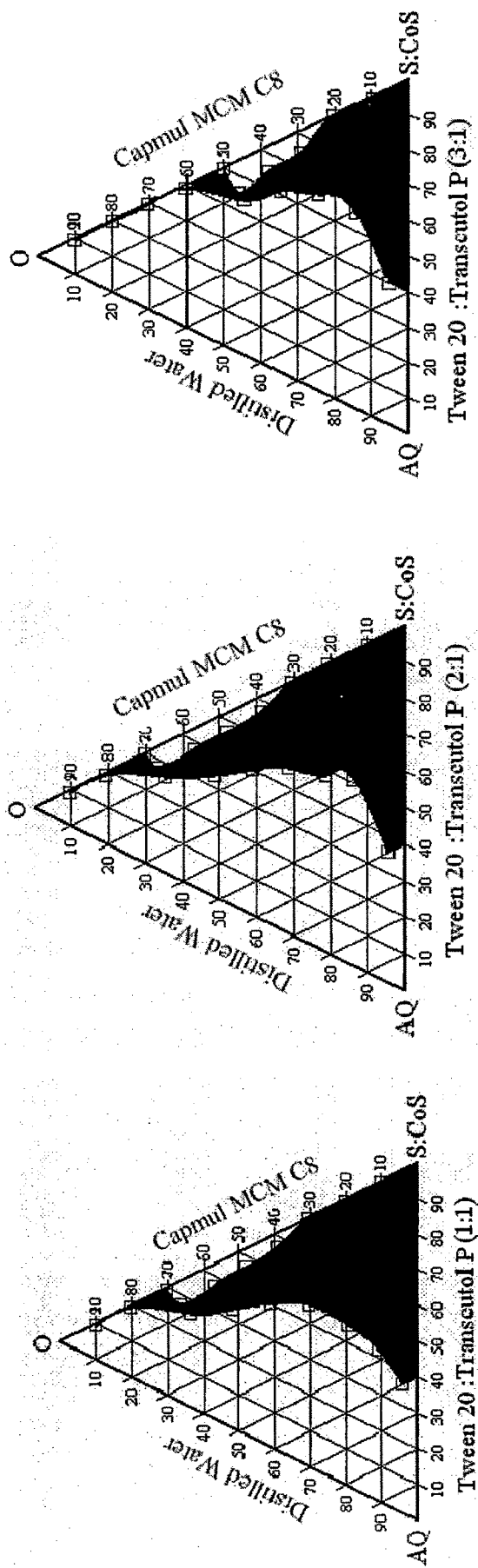


Figure 3.2.1.3. Pseudo-ternary phase diagrams for CME 2 (System 2) showing ME regions (Shaded) at S: CoS ratio 1:1, 2:1 and 3:1.

3.2.2.Characterization

Prepared Oral microemulsions of Cilostazol were further characterized for its pH globule size, zeta potential, viscosity , electroconductivity and % Transmittance.

3.2.2.1. Appearance :

Appearances of CME1 and CME2 were tested against white and black background and turbidity were checked. The test was carried out as described in the Indian Pharmacopoeia (1996) and United States Pharmacopoeia (2003).

3.2.2.2. Stability as per stomach condition and pH Determination :

The pH of CME 1 and CME 2 were measured by diluting the 5 mL of respective test sample of ME with 10 parts, 100 parts and 1000 parts of distilled water. The resultant solution/dispersion was stirred for 5 min and the stability was checked. The pH were recorded for stable solutions/dispersions by using calibrated digital pH meter at $25^{\circ}\text{C} \pm 1^{\circ}\text{C}$ ¹³. The pH was recorded in triplicate when the pH gets stabilized. pH meter was calibrated daily using standard buffer solutions (pH 4.2, pH 7.00 and pH 9.2) prior to recording the observations.

3.2.2.3. Globule size Determination :

The globule size^{12,14} of CME1 and CME 2 were determined using photon correlation spectroscopy (PCS) method with in-built Zetasizer (Model: Nano ZS, Malvern Instruments, UK) at 633 nm. The equipment was filled with 18 mm width, helium-neon gas laser source having intensity of 4 mW. The mean PCS diameter is the so-called intensity-weighted “z-average” (mean particle size). Average of three measurements of each sample was used for derivation of mean particle size. Latex dispersion having mean particle size $60\text{ nm} \pm 5\text{ nm}$ was used as a standard. The standard was evaluated after every 60 min during measurement of test samples in order to validate the equipment.

3.2.2.4. Zeta Potential Determination :

The Nano ZS Zetasizer (Malvern Instrument,UK) was used to measure the zeta potential by electrophoresis and electrical conductivity of the formed ME was also performed using in built conductivity option (Zeta potential) of the Zetasizer¹². The electrophoretic mobility ($\mu\text{m/s}$) was converted to zeta potential by in-built software using Helmholtz-Smoluchowski equation. Measurements were performed using small volume disposable zeta cell. Average of three measurements of each sample was used to derive average zeta potential. Latex dispersion having zeta potential $-50\text{ mV} \pm 2.5\text{ mV}$ was used as a standard.

The standard was evaluated after every 60 min during measurement of test samples in order to validate the results of test formulation.

3.2.2.5. Viscosity Measurement :

The rheological property of the CME1 and CME 2 were evaluated¹³ by a Brookfield LVDV 111 + CP viscometer (Stoughton, MA) at 30 °C using a CPE 42 spindle at 5 rpm. Experiment was performed in triplicate for each sample, and results were presented as average ± standard deviation.

3.2.2.6. Electroconductivity Measurement :

The electroconductivity of the resultant system was measured by an electroconductometer (CM 180 conductivity meter, Elico, Mumbai, India). For the conductivity measurements, the tested microemulsions were prepared with a 0.01N aqueous solution of sodium chloride instead of distilled water.

3.2.2.7. % Transmittance Measurement :

The percent transmittance of CME1 and CME 2 were measured at 650 nm using UV spectrophotometer (UV 1601, Shimadzu, Japan) keeping distilled water as a blank.

3.2.2.8 Active Ingredient Analysis :

CME1 and CME 2 were analyzed for presence of Cilostazol ingredient using the developed spectrophotometric method of analysis for analyzing formulations described in under sections 3.1.1.4.5.

Table 3.2.2.1. Compositions and characterization of Cilostazol microemulsion system 1 (CME 1) as per stomach condition.

System	O (%)	S (%)	CoS (%)	AQ (%)	Globule size (nm) \pm SD		Zeta potential (mV) \pm SD		Transmittance (%) \pm SD	
					Initial	After 3 Hr.	Initial	After 3 Hr.	Initial	After 3 Hr.
	15	26.25	8.75	50	82.2 \pm 0.32	82.1 \pm 0.55	-2.48 \pm 0.46	-2.47 \pm 0.54	99.85 \pm 0.19	99.71 \pm 0.36
CME 1 DILUTED BY 10 TIMES WITH AQUEOUS PHASE										
	10	17.5	5.83	66.66	92.8 \pm 0.45	93.2 \pm 0.21	-2.90 \pm 0.82	-2.88 \pm 0.44	99.69 \pm 0.69	99.58 \pm 0.16
CME 1 DILUTED BY 100 TIMES WITH AQUEOUS PHASE										
	1.42	2.5	0.833	95.23	104.4 \pm 0.31	106.5 \pm 0.56	-5.01 \pm 0.21	-4.90 \pm 0.38	99.42 \pm 0.82	99.34 \pm 0.35
CME 1 DILUTED BY 1000 TIMES WITH AQUEOUS PHASE										
	0.149	0.261	0.087	99.50	123.3 \pm 0.56	129.9 \pm 0.65	-6.9 \pm 0.39	-6.36 \pm 0.71	99.10 \pm 0.58	98.91 \pm 0.24

The results are mean values \pm SD derived from three different experimental batches. O is denoted for Oil Phase (Capmul MCM C8[®]), S for surfactant (Labrafil M 1944[®]), Co-S for co-surfactant (Transcutol P[®]) and AQ is denoted for aqueous phase (Distilled Water). The CME formulations contain Cilostazol – 10 mg/mL.

Table 3.2.2.2. Compositions and characterization of Cilostazol microemulsion system 2 (CME 2) as per stomach condition.

System	O (%)	S (%)	CoS (%)	AQ (%)	Globule size (nm) \pm SD		Zeta potential (mV) \pm SD		Transmittance (%) \pm SD	
					Initial	After 3 Hr.	Initial	After 3 Hr.	Initial	After 3 Hr.
	13.8	16.24	16.24	53.72	66.1 \pm 0.67	71.29 \pm 0.63	-4.88 \pm 0.30	-4.10 \pm 0.31	99.80 \pm 0.68	99.54 \pm 0.59
CME 2 DILUTED BY 10 TIMES WITH AQUEOUS PHASE										
	9.4	11.59	11.59	67.38	75.7 \pm 0.54	86.9 \pm 0.54	-5.23 \pm 0.45	-4.88 \pm 0.77	99.24 \pm 0.34	99.18 \pm 0.67
CME 2 DILUTED BY 100 TIMES WITH AQUEOUS PHASE										
	1.33	1.64	1.64	95.38	86.9 \pm 0.61	91.86 \pm 0.54	-6.2 \pm 0.68	-6.9 \pm 0.59	99.06 \pm 0.41	99.00 \pm 0.25
CME 2 DILUTED BY 1000 TIMES WITH AQUEOUS PHASE										
	0.139	0.171	0.171	99.51	98.23 \pm 0.38	105.23 \pm 0.66	-7.22 \pm 0.23	-7.55 \pm 0.91	98.90 \pm 0.38	98.78 \pm 0.32

The results are mean values \pm SD derived from three different experimental batches. O is denoted for Oil Phase (Capmul MCM C8[®]), S for surfactant (Twen - 20[®]), CoS for Co-surfactant (Transcutol P[®]) and AQ is denoted for aqueous phase (Distilled Water). The CME formulations contain Cilostazol - 10 mg/mL.

Table 3.2.2.3. Characterization of Cilostazol microemulsions (CME 1 and CME 2).

Microemulsion	O (%)	S (%)	CoS (%)	AQ (%)	pH \pm SD	Conductivity (μ semence) \pm SD	Viscosity (Cps) \pm SD
CME 1	15	26.25	8.75	50	4.66 \pm 0.42	168.2 \pm 0.3	26.3 \pm 1.1
CME 2	13.8	16.24	16.24	53.72	4.58 \pm 0.26	121.0 \pm 0.73	29.39 \pm 0.48

3.2.3. Physical Stability

CMEs were evaluated for their physical and chemical stability¹⁵. The prepared MEs were subjected to accelerated centrifugation for the assessment of physical phase separation, if any between the oil and aqueous phase. Some of the batches meeting the criteria mentioned below were selected for further studies¹⁶.

Criteria for selection of batches

1. Microemulsions having mean globule size below 100 nm; and
2. Zeta potential at least -5 mV

Microemulsions having least globule size are expected to have larger surface area and therefore, may get absorbed or may transverse rapidly across the intestinal mucosa. Moreover, literature citation revealed that ME which are negatively charged and having zeta potential close to -5 mV or less exhibits moderate to excellent physical stability^{12,17}. Therefore, both the selection criteria were used as a filter prior to assessment of accelerated physical stability. These experimental batches are marked in bold face fonts (Table 3.2.1.3.).

Method

Approximately 5 mL of the ME was charged to the centrifugation tube and the top of the tube was tightly closed using screw-on cap. Phase separation study of the globule size and zeta potential-fractionated ME were performed using accelerated centrifugation at 3.6 x 1x g at 4° C ± 2° C temperature for 15 min¹². Sample from top, middle and bottom were collected using 24" needle fitted on 1 mL syringe and globule size determination was performed using photon correlation spectroscopy (as mentioned under characterization in this chapter, section 3.2.2.). The results of globule size following accelerated centrifugation for selected batches of CME are recorded in Table 3.2.3.1 A few representative batches wherein the physical separation was noticed (different globule size compared to initial values) were also analyzed for active ingredient content to reconfirm the separation. The results of the promising batches with acceptable globule size difference (± 5 nm) as compared to initial values (marked in bold face font in Table 3.2.3.1.) have been evaluated for chemical stability followed by *in vitro* drug diffusion studies^{18,19} using dialysis bag technique and intestinal permeability study to assess diffusion coefficient and release kinetics²⁰.

Table 3.2.3.1. Accelerated physical stability of Cilostazol microemulsions.

System	Ratio of S:CoS	O (%)	S (%)	CoS (%)	AQ (%)	Globule size (nm)		
						Top layer	Middle layer	Bottom layer
CME 1	3:1	15	26.25	8.75	50	84.04 ± 3.23	81.23 ± 3.52	78.56 ± 2.89
CME 2	1:1	13.8	16.24	16.24	53.72	71.35 ± 0.87	68.87 ± 0.72	63.05 ± 0.64

3.2.4. Chemical Stability (Drug Retention Studies)

Cilostazol microemulsions were subjected to accelerated temperature and stress conditions (<http://www.nihs.go.jp/dig/ich/quality/q1e/Q1E>). The MEs were analyzed for physical and chemical stability. Approximately 10 mL of the formulation was filled in USP type III glass vials and sealed using VP6 crimp on spray pump fitted with 10 μ m actuator. Physical stability was assessed using accelerated centrifugation technique as described previously in this chapter (section 3.2.3.)¹³.

The stress stability was conducted at 60° C \pm 2° C in an incubator. The accelerated stability was performed at 30° C \pm 2° C / 65% \pm 5% relative humidity (RH) and 40° C \pm 2° C / 75% \pm 5% RH. The duration of stability was 6 months and samples were withdrawn at predetermined time intervals after 1 month, 2 months, 3 months and 6 months (<http://www.nihs.go.jp/dig/ich/quality/q1e/Q1E>). The parameters such as physical separation at accelerated gravitational force, active ingredient content, globule size determination, zeta potential measurement, appearance, cracking or physical separation, solidification/ gel formation etc. were assessed. These parameters were evaluated as per the methods described in the section 3.2.2 and 3.2.3. The results for Cilostazol microemulsions drug retention studies are recorded in Table 3.2.4.1.

Table 3.2.4.1. Accelerated chemical stability of Cilostazol microemulsions at 40°C/75% RH and 30°C/65% RH

System	Ratio of S:CoS	O (%)	S (%)	CoS (%)	AQ (%)	Period (month)	40°C/75% RH				30°C/65% RH			
							Globule size (nm) ± SD	Zeta potential (mV) ± SD	Transmittance (%) ± SD	Drug content (%) ± SD	Globule size (nm) ± SD	Zeta potential (mV) ± SD	Transmittance (%) ± SD	Drug content (%) ± SD
CME 1	3:1	15.00	26.25	8.75	50.00	0	83.45 ± 0.40	-2.50 ± 0.51	99.28 ± 0.72	99.67 ± 0.35	83.59 ± 0.40	-2.05 ± 0.21	99.88 ± 0.42	99.85 ± 0.35
						1	85.46 ± 0.33	-2.87 ± 0.81	99.33 ± 0.55	99.18 ± 0.44	82.85 ± 0.28	-2.22 ± 0.87	99.56 ± 0.74	99.35 ± 0.29
						2	82.42 ± 0.39	-2.39 ± 0.35	99.21 ± 0.79	98.87 ± 0.50	84.15 ± 0.32	-2.84 ± 0.67	99.62 ± 0.34	98.92 ± 0.63
						3	84.27 ± 0.56	-2.85 ± 0.11	98.98 ± 0.31	98.12 ± 0.61	84.85 ± 0.91	-2.72 ± 0.32	99.69 ± 0.39	98.55 ± 0.40
						6	85.46 ± 0.65	-2.88 ± 0.73	99.04 ± 0.38	97.56 ± 0.86	85.18 ± 0.72	-2.66 ± 0.82	99.26 ± 0.53	97.62 ± 0.85
						0	68.00 ± 0.45	-4.37 ± 1.27	99.52 ± 0.25	99.55 ± 0.32	64.46 ± 0.57	-4.26 ± 1.07	99.52 ± 0.86	99.39 ± 0.64
CME 2	1:1	13.80	16.24	16.24	53.72	1	71.35 ± 0.33	-4.12 ± 1.18	99.46 ± 0.64	99.19 ± 0.46	67.58 ± 0.91	-4.8 ± 1.07	99.36 ± 0.74	99.45 ± 0.85
						2	69.64 ± 0.86	-3.97 ± 1.28	99.30 ± 0.24	98.77 ± 0.45	68.68 ± 0.84	-4.89 ± 0.88	99.54 ± 0.83	98.82 ± 0.64
						3	68.75 ± 0.83	-4.53 ± 1.36	99.05 ± 0.35	98.38 ± 0.57	65.80 ± 0.60	-4.17 ± 1.66	99.57 ± 0.51	98.36 ± 0.77
						6	69.82 ± 0.35	-4.43 ± 0.94	98.94 ± 0.28	97.56 ± 0.38	69.45 ± 0.84	-4.53 ± 1.83	99.06 ± 0.45	97.16 ± 0.87

3.2.5. Drug Diffusion Study.

In vitro permeation/diffusion of formulations is a valuable tool to predict behavior of a particular formulation with respect to drug transport across the membrane. Under the testing conditions *in vitro* studies can be helpful to assess the relative drug permeation/diffusion behavior across the membrane^{21,22}. Various physicochemical parameters pertaining to formulations such as flux, partition coefficient, diffusion coefficient and permeation coefficient can be derived using *in vitro* evaluation techniques. One of the disadvantages of *in vitro* evaluation techniques is that method does not mimic the behavior of living tissues/organs, for example, degradation of drug compound in presence of enzymes, capricious blood supply or metabolism etc. In practice, it virtually becomes difficult task to perform the biological studies using animals or on humans for the assessment of different formulations from the perspective of economy and time requirement. At the same time, *in vitro* models can serve as second line option which will be indicative kind of tool prior to proceeding for animal or human studies.

In this investigation, all the test formulations were assessed for *in vitro* diffusion across the dialysis technique and *in vitro* permeation across Male Sprague Dawley rat's duodenum in triplicate and the physicochemical parameters were calculated as mentioned below²³.

(A) Percent Drug Diffused

The percent drug diffused across the sheep nasal mucosa at predetermined sampling time interval was determined using formula mentioned below.

$$\% \text{ Drug Diffused} = \frac{c_r v_r}{c_d v_d} \times 100$$

Where, C_r = Concentration of the drug in receptor compartment

V_r = Volume of the receptor compartment

C_d = Initial concentration of the drug in donor compartment

V_d = Initial volume in the donor compartment

(B) Kinetics of Release

In order to investigate the mechanism of drug release from the formulation, the release rates were integrated into each of the following equation and the regression coefficient was investigated from each of the regressed graph.

Zero-order equation:

$$Q = K_0 t$$

Where, Q = Amount of drug released at time t

t = Time in hours

K_0 = Zero-order release rate constant

First-order equation:

$$Q = Q_0 e^{-K_1 t}$$

Where, Q = Amount of drug released at time t

t = Time in hours

K_1 = First-order release rate constant

Higuchi's equation:

$$Q = K_H \times \sqrt{t}$$

Where, Q = Amount of drug released at time t

t = Time in hours

K_H = Higuchi's diffusion rate constant

The order of drug release was determined by performing the regression over the mean values of percent drug diffusion vs. time (for Zero-order), log percent drug diffusion vs. time (for First-order) and percent drug diffusion vs. square root of time (for Higuchi).

3.2.5.1. Experimental design.

3.2.5.1.1 Dialysis Bag Technique^{24,25}.

In vitro diffusion study was performed for all prepared MEs of Cilostazol by using the dialysis bag technique. Experiments were carried out by using a cellulose dialysis bag (7 cm in length), having a circular tubing shape with both open ends as shown in Figure 3.2.5.1.(a). Dialysis bag was soaked for over night into a phosphate buffer pH 6.8 for saturation purpose and then it was used for further experimental study. The dialysis medium was 30 mL of phosphate buffer pH 6.8. One end of the prepared dialysis bag was tied with thread, and then 1 mL of concentrated ME (2 mg of drug) was placed into it along with 0.5 mL of diffusion medium. The other end of the dialysis bag was also secured with thread and was allowed to rotate freely in 30 mL of dialysis medium and stirred continuously for 100 rpm with magnetic bead on magnet plate

at 37 °C (Figure 3.2.5.2.(b)). Aliquots of 0.250 mL were withdrawn at different time intervals and volume of aliquots replaced with fresh dialysis medium each time. The samples were analyzed quantitatively for Cilostazol dialyzed across the membrane at corresponding time by using UV-Visible spectrophotometer (Shimadzu UV 1601 , Japan) as mentioned under Section 3.1.1.4.6. The experiments were run in triplicate and the mean cumulative % drug diffused along with SD of pure Cilostazol, Marketed formulation (Tablet, Pletoz-50) and prepared ME are shown in Table 3.2.5.2 and Table 3.2.5.3. These are represented graphically in Figure 3.2.5.2.(a). The release kinetics of diffusion was studied by calculating the regression coefficient for zero order, first order, and Higuchi's equations. The regression coefficients for the different formulations of Cilostazol are recorded in Table 3.2.5.4.

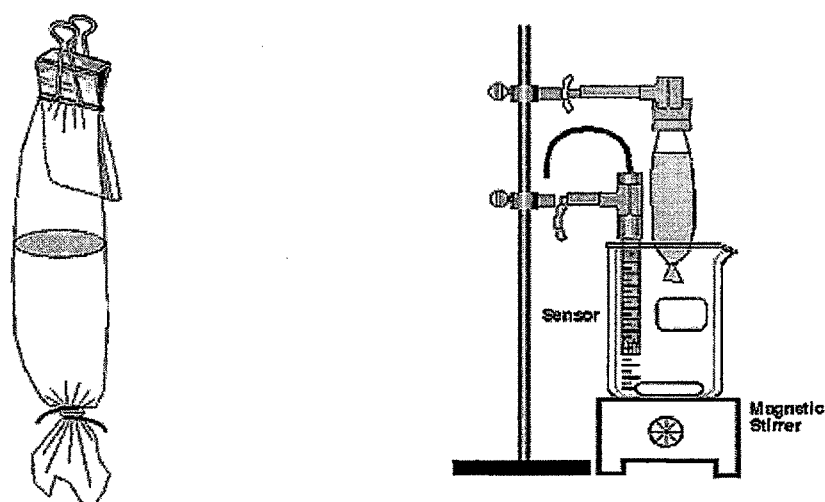


Fig. 3.2.5.1 (a) Preparation of Dialysis bag (b) Experimental Set up

3.2.5.1.2 Intestinal Permeability Study

The experimental procedure described by P. Smith²⁶ and P. K. Ghish¹³ was modified for permeation study. Male Sprague Dawley rats (250 – 300 gm) were killed by over dose with pentobarbitone administered by intravenous injection. Our basic aim was to check the intestinal permeability of the drug, orally administered as ME base. To check the intraduodenal permeability, the duodenal part of the small intestine was isolated and used for *in vitro* intestinal study. Separated duodenal part was washed with cold Ringer solution to remove mucous and lumen contents and one end of the duodenum was tied with thread. Prepared concentrated ME of

Cilostazol was diluted outside with 1 mL of Phosphate buffer pH 6.8 for 5 minute by vortex mixture. A suspension of marketed formulation (Tablet, Pletoz – 50) was formed by using 1 mL of Phosphate buffer pH 6.8. The resultant solution (2mg/mL) was injected into the lumen of the duodenum using a syringe and another side of the lumen was tightly closed with the thread. The tissue was placed in a chamber of organ bath with continuous aeration and a constant temperature of 37 °C. The receiver compartment was filled with 30 mL of phosphate buffer pH 6.8. Aliquots of 0.250 mL were removed at different time intervals and volume of aliquots replaced with fresh dialysis medium each time. The samples were analyzed quantitatively for Cilostazol dialyzed across the membrane at corresponding time by using UV-Visible spectrometric method as mentioned in Chapter 3.1, Section 3.1.1.4.6. The experiments were run in triplicate and the mean cumulative % drug diffused along with SD of Cilostazol, Marketed formulation and prepared MEs are shown in Table 3.2.5.2. and Table 3.2.5.3. and graphically they are represented in Figure 3.2.5.2(b). The release kinetics of diffusion was studied by calculating the regression coefficient for zero order, first order, and Higuchi's equations. The regression coefficients for the different formulations of Cilostazol are recorded in Table 3.2.5.5.^{27,28}.

Table 3.2.5.1. Promising compositions of Cilostazol microemulsions for *in vitro* diffusion study :

System	Ratios of S : CoS	O %	S %	CoS %	AQ %
CME 1	3 : 1	15	26.25	8.75	50
CME 2	1 : 1	13.8	16.24	16.24	53.72

Table 3.2.5.2. Cumulative % drug diffused from Pure Cilostazol and its marketed formulation at different time intervals .

Time (h)	Cumulative % drug diffused [#] System (Formulation)					
	Pure Cilostazol			Pletoz - 50 (Tablet)		
	Dialysis bag Technique	Intestinal Permeability Study	Intestinal Permeability Study	Dialysis bag Technique	Intestinal Permeability Study	Intestinal Permeability Study
0.15	0.36 ± 0.56	0.21 ± 0.11	0.21 ± 0.11	2.98 ± 0.26	3.81 ± 0.43	3.81 ± 0.43
0.30	0.86 ± 0.85	0.99 ± 0.31	0.99 ± 0.31	4.11 ± 0.55	4.35 ± 0.57	4.35 ± 0.57
0.45	1.11 ± 0.69	1.21 ± 0.66	1.21 ± 0.66	6.92 ± 0.35	5.27 ± 0.66	5.27 ± 0.66
1	2.47 ± 0.29	2.09 ± 0.43	2.09 ± 0.43	8.43 ± 0.78	7.56 ± 0.89	7.56 ± 0.89
2	3.65 ± 0.19	3.26 ± 0.76	3.26 ± 0.76	11.33 ± 0.87	9.88 ± 0.62	9.88 ± 0.62
3	4.99 ± 0.24	4.31 ± 0.68	4.31 ± 0.68	13.65 ± 0.91	11.22 ± 0.92	11.22 ± 0.92
4	5.15 ± 0.35	5.11 ± 0.42	5.11 ± 0.42	15.85 ± 0.72	14.34 ± 0.81	14.34 ± 0.81
5	6.43 ± 0.75	5.91 ± 0.87	5.91 ± 0.87	16.93 ± 0.55	15.96 ± 0.63	15.96 ± 0.63
6	7.32 ± 0.88	6.86 ± 0.24	6.86 ± 0.24	18.07 ± 0.71	17.35 ± 0.72	17.35 ± 0.72
7	8.81 ± 0.45	7.34 ± 0.91	7.34 ± 0.91	20.26 ± 0.91	18.57 ± 0.44	18.57 ± 0.44
8	9.11 ± 0.91	8.01 ± 0.79	8.01 ± 0.79	22.62 ± 0.84	19.84 ± 0.63	19.84 ± 0.63

[#] All values are represented as mean ± SD (±n=3).

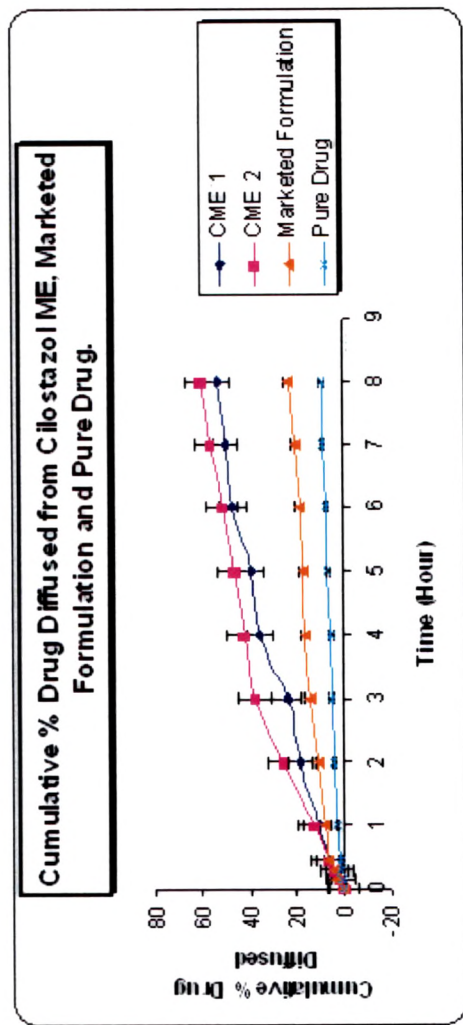
Table 3.2.5.3. Cumulative % drug diffused from different Cilostazol microemulsion at different time intervals .

Time (h)	Cumulative % drug diffused [#] System (Formulation)					
	CME1			CME2		
	Dialysis bag Technique	Intestinal Permeability Study	Dialysis bag Technique	Dialysis bag Technique	Intestinal Permeability Study	Intestinal Permeability Study
0.15	1.32 ± 0.77	0.51 ± 0.20	1.75 ± 0.20	1.75 ± 0.20	0.58 ± 0.19	0.58 ± 0.19
0.30	1.99 ± 0.53	2.89 ± 0.58	3.88 ± 0.34	3.88 ± 0.34	3.19 ± 0.36	3.19 ± 0.36
0.45	6.03 ± 0.69	8.48 ± 1.05	7.10 ± 0.77	7.10 ± 0.77	9.57 ± 0.61	9.57 ± 0.61
1	11.33 ± 0.86	17.45 ± 0.97	12.56 ± 1.34	12.56 ± 1.34	19.12 ± 0.82	19.12 ± 0.82
2	17.85 ± 0.94	27.44 ± 1.22	25.67 ± 1.23	25.67 ± 1.23	27.75 ± 1.27	27.75 ± 1.27
3	23.96 ± 1.31	36.38 ± 1.48	37.43 ± 1.64	37.43 ± 1.64	37.64 ± 0.77	37.64 ± 0.77
4	35.32 ± 1.28	43.39 ± 1.18	42.19 ± 1.42	42.19 ± 1.42	43.23 ± 1.19	43.23 ± 1.19
5	39.39 ± 1.32	47.65 ± 1.38	46.43 ± 1.71	46.43 ± 1.71	48.86 ± 1.66	48.86 ± 1.66
6	46.86 ± 1.56	48.31 ± 1.66	51.42 ± 1.82	51.42 ± 1.82	50.21 ± 1.33	50.21 ± 1.33
7	49.83 ± 1.32	50.29 ± 1.63	56.76 ± 1.25	56.76 ± 1.25	54.10 ± 1.25	54.10 ± 1.25
8	53.33 ± 1.55	52.04 ± 1.57	60 ± 1.16	60 ± 1.16	57.32 ± 1.35	57.32 ± 1.35

[#] All values are represented as mean ± SD (±n=3).

Figure 3.2.5.2. Cumulative % drug diffused from Cilostazol MEs, Marketed Formulation (Tablet- Pletoz-50) and Pure Drug at different time intervals. Error bars represent SD (n=3).

(a) Cumulative % Drug Diffused by Dialysis Bag Study.



(b) Cumulative % Drug Diffused by Intestinal Permeability Study.

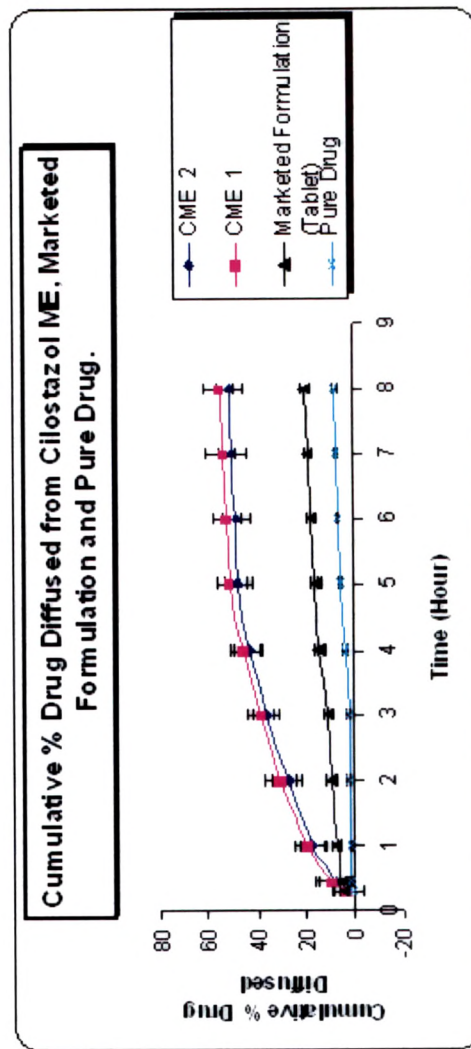


Table 3.2.5.4. Regression coefficients of different Cilostazol microemulsions (CME 1 and CME 2), Pletoz-50 and Pure Cilostazol derived using regressed graphs by Dialysis Bag Method.

System (Formulation)	Zero-order equation	First-order equation	Higuchi's equation
	r^2	r^2	r^2
CME 1	0.9811	0.7592	0.9728
CME 2	0.9531	0.7207	0.9846
Pletoz-50	0.926	0.6675	0.9923
Pure Drug	0.9749	0.7834	0.9808

Table 3.2.5.5. Regression coefficients of different Cilostazol microemulsions (CME 1 and CME 2), Pletoz-50 and Pure Cilostazol derived using regressed graphs by Intestinal Permeability Study.

System (Formulation)	Zero-order equation	First-order equation	Higuchi's equation
	r^2	r^2	r^2
CME 1	0.8872	0.612	0.9707
CME 2	0.8912	0.6087	0.9742
Pletoz-50	0.9411	0.6913	0.9954
Pure Drug	0.9739	0.8432	0.989

3.2.6. Results and Discussion

Cilostazol microemulsions (CME 1 and CME 2) were successfully prepared using the titration technique followed by construction of pseudo-ternary phase diagrams²⁹. As per the solubility data shown in Table 3.2.1.1, the solubility of drug in cotton seed oil, peanut oil, Labrafac PG and Capmul MCM C10 was less than 5 mg/mL but showed maximum solubility in Capmul MCM C8[®] (> 11 mg/mL), hence it was selected to formulate MEs. As oral formulations should be dose dependent and compatible with stomach condition (acidic pH as well as excess amount of aqueous phase (> 1000 ml)), the ME base was selected on the merits of stability of micells when concentrated ME was contacted with excess of aqueous phase as well as solubilization capacity of drug. The selection of surfactant and co-surfactant mixture was on the basis of HLB values. The mixtures of S:CoS reported in literature and which can provide HLB value between 9 and 12 were selected.

To screen out a drug vehicle suitability for oral delivery of Cilostazol, two different ME systems were prepared wherein CME 1 and CME 2 comprised of Capmul MCM C8[®] as an oil phase, Transcutol P[®] as a co-surfactant and distilled water as an aqueous phase. Labrafil M 1944[®] and Tween 20[®] were used as surfactant for CME 1 and CME 2 respectively. Both MEs (CME 1 and CME 2) were formulated at different S:CoS ratios: 1:1, 2:1 and 3:1 and phase studies were done to investigate the effect of S:CoS ratio on the existence ranges of stable o/w ME region. The transparent ME area is presented in the phase diagrams as shaded region. No distinct conversion from w/o to o/w ME was seen; therefore, this single isotropic region is considered as a bicontinuous ME. The rest of the region on the phase diagram represented the viscous gel area or turbid and conventional emulsions based on visual identification. The pseudo-ternary phase diagrams of CME 1(three formulations) and CME 2(three formulations) are displayed in Figures. 3.2.1.2. and 3.2.1.3. respectively.

It can be concluded from the phase diagrams, 3:1 S:CoS ratio of CME 1 and S:CoS ratio 1:1 of CME 2 showed maximum microemulsion region and its compositions are shown in Table 3.2.6.1. The data obtained from the phase diagram study suggested that, increased ME region was towards the oil–water axis, there by indicating at optimum surfactant concentration, the amount of water and oil that could be solubilized into the ME is increased^{30,31}.

Table 3.2.6.1.: Excipients and its composition for the preparation of CME 1 and CME 2.

System (S:CoS) ratio	Oil (%)	Surfactant (%)	Co-surfactant (%)	Aqueous phase (%)	Amount of Cilostazol (mg/mL)
CME 1 (S: CoS ratio 3:1)	Capmul MCM C8 (15%)	Labrafil M1944 (26.25%)	Transcutol P (8.75%)	Water (50%)	10
CME 2 (S: CoS ratio 1:1)	Capmul MCM C8 (13.8%)	Tween 20 (16.24%)	Transcutol P (16.24%)	Water (53.72%)	10

The optimized formulations of CME 1 and CME 2 were further selected for characterization studies like, globule size, zeta potential and % Transmittance and the results along with \pm SD are mentioned in Table 3.2.6.2.

Table 3.2.6.2. Characterization of Cilostazol microemulsion systems (CME 1 and CME 2).

Formulations	S:CoS ratio	Globule size (nm) \pm SD		Zeta potential (mV) \pm SD		% Transmittance \pm SD	
		Initial	After 3 Hr.	Initial	After 3 Hr.	Initial	After 3 Hr.
		CME 1 (S: CoS ratio 3:1)	82.2 \pm 0.32	82.1 \pm 0.55	-2.48 \pm 0.46	-2.47 \pm 0.54	99.85 \pm 0.19
CME 2 (S: CoS ratio 1:1)	66.1 \pm 0.67	71.29 \pm 0.63	-4.88 \pm 0.30	-4.10 \pm 0.31	99.80 \pm 0.68	99.54 \pm 0.59	

It was observed from the result that, increase in concentration of oil phase, resulted in increase in globule size (CME 1 containing higher oil phase compare with CME 2). This may be due to fact that parts of the oil phase which increase the interfacial tension between oil and water³². The globule size and zeta potential were fairly reproducible within \pm 5 nm / \pm 1 mV range respectively for initially and after 3 Hr. Comparing globule size of CME 1 and CME 2 with varying concentrations of S:CoS mixture, it was observed that the excess amount of S:CoS mixture concentrations results in the increase in the globule size. So, it was concluded that the

excess concentration of S:CoS mixture may be critical for the formation of CME¹⁷ (as S:CoS of CME 1 is greater than CME 2). Also, ME with less globule size may have larger surface area and better absorption across the intestinal spaces. Therefore, less globule sizes (CME 2) were identified as a filter for the selection criteria for further studies.

It was also observed that increase in the aqueous phase concentration resulted an increase in the zeta potential (anionic) (Table 3.2.6.2.). Reports in the literature revealed that ME having negative charged zeta potential exhibit moderate to best physical stability in terms of phase separation¹². Therefore, ME having maximum zeta potential up to -10 mV were selected for further studies^{16,17}.

Comparing CME 1 and CME 2 for the ME region (Figure 3.2.1.2. and 3.2.1.3. respectively), the ME region obtained with Labrafil M 1944[®] was found to be wider in comparison to those obtained with Tween 20[®]. This may be attributed to the lower HLB value of Labrafil M 1944[®] which is responsible for more oil solubilization. The pH of the prepared ME systems were similar to the pH of water which proved the ME systems were stable at stomach condition. Viscosity of CME 1 and CME 2 were found to be 26.6 and 29.39 cps which were suitable for the preparation of oral liquid formulation. Both ME containing non-ionic surfactant-co-surfactant mixture, oil and water showed electroconductivity behavior in spite of its non ionic nature. From the favourable data of Viscosity and electroconductivity, it can be concluded that the ME systems were purely o/w type.

Concentrated CME 1 and CME 2 were further diluted with 10 times, 100 times and 1000 times of aqueous phase and results are mentioned in Table 3.2.2.1. and 3.2.2.2. The increase in the globule size up on dilution of CME 2 was found to be lower (105.23 ± 0.66 nm) than CME 1 (129 ± 0.65 nm)¹³. Zeta potential of CME 2 was also reduced up to -7.5 mV because with the increasing anionic phase the negative charge was also increased into the ME. Diluted MEs showed decrease in the % Transmittance (between 98.66 to 99.08 %) with increase in the globule size and they have been further evaluated for physical and chemical stability.

CME 1 and CME 2 were subjected to accelerated centrifugation for assessment of physical stability study and the results are shown in Table 3.2.3.1..The data revealed that there was no appreciable change before and after centrifugation for 15 min at accelerated conditions. Moreover, the layers from top, middle and bottom following centrifugation were sampled and analyzed to determine homogeneity. The globule size of the CMEs in top, middle and bottom

layer for CME 1 and CME 2 were within ± 5 nm from the initial values. The data clearly suggested that CME 1 and CME 2 were physically stable under the testing conditions. The MEs were selected on the basis of globule size. All the batches of MEs were having globule size less than 85 nm and zeta potential close to -2 mV or less. Microemulsions which are bicontinuous, w/o or o/w were found to be stable.

Drug retention study was performed on physically stable CME 1 and CME 2 by subjecting Cilostazol microemulsions at 30°C / 65% RH and 40°C / 75% RH. The samples were withdrawn at the period of 1, 2, 4 and 6 months respectively and were subjected to globule size, size distribution, zeta potential, percent transmittance and drug content. The data was recorded in Table 3.2.4.1. As seen from the table, globule size for both CME 1 and CME 2 were within the range of ± 5 nm from the initial values and no abnormal changes in the globule size were noticed at both the accelerated testing conditions. The zeta potential values were also found to be consistent and within the range ± 5 mV from the initial values. The data clearly indicated that the formulations were physically stable at 30°C / 65% RH and 40°C / 75% RH without noticeable change in the zeta potential values. Percent transmittances for all the experimental batches were found to be greater than 99% which indicated the clarity of the tested ME and indirectly gives an indication that no separation was observed in the Cilostazol microemulsions. Drug content for different CME formulations were found to be more than 95 %. It was concluded from the above data that the formulations were found to meet the general monograph of Pharmacopoeia and criteria stipulated therein for the liquid preparations. Physically and chemically stable CME 1 and CME 2 were further taken up for the *in vitro* diffusion studies to evaluate the potential.

In vitro diffusion studies were performed to evaluate relative diffusion behavior of different formulations of Cilostazol. Cumulative drug diffused across dialysis bag and intestinal mucosa of CME 1 and CME 2 up to 8 h have been recorded in Table 3.2.5.2 and Table 3.2.5.3. These are graphically shown in Figure 3.2.5.1.(a) and Figure 3.2.5.2.(b) respectively. As shown in the data, CME 2 was found to have substantially higher diffusion than CME 1, marketed formulation Pletoz -50 and pure Cilostazol across the dialysis bag (60.00%) and intestinal mucosa (57.32%). In all the cases higher diffusion was observed by using dialysis bag technique because an active membrane of intestine is NOT a simple bag holding cell parts but the anchorage site for many enzymes, coenzymes and receptors which will effect the rate of diffusion through membrane. The mechanism of drug diffusion was also predicted by inputting

the regressed data into the excel spread sheet and the result are recorded in Table 3.2.5.4. and Table 3.2.5.5. It was found that all MEs, marketed formulation (Pletoz-50) and pure drug follow Higuchi's kinetics whereas, the regression coefficient values were found less for zero-order and first-order compared to Higuchi's kinetic fit²³. On comparing Cilostazol solution and marketed formulation (Pletoz – 50) with optimized Cilostazol microemulsion (CME 2), it was observed that microemulsion showed better drug diffusion compared to marketed formulation and drug solution (Table 3.2.5.2 and Table 3.2.5.3.). Cilostazol microemulsion (CME 2) showed 2.85-fold higher diffusion compared to marketed formulation (Pletoz – 50) and 6.58-fold higher diffusion compared to Cilostazol solution (Figure 3.2.5.2. (a)) by dialysis bag study and 2.88-fold higher diffusion compared to marketed formulation (Pletoz–50) and 7.49-fold higher diffusion compared to Cilostazol solution (Figure 3.2.5.2.(b)) by intestinal permeability study. This may be attributed to the fact that microemulsion enhances transport of drug across mucosa³².

It can be concluded that, *in vitro* diffusion study across the dialysis bag and intestinal mucosa may be a reasonable tool for comparative evaluation of different formulations. The non linearity of percent drug diffused vs. time graphs suggested that the diffusion pattern does not follow zero order kinetics³³. However, the correlation coefficients indicated that Higuchi's model was found to be the best-fit curve for all the tested formulations. This may be attributed to the fact that the systems tested has reservoir compartment, dialysis bag and intestinal mucosa as a barrier or controlling membrane hence, the drug diffusion will more mimic and closer to reservoir system rather than zero-order or first-order (concentration gradient) diffusion³⁴.

It was observed from the results of characterization and evaluation for CME 1 and CME 2, CME 2 showed less globule size and low zeta potential as compared to CME 1. The viscosity, pH, % Transmittance and Conductivity data were found to be suitable for oral delivery of Cilostazol. In vitro diffusion study supported the fact that CME 2(1:1 S: CoS ratio) is more convincing formulation for oral drug delivery then all tested formulations and hence, CME 2 was selected for in vivo pharmacokinetic study.

3.2.7. References

1. Shinoda K, Araki M, Sadaghiani M, Khan A, Lindman B. Lecithin based microemulsions: phase behavior and microstructure. *J. Phys. Chem.* 1991; 95:989-993.
2. Shinoda K, Friberg S. Microemulsions. Colloidal aspects. *Adv. Colloid Interface Sci.* 1975; 4:281-300.
3. Shinoda K, Kunieda H. Conditions to produce so-called microemulsions. Factors to increase the mutual solubility of oil and water by solubilizer. *J. Colloid Interface Sci.* 1973; 42:381-387.
4. Lawrence JM, Rees GD. Microemulsion-based media as novel drug delivery systems. *Adv. Drug Deliv. Rev.* 2000; 45:89-121
5. Constantinides PP, Scalart JP, Lancaster C, et al. Formulation and intestinal absorption enhancement evaluation of water in oil microemulsion incorporating medium chain glycerides. *Pharm Res.* 1994;11(10):1385-1390.
6. Beskid G, Unowsky J, Behl CR, et al. Enteral, oral and rectal absorption of ceftriaxone using glyceride enhancers. *Chemotherapy.* 1988;84:77-84.
7. Plain KJ, Phillips AJ, Ning A. The oral absorption of cefoxitin from oil and emulsion vesicles in rats. *Int. J. Pharm.* 1986;33:99- 104.
8. Hauser B, Meinzer A, Posanski U, Richter F. Cyclosporin emulsion composition. GB patent application 2 222 770. March 21, 1990.
9. Skodvin T, Sjoblem J, Saeten J O, Gestblom B. Solubilizations of drugs in microemulsions as studied by dielectric spectroscopy. *J. Colloid Interface Sci.* 1993; 155:392-401.
10. Lawrence JM, Rees GD. Microemulsion-based media as novel drug delivery systems. *Adv. Drug Deliv. Rev.* 2000; 45:89-121
11. Prince LM. A theory of aqueous emulsion. I. Negative interfacial tension at the oil/water interface. *J. Colloid Interface Sci.* 1967; 23:165-173.
12. Roland I, Piel G, Delattre L, Evrard B. Systemic characterization of oil-in-water emulsions for formulation design. *Int. J. Pharm.* 2003; 263:85-94.

13. P. K. Ghosh, R. J. Majethia, M. L. Umrethia and R. S. R. Murthy, Design and Development of Microemulsion Drug Delivery System of Acyclovir for Improvement of Oral Bioavailability, *AAPS Pharm.Sci.Tech.* 2006; 7 (3): E1 –E6.
14. Kaler EW, Prager S. A model of dynamic scattering by microemulsions. *J. Colloid Interface Sci.* 1982; 86:359-369
15. Kantaria S, Rees GD, Lawrence JM. Gelatin-stabilized microemulsion-based organogels: rheology and application in iontophoretic transdermal drug delivery. *J. Control Release* 1999; 60:355-365.
16. Block LH. Pharmaceutical emulsions and microemulsions. In: Lieberman HA, Rieger MM, Banker GS. (Second edition, Revised and Expanded). *Pharmaceutical Dosage Forms.* 2001(1): 47-110.
17. Nash RA. 2001. Pharmaceutical suspensions. In: Lieberman HA, Rieger MM, Banker GS. (Second edition, Revised and Expanded). *Pharmaceutical Dosage Forms.* 1:1-47
18. Khoshnevis P, Mortazavi SA, Lawrence MJ, Aboofazil R. *In vitro* release of sodium salicylate from water-in-oil phospholipids microemulsions. *J. Pharm. and Pharmacol.* 1997; 49(S4):47.
19. Koziara JM, Lockman PR, Allen DD, Mumper RJ. In situ blood-brain barrier transport of Nanoparticles. *Pharm. Res.* 2003; 20(11):1772-1778.
20. Gavini E, Rassu G, Sanna V, Cossu M, Giunchedi P. Mucoadhesive microspheres for nasal administration of an antiemetic drug, metoclopramide: in-vitro/ex-vivo studies. *J. Pharm. And Pharmacol* 2005; 57(3):287-294.
21. Akiyama Y., Nagahara N., Kashihara T., Hirai S., Toguchi H. In vitro and in vivo evaluation of Mucoadhesive microspheres prepared for the gastrointestinal tract using polyglycerol esters of fatty acids and poly (acrylic acid) derivatives. *Pharm. Res.* 1995; 12:397-405.
22. Aspden T.J., Adler J., Davis S.S., Skaugrud Q., Illum L. Chitosan as a nasal delivery system: evaluation of the effect of chitosan on mucociliary clearance rates in the frog palate model. *Int. J. Pharm.* 1995; 122:69-78.

-
23. Higuchi T. Rate of release of medicaments from ointment bases containing drugs in suspension. *J. Pharm. Sci.* 1961; 50:874-875.
 24. Ho J. K., Kyung. A. Y., Mikyoung H., Eun S. P., and Sang C. C., Preparation and In-vitro evaluation of self-microemulsifying drug delivery system containing Idebenone, *Drug Dev. and Ind. Pharmacy*, 2000, 26(5), 523-529.
 25. Pradeep P., Prasad J. and Anant P. Effect of formulation variables on preparation and evaluation of Gelled Self Microemulsifying drug delivery system of Ketoprofen, *AAPS Pharm. Sci. Tech.* 2004, 5(3), 1-8.
 26. Smith P. Method for evaluating intestinal permeability and metabolism *in vitro*. *Pharm. Biotech.* 1996, 8, 13-34.
 27. Gupta P.K., Leung S.H.S., Robinson J.R. Bioadhesives/Mucoadhesives in drug delivery to the gastrointestinal tract. In: Lenaerts V, Gurny R. (Eds.), *Bioadhesive Drug Delivery Systems*, CRC Press, Boca Raton, FL, 1990; 65-92.
 28. Morimoto K., Morisaka K., Kamada A. Enhancement of nasal absorption of insulin and calcitonin using polyacrylic acid gel. *J. Pharm. Pharmacol.* 1985; 37(2):134-136.
 29. Lianli L, Nandi I, Kim KH. Development of an ethyl laurate-based microemulsion for rapid-onset intranasal delivery of diazepam. *Int. J. Pharm.* 2002; 237:77-85.
 30. Zhang Q, Jiang X, Xiang W, Lu W, Su L, Shi Z. Preparation of nimodipine-loaded microemulsion for intranasal delivery and evaluation of the targeting efficiency to brain. *Int. J. Pharm.* 2004; 275:85-96.
 31. Attwood D. Microemulsions, University of Manchester, Manchester, U.K.
 32. Lawrence MJ, Rees GD. Microemulsion-based media as novel drug delivery systems. *Adv. Drug Del. Rev.* 2000; 45:89-121.
 33. Vincent HL, Robinson RJ. In *Controlled Drug Delivery*, Marcel Dekker, Inc. New York and Basel, 1995; 99.
 34. Swardick J, Boylan JC. Mucosal Adhesive Preparation. *Encyclopedia of Pharmaceutical Technology*, Vol. 10, Marcel and Dekker Inc., NY, 1994; 144.

3.3.1. Preparation of Inclusion Complexes :

An inclusion complex is a unique form of inclusion chemical complex. Here one molecule is enclosed within another molecule or structure of molecules. The combination is characterized by absence of ordinary chemical bonds, the essential criteria is that enclosed molecule or guest should be of a suitable size and shape to fit into a cavity within a solid structure formed by a host molecule. The stereochemistry of host and guest molecules determines whether the inclusion complex can occur. These noncovalent complexes show new physicochemical characteristics when complexes with the guest molecule. They include better stability, higher aqueous solubility, increased bioavailability and less undesirable side effects.¹⁻⁴.

3.3.1.1. Material and Reagents :

Cilostazol was generously provided by Cadila Pharmaceutical Laboratory, Ahmedabad as a gift sample. β -Cyclodextrin (β -CD) was purchased from Hi-media Laboratories Pvt. Ltd. Mumbai. Hydroxy propyl β -Cyclodextrin (HP- β -CD) was obtained as a gift sample from Sun Pharma Advance Research Company, Vadodara. γ -Cyclodextrin (γ -CD) and Dimethyl- β -Cyclodextrin (DM- β -CD) were procured as a gift samples from Roquette Pharma, U.S.A. Methanol and Chloroform (HPLC grade, S.D. Fine Chemical, Bombay, India), and, triple distilled water were used in the study.

3.3.1.2. Preparation of Cilostazol Inclusion Complexes :

The cyclodextrins(CDs) used for the preparation of inclusion complexes were β -CD, γ -CD, HP- β -CD and DM- β -CD. Cilostazol-CDs inclusion complexes were prepared in 1:1, 1:2 and 1:3 molar ratios by using two different method (1) Kneading Method and (2) Coprecipitation method and compared with physical mixtures of Cilostazol-CDs⁵.

(1) Physical Mixture :

The physical mixture was prepared by mixing of pulverized powder of drug and different CDs like, β -CD and γ -CD and derivatives of β -CD like, HP- β -CD and DM- β -CD in different drug-CD ratios like, 1:1, 1:2 and 1:3 then passed through sieve mesh # 100 and stored in dessicator until further evaluation.

(2) Kneading Method :

A paste containing one part of drug and 3 parts of any one CD like, β -CD, γ -CD, HP- β -CD and DM- β -CD was introduced in to a kneading machine with progressive addition of the drug. The paste was mixed for 1 hr. The viscosity of the mixture increased indicating the formation of the complex. Auxiliary step involved washing the paste with solvent and water

followed by filtration. Finally the paste was dried in an oven at 45 °C until dry. The paste was ground to get a fine powder and passed through sieve mesh # 100. All the prepared inclusion complexes were stored in dessicator until further evaluation.

(3) Co – precipitation method :

In this method, an organic solution of the drug was poured under agitation into an aqueous solution of CD with contentious stirring. Sometime it was required to use a hot solution of CD and maintaining the temperature during agitation.

A solid inclusion complex was obtained either spontaneously or after evaporation of excess solvent. After the precipitation step, the inclusion complex was thoroughly washed with solvent and water, filtered and dried to get a pure inclusion complex. Finally dried complex was passed through sieve mesh # 100 and stored in desiccator until further evaluation.

3.3.2. Characterization of prepared Cilostazol-Cyclodextrins

Inclusion Complexes

Prepared CDs inclusion complexes of Cilostazol were further characterized by Phase solubility Study, Inclusion efficiency study, IR Spectroscopy study, Differential scanning calorimetry study and X-ray powder diffraction study.

3.3.2.1. Phase solubility study :

The phase solubility of Cilostazol was conducted according to Higuchi and Connors⁶. An excess amount of Cilostazol (50 mg) was added to 5 mL of water or aqueous solutions of CDs and its derivatives (10 – 50 mM/L) individually in 10 mL stoppered glass tubes, and the tubes were shaken for 24 h at 50 cycle/min in a water bath at $37 \pm 0.5^\circ \text{C}$. At equilibrium after 2 days, aliquots were withdrawn, filtered (0.45- μm cellulose nitrate filters) and suitably diluted. Concentration of Cilostazol was determined spectrophotometrically. The phase solubility study was further carried out in HCl buffer pH1.2 and Phosphate buffer pH 6.8.

A plot of total molar concentration of the drug against the total molar concentration of CDs gave phase-solubility diagrams from where the apparent solubility constant, K_C were calculated for all the pH values using their regression lines to the following equation.

$$\text{Stability constant } (K_C) = \frac{\text{Slope}}{S_0(1 - \text{Slope})}$$

Where S_0 is the intrinsic solubility of the drug studied under the conditions^{7,8,9}.

3.3.2.2. Inclusion efficiency study :

All inclusion complexes of Cilostazol and their physical mixtures (25 mg) were taken in 25 ml volumetric flasks. 10 mL of methanol was added to it, mixed thoroughly and sonicated it for 30 min at ambient temperature. The volume was made up to mark with methanol. The solution was suitably diluted with methanol to get the concentration of 10 μg of drug per ml of solution and spectrophotometrically assayed for drug content at 257.00 nm. Inclusion efficiency was calculated using the formula:-

$$\text{Inclusion efficiency} = (\text{estimated \% drug content} / \text{theoretical \% drug content}) \times 100$$

3.3.2.3. IR spectroscopy study :

The IR spectra were obtained using a Shimadzu FTIR-8400S spectrophotometer with IR solution software (Shimadzu). The samples were prepared by grinding a small amount of the dried sample and the corresponding amount of potassium bromide (2/98 w/w). in an agate

mortar. Data were collected over a spectral region from 4000 to 650 cm^{-1} with resolution 4 cm^{-1} and 100 scans.

3.3.2.4. Differential scanning calorimetry :

Differential scanning calorimetry (DSC) analysis was performed for pure Cilostazol, pure CDs and its derivatives, physical mixtures of drug-CDs and inclusion complexes using a Shimadzu DSC (Model DT-60) instrument. Samples (0.5-1.0 mg) were weighed on Shimadzu libror AEG 220 electronic balance and transferred to the aluminium boat, crimped and hermetically sealed by using crimping machine. An empty aluminium boat was used as reference. Samples were heated in sealed aluminium boat at a rate of $10^{\circ}\text{C}/\text{min}$ in a $0-400^{\circ}\text{C}$ temperature range under nitrogen stream. The analysis was repeated after cooling down to temperature in order to estimate the DSC baseline. The instrument was calibrated using indium (melting point, 156.61°C ; enthalpy of fusion, 28.71 J/g)^{5,10}.

3.3.2.5. X-ray powder diffraction study :

X- diffraction pattern (XRD) of pure Cilostazol, pure CDs and its derivatives, physical mixtures of drug-CDs and inclusion complexes were collected with a PW1701 diffractometer at 30 mA and 40 KV using $\text{Cu K}\alpha$ radiation and equipped with a graphite monochromator on the diffracted beam. The powdered samples (a fraction of 100 – 180 μm sieved powder) were deposited on an adhesive support and placed in the diffractometer. XRD pattern were recorded in step scan mode in the range $3^{\circ} \leq 2\theta \leq 60^{\circ}$ with step size 0.06. The scanning rate employed was $1^{\circ} \text{ min}^{-1}$ over the $0-100^{\circ}$ diffraction angle (2θ) range. The divergence and receiving slits were chosen in order to ensure a high resolution mode for the crystalline phases¹¹.

3.3.2.1. Phase solubility diagrams of Cilostazol (Each point represent the mean of 5 experiments).

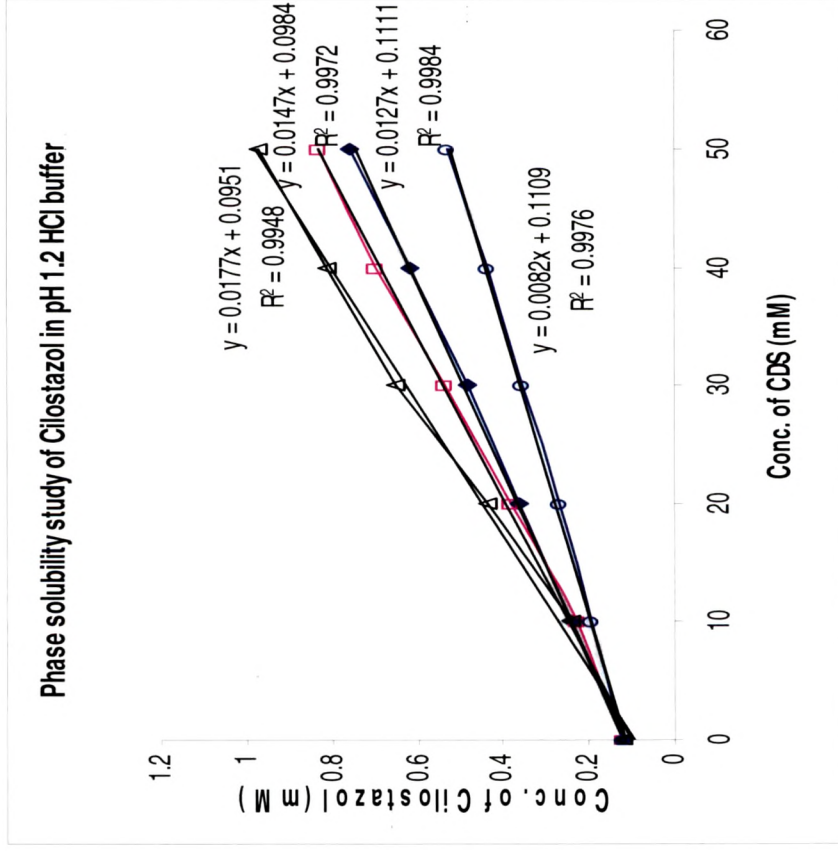


Figure 3.3.2.1.1. Phase solubility study of Cilostazol in 1.2 pH HCl at 257.2 nm. Key (Δ) DM-β-CD; (□) HP-β-CD; (○) β-CD; (◇) γ-CD; (◊) HP-γ-CD.

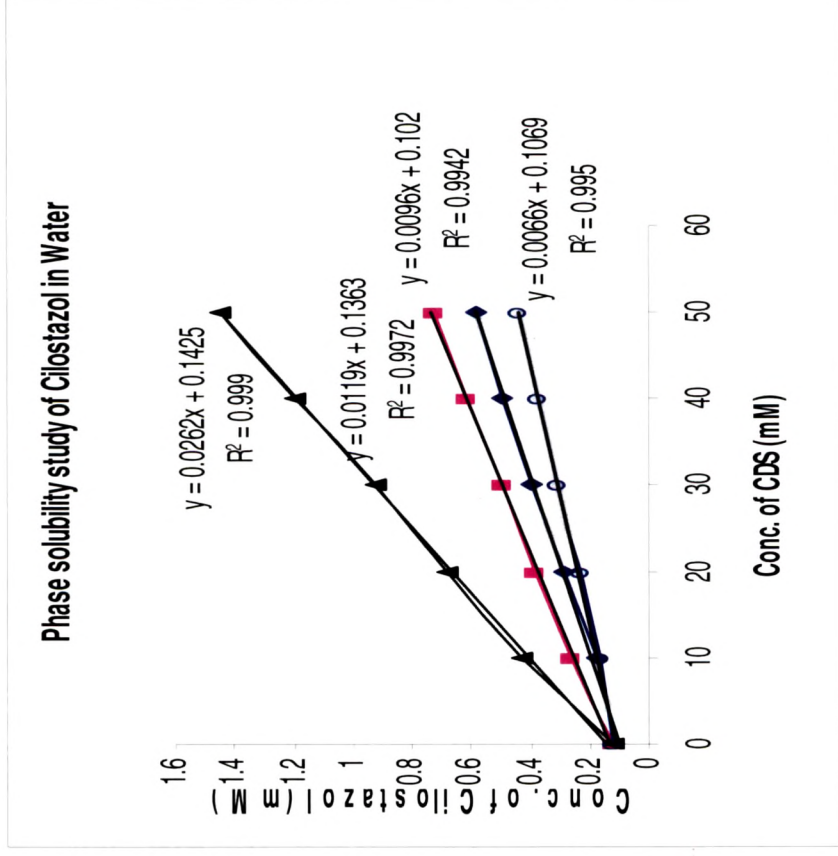


Figure 3.3.2.1.2. Phase solubility study of Cilostazol in Water at 257.00 nm. Key (▲) DM-β-CD; (■) HP-β-CD; (○) β-CD; (◇) γ-CD; (◊) HP-γ-CD.

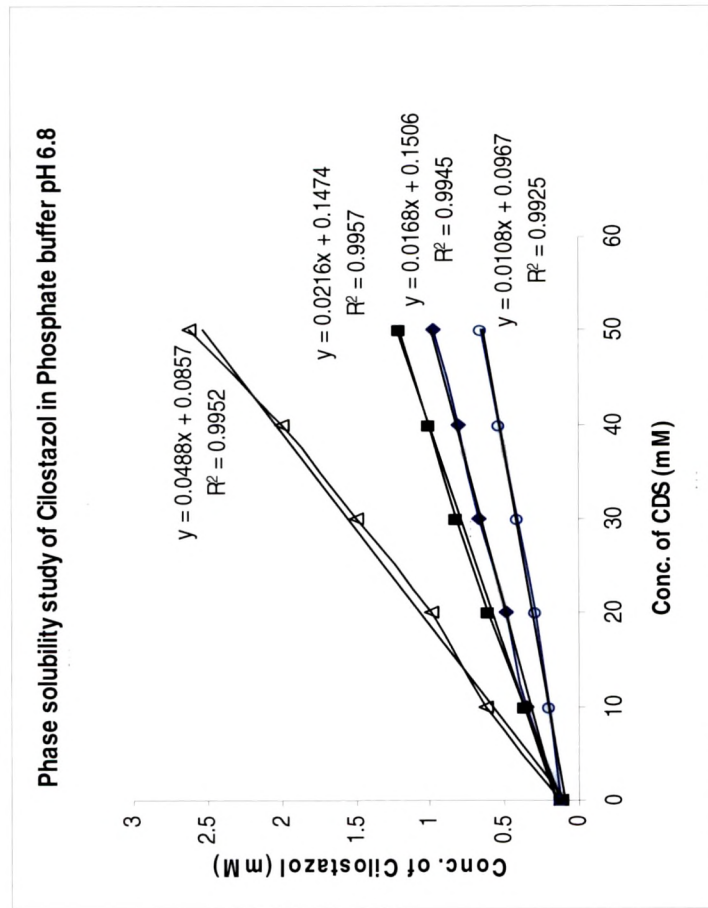


Figure 3.3.2.1.3. Phase solubility study of Cilostazol in Water at 257.8 nm. Key (Δ) DM- β -CD; (\blacksquare) HP- β -CD; (\blacklozenge) β -CD; (\circ) γ -CD.

Table 3.3.2.1.1. Apparent Inclusion complex Stability constant (Kc) of Cilostazol with different CDs at 37 °C and types of phase solubility curve for Cilostazol with various CDs at different pH solutions.

CDs	Cilostazol			
	Solutions	K 1:1 [M ⁻¹] ± SD	R ²	Type of Curve
B-CD	HCl buffer pH 1.2	105.367 ± 7	0.9984	A _L
	Water	79.89 ± 5	0.9942	A _L
γ-CD	Phosphate buffer pH 6.8	138.804 ± 11	0.9945	A _L
	HCl buffer pH 1.2	68.34 ± 6	0.9976	A _L
	Water	55.09 ± 4	0.995	A _L
	Phosphate buffer pH 6.8	89.77 ± 8	0.9925	A _L
HP-β-CD	HCl buffer pH 1.2	121.713 ± 11	0.9972	A _L
	Water	101.81 ± 13	0.9972	A _L
	Phosphate buffer pH 6.8	177.591 ± 15	0.9957	A _L
DM-β-CD	HCl buffer pH 1.2	146.106 ± 17	0.9948	A _L
	Water	214.3997 ± 20	0.999	A _L
	Phosphate buffer pH 6.8	390.071 ± 35	0.9952	A _L

3.3.2.2. Inclusion efficiency study.

Table 3.3.2.2.1. Inclusion efficiency data for Cilostazol- β -CD Inclusion complex.

Cilostazol- β -CD(w/w)	Inclusion efficiency \pm SD [#]	%RSD [#]
1:1	75.2 \pm 2.12	2.16
1:2	87.4 \pm 2.23	2.29
1:3	98.9 \pm 1.22	1.23
1:1*	55.5 \pm 1.50	1.51
1:2*	61.6 \pm 0.8	1.05
1:3*	68.5 \pm 1.2	1.3

mean of three determinations

*physical mixture

Table 3.3.2.2.2. Inclusion efficiency data for Cilostazol - γ -CD Inclusion complex.

Cilostazol- γ -CD(w/w)	Inclusion efficiency \pm SD [#]	%RSD [#]
1:1	69.2 \pm 0.92	1.36
1:2	80.4 \pm 0.83	1.89
1:3	99.4 \pm 2.06	2.23
1:1*	49.0 \pm 1.53	1.81
1:2*	58.9 \pm 0.85	1.55
1:3*	67.5 \pm 1.72	0.83

mean of three determinations

*physical mixture

Table 3.3.2.2.3. Inclusion efficiency data for Cilostazol – HP-β-CD Inclusion complex.

Cilostazol-HP-β-CD (w/w)	Inclusion efficiency ± SD[#]	%RSD[#]
1:1	67.6 ± 2.32	1.31
1:2	83.94 ± 1.66	2.39
1:3	98.9 ± 0.81	1.69
1:1*	57.50 ± 1.23	1.91
1:2*	79.1 ± 1.35	1.55
1:3*	84.7 ± 1.92	1.23

mean of three determinations

*physical mixture

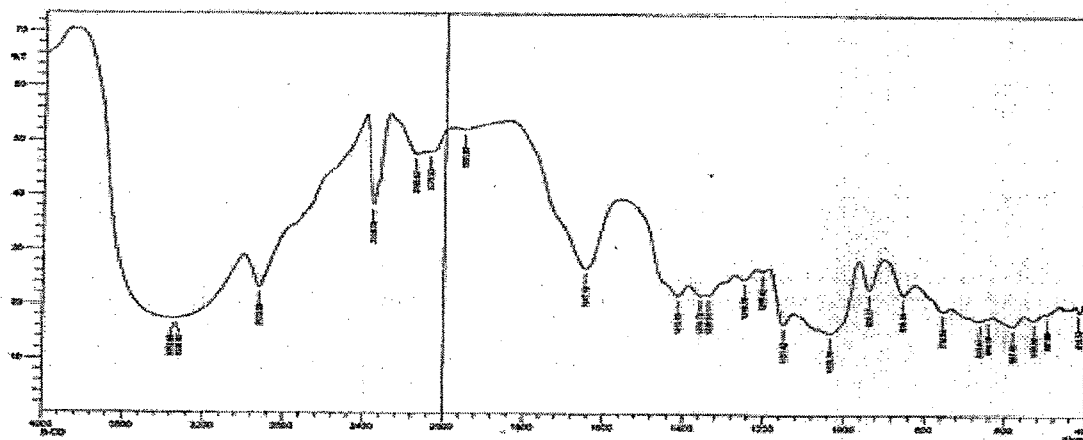
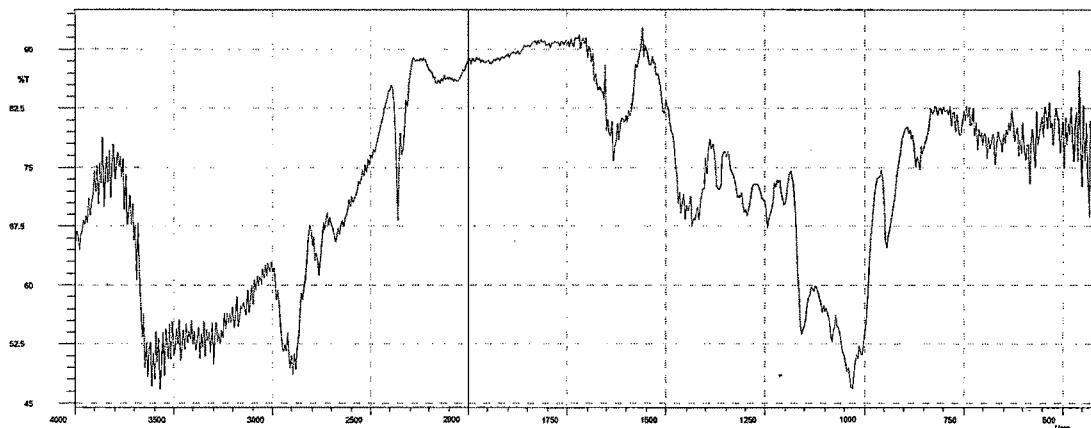
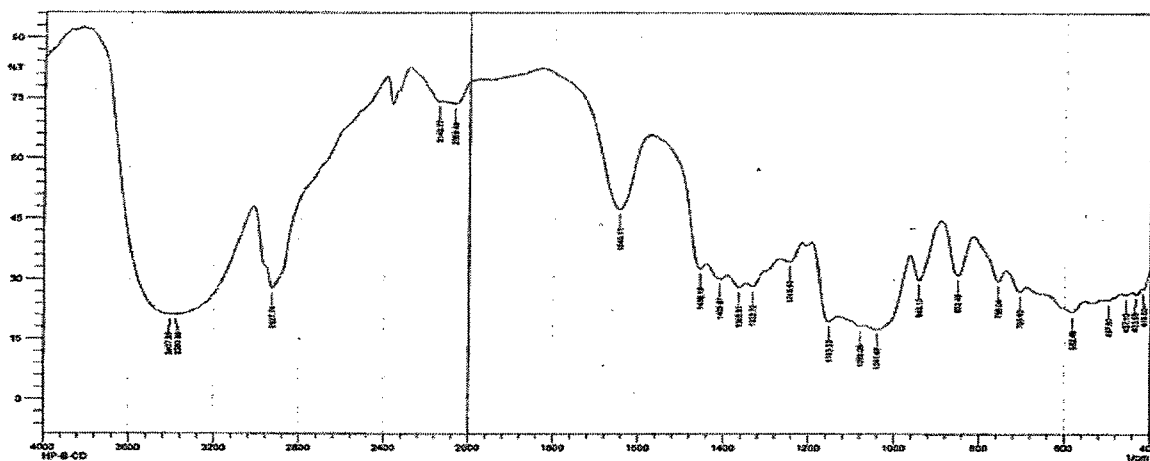
Table 3.3.2.2.4. Inclusion efficiency data for Cilostazol – DM-β-CD Inclusion complex.

Cilostazol-DM-β-CD (w/w)	Inclusion efficiency ± SD[#]	%RSD[#]
1:1	77.2 ± 1.12	1.96
1:2	89.4 ± 1.33	1.89
1:3	99.64 ± 1.86	1.73
1:1*	68.7 ± 0.50	2.51
1:2*	79.3 ± 0.45	1.65
1:3*	88.9 ± 0.2	2.39

mean of three determinations

*physical mixture

3.3.2.3. IR Spectrum of CDs, Physical mixtures and Inclusion complexes of Cilostazol.

Figure 3.3.2.3.1. IR Spectrum of Pure β -CD.Figure 3.3.2.3.2. IR Spectrum of Pure γ -CD.Figure 3.3.2.3.3. IR Spectrum of Pure HP- β -CD.

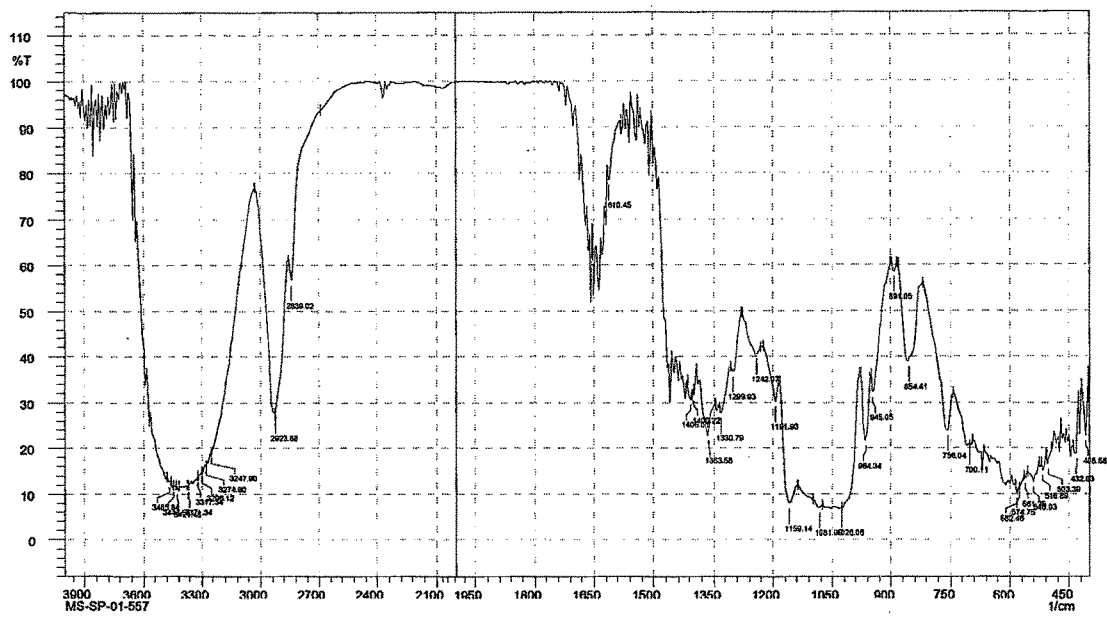


Figure 3.3.2.3.4. IR Spectrum of Pure DM- β -CD.

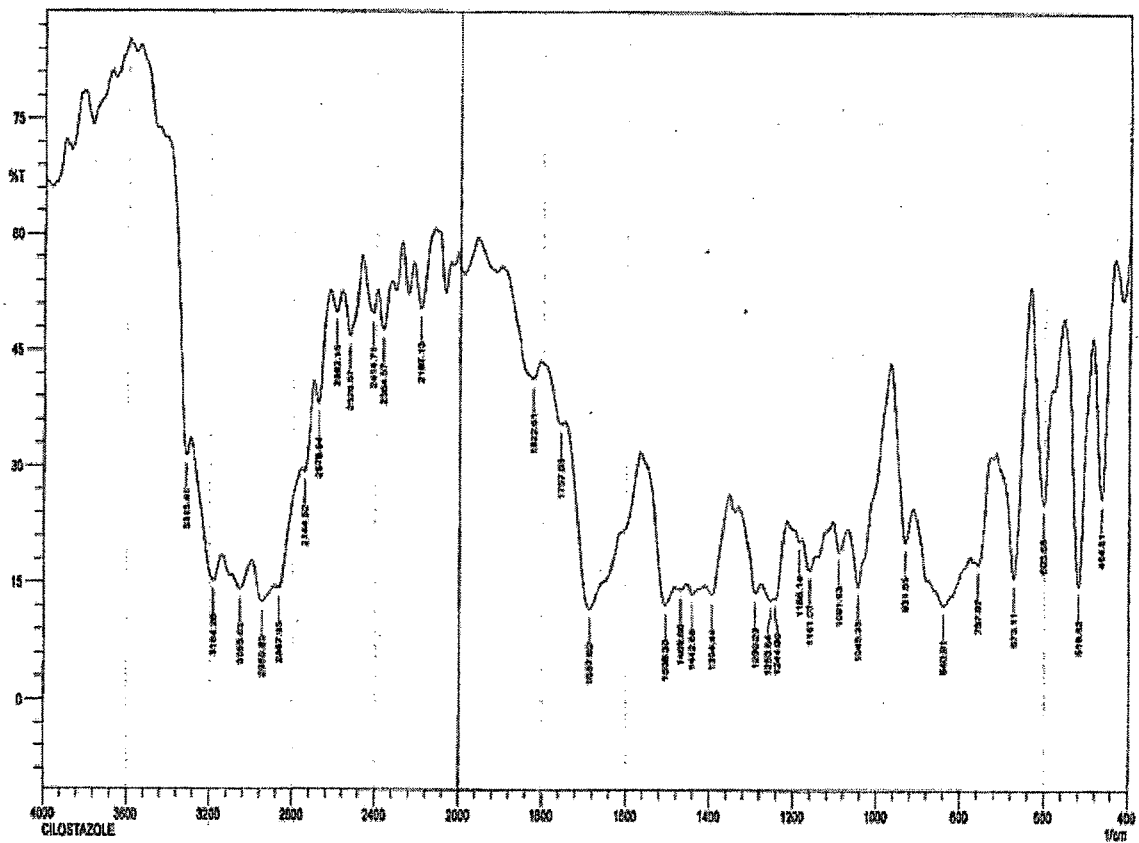
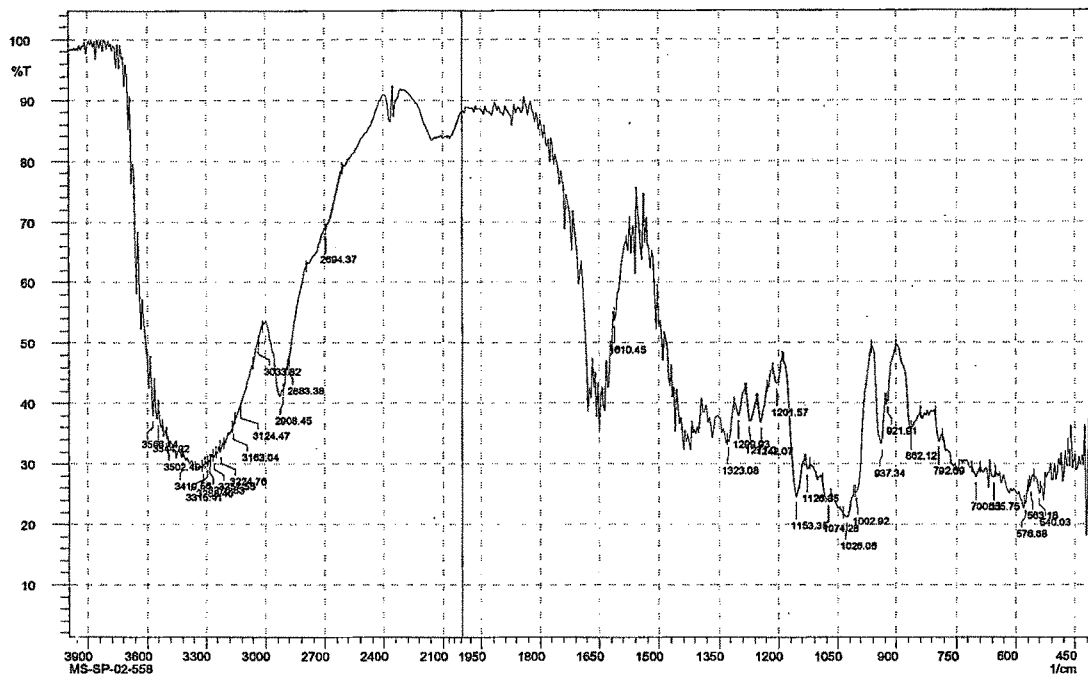
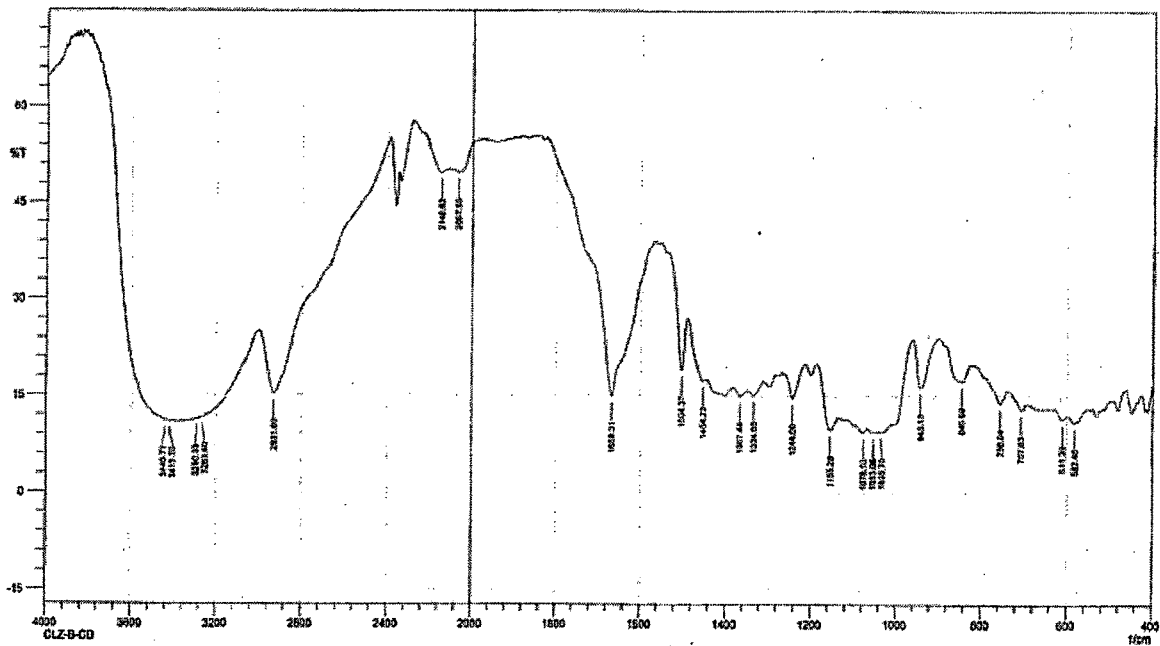
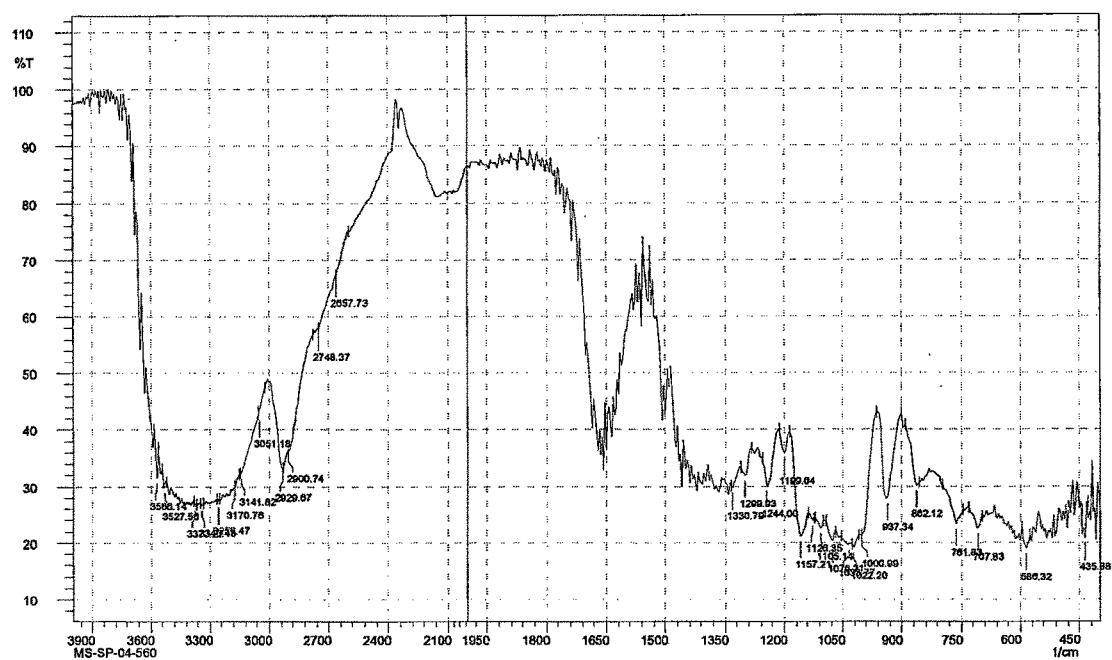
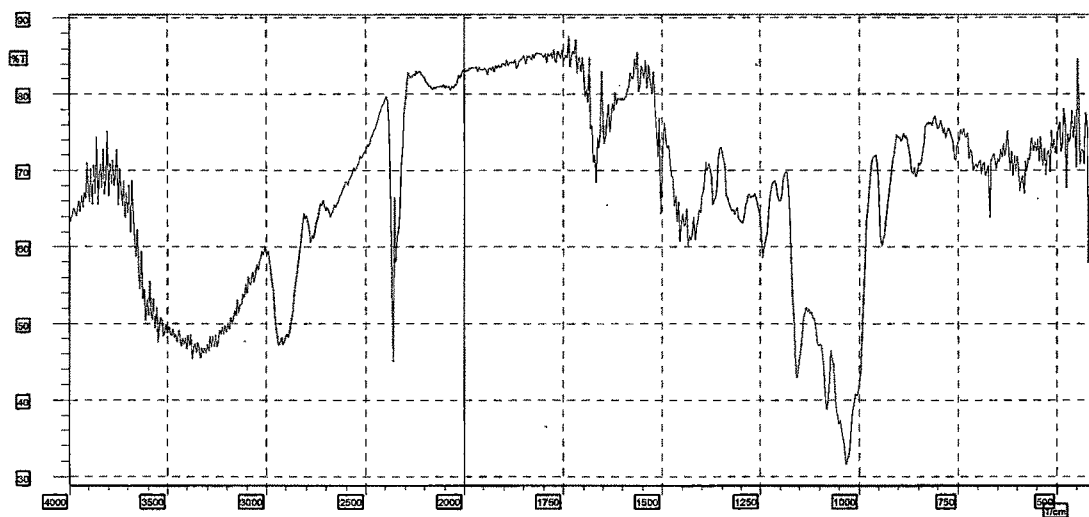


Figure 3.3.2.3.5. IR Spectrum of Pure Cilostazol.

Figure 3.3.2.3.6. IR Spectrum of β -CD-Cilostazol physical mixture(3:1).Figure 3.3.2.3.7. IR Spectrum of β -CD-Cilostazol inclusion complex(3:1).

Figure 3.3.2.3.8. IR Spectrum of γ -CD-Cilostazol physical mixture(3:1).Figure 3.3.2.3.9. IR Spectrum of γ -CD-Cilostazol inclusion complex(3:1).

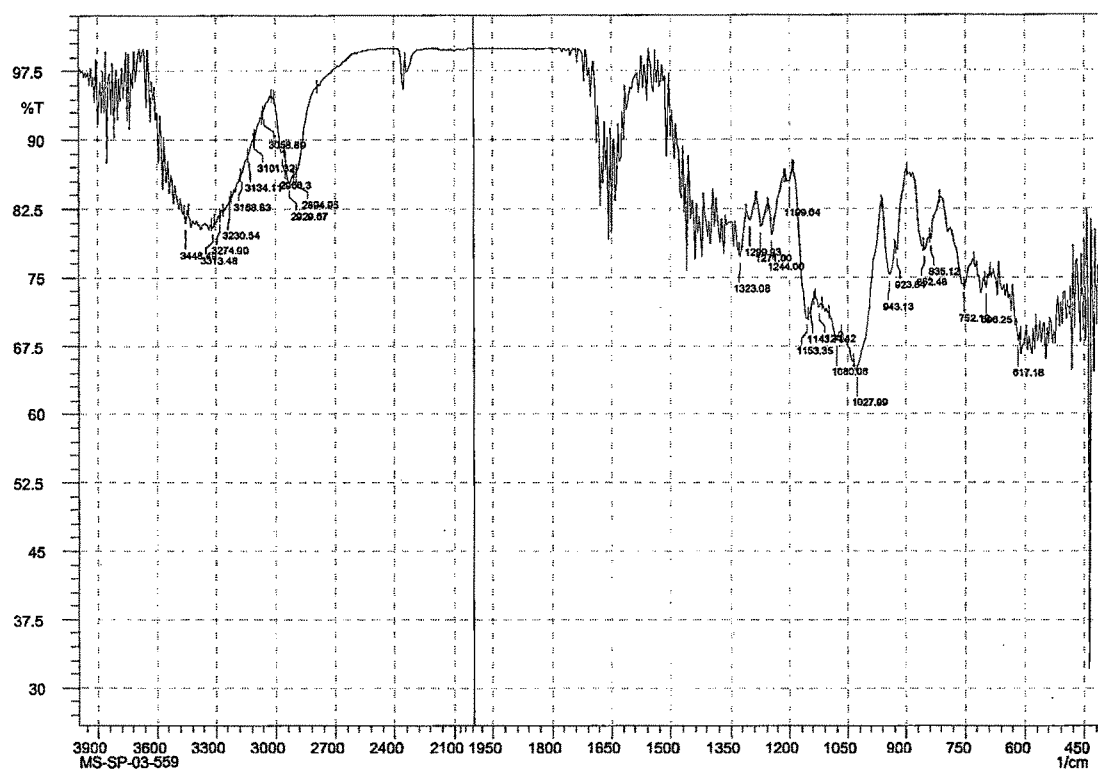


Figure 3.3.2.3.10. IR Spectrum of HP-β-CD-Cilostazol physical mixture(3:1).

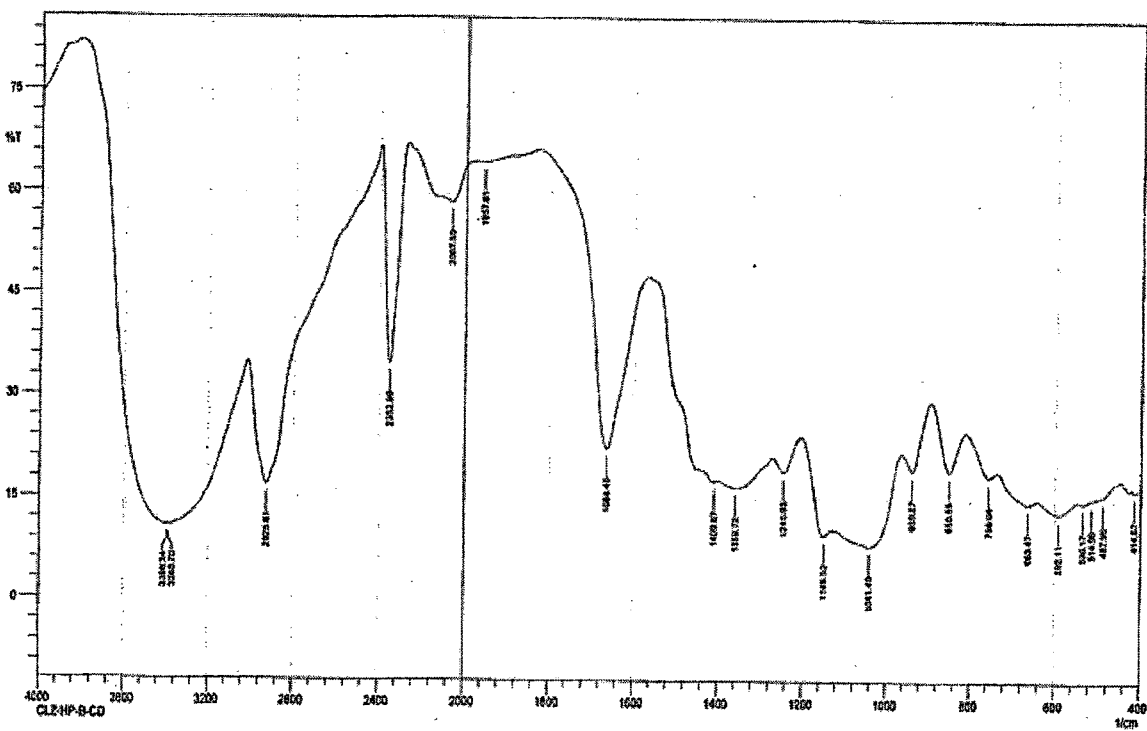


Figure 3.3.2.3.11. IR Spectrum of HP-β-CD-Cilostazol inclusion complex(3:1).

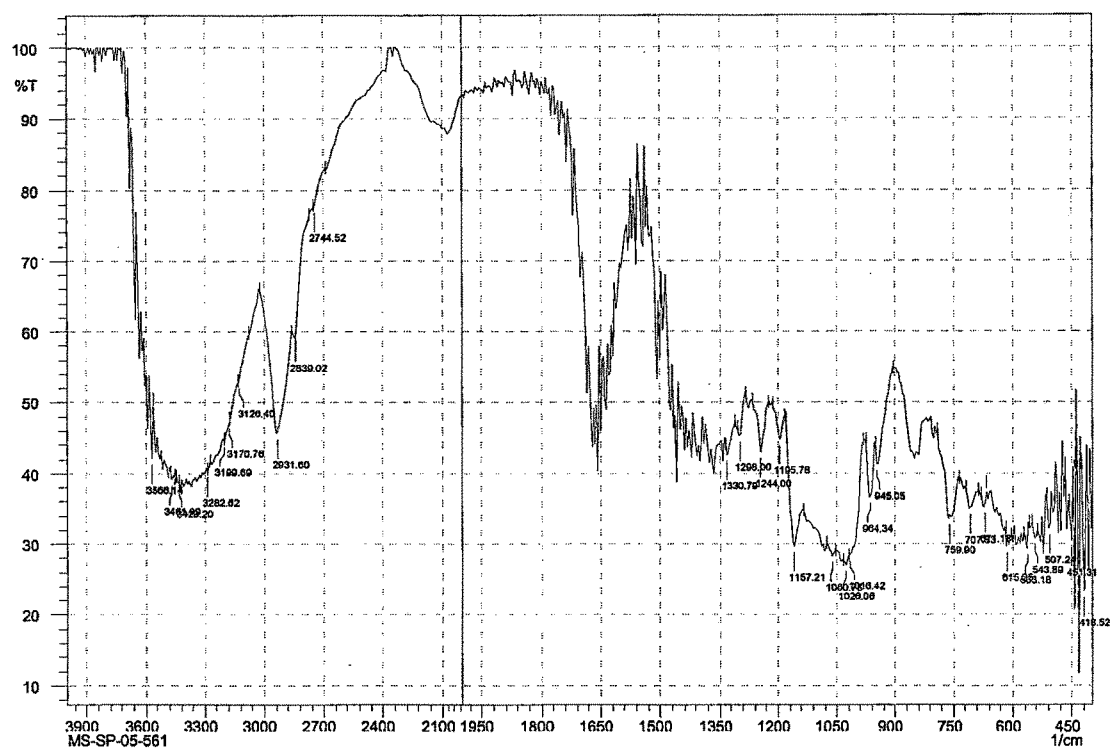


Figure 3.3.2.3.12. IR Spectrum of DM-β-CD-Cilostazol physical mixture(3:1).

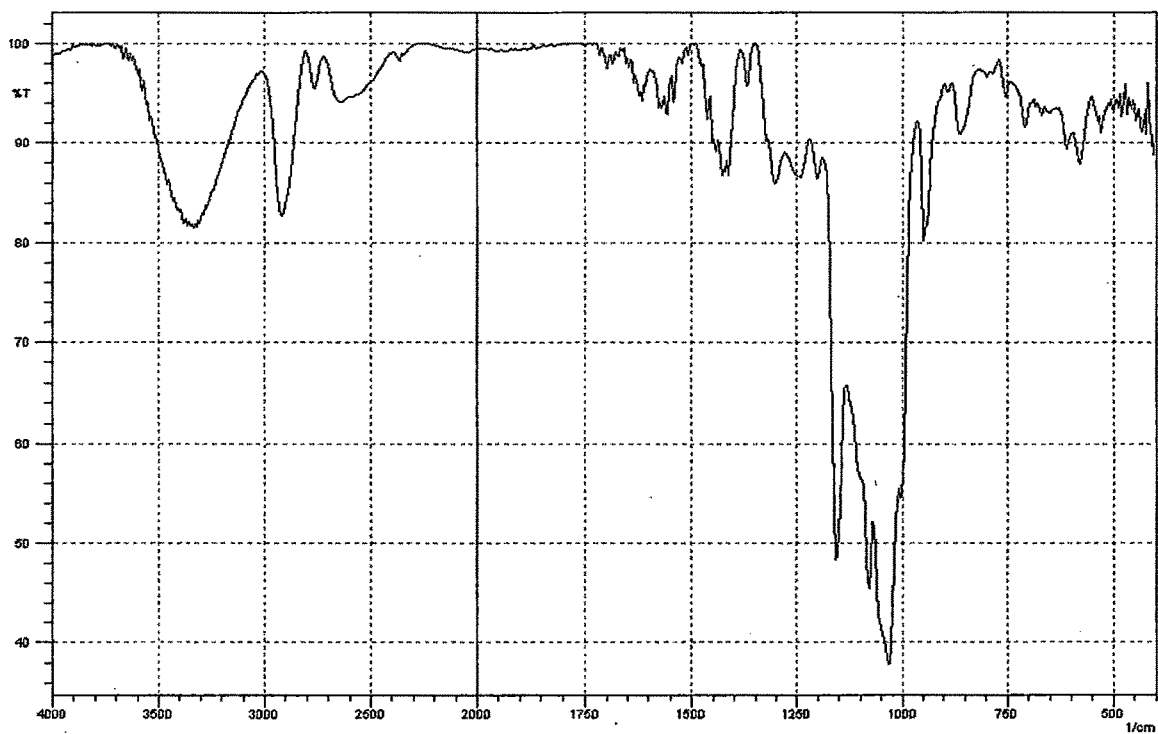


Figure 3.3.2.3.13. IR Spectrum of DM-β-CD-Cilostazol inclusion complex(3:1).

3.3.2.4. DSC thermograms of Cilostazol, CDs, its Physical mixtures and its Inclusion complexes.

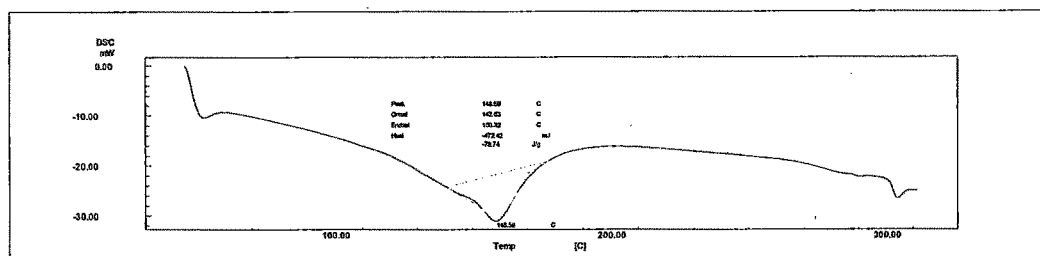


Figure 3.3.2.4.1. DSC thermogram of pure β -CD.

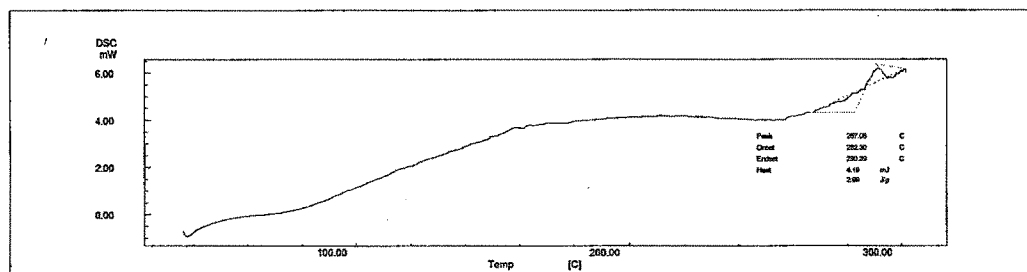


Figure 3.3.2.4.2. DSC thermogram of pure γ -CD.

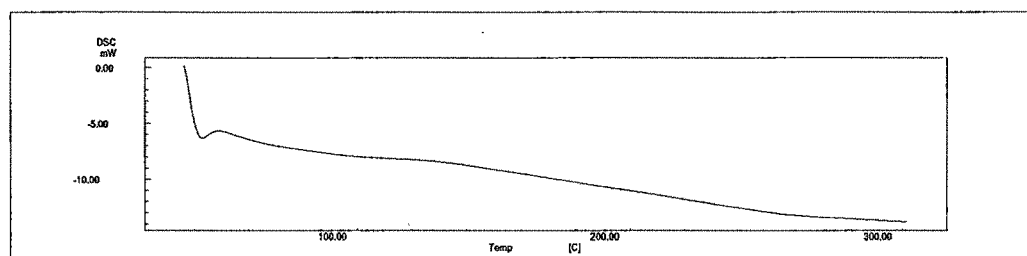


Figure 3.3.2.4.3. DSC thermogram of pure HP- β -CD.

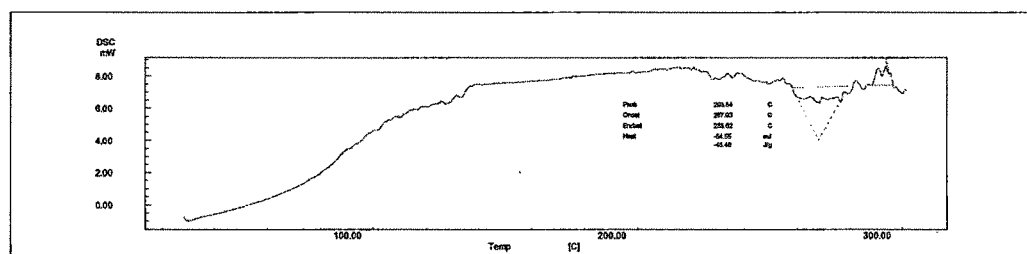


Figure 3.3.2.4.4. DSC thermogram of pure DM- β -CD.

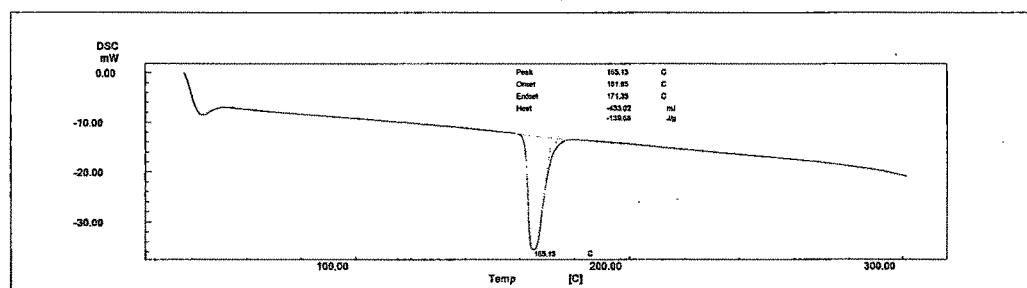
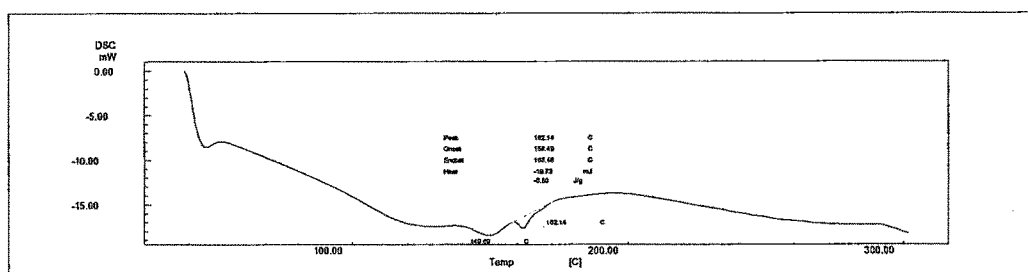
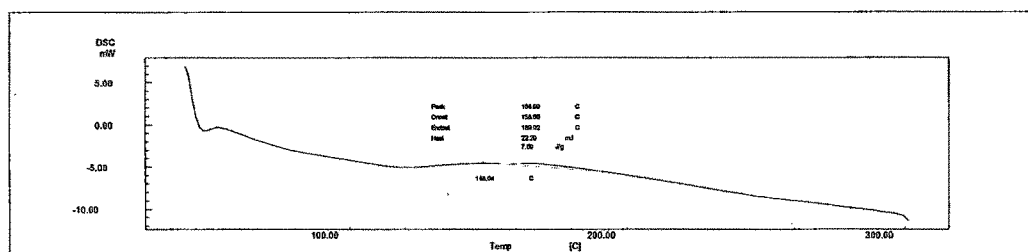
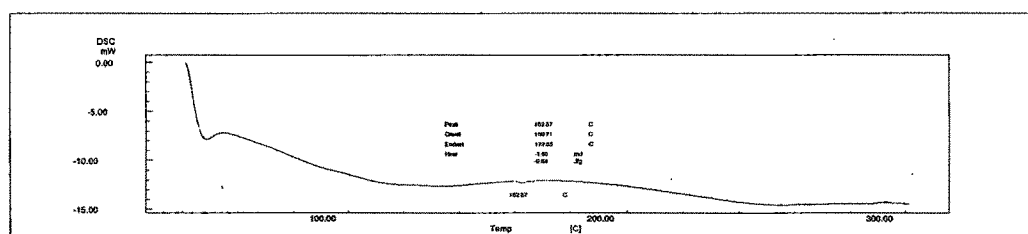
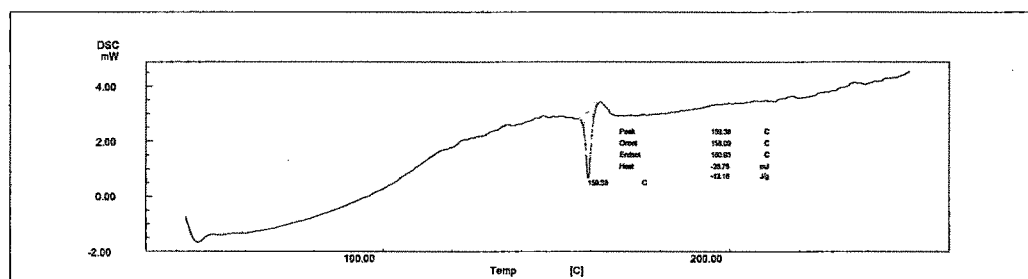
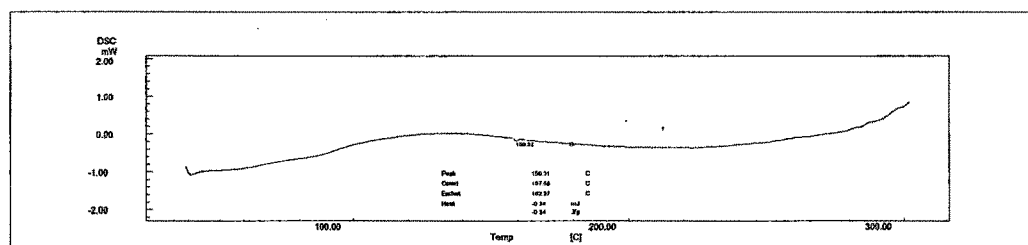


Figure 3.3.2.4.5. DSC thermogram of pure Cilostazol.

Figure 3.3.2.4.6. DSC thermogram of β -CD-Cilostazol physical mixture (3:1).Figure 3.3.2.4.7. DSC thermogram of β -CD-Cilostazol Inclusion complex by co-precipitation method (3:1)Figure 3.3.2.4.8. DSC thermogram of β -CD-Cilostazol Inclusion complex by kneading method (3:1)Figure 3.3.2.4.9. DSC thermogram of γ -CD-Cilostazol physical mixture (3:1).Figure 3.3.2.4.10. DSC thermogram of γ -CD-Cilostazol Inclusion complex by co-precipitation (3:1)

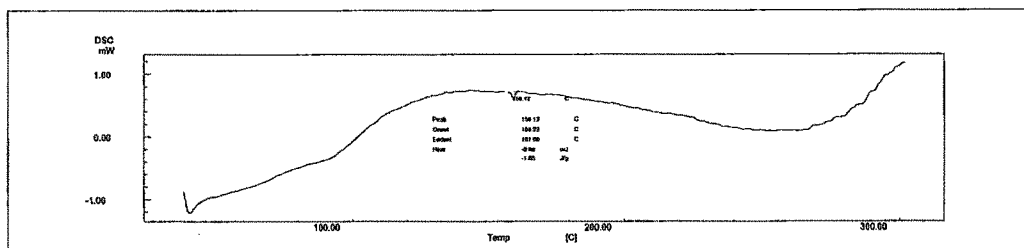


Figure 3.3.2.4.11. DSC thermogram of γ -CD-Cilostazol Inclusion complex by kneading method (3:1)

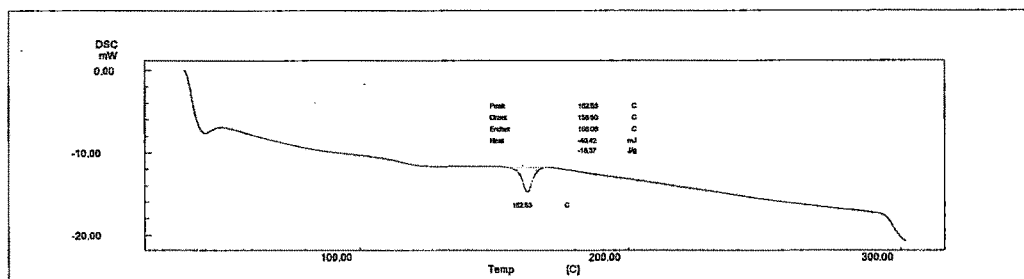


Figure 3.3.2.4.12. DSC thermogram of HP- β -CD-Cilostazol physical mixture (3:1).

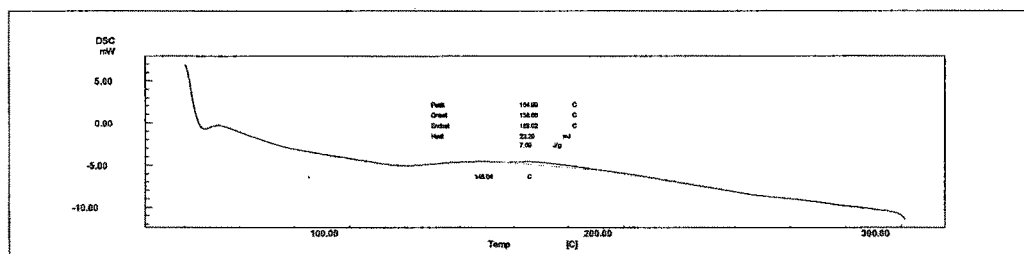


Figure 3.3.2.4.13. DSC thermogram of HP- β -CD-Cilostazol Inclusion complex by co-precipitation method (3:1)

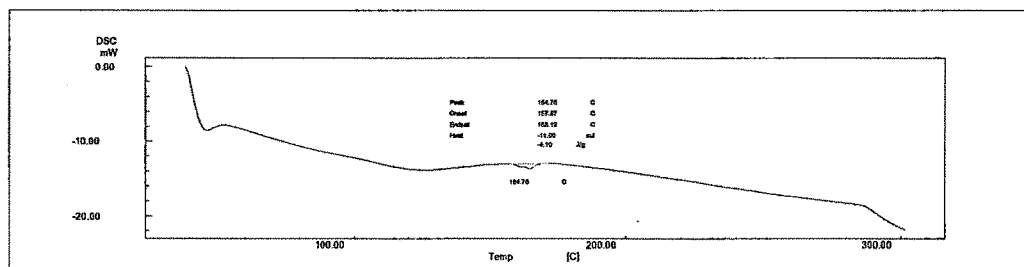


Figure 3.3.2.4.14. DSC thermogram of HP- β -CD-Cilostazol Inclusion complex by kneading method (3:1)

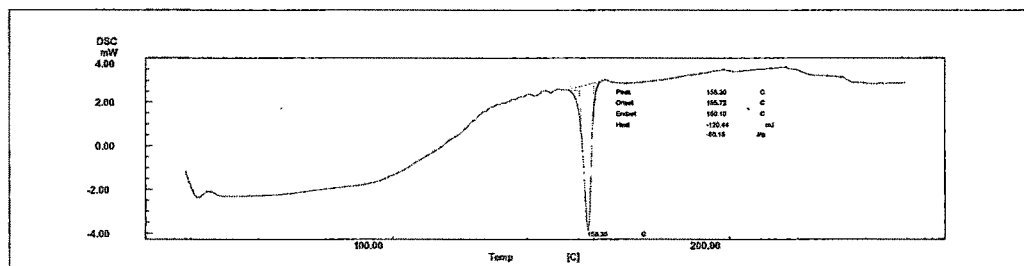


Figure 3.3.2.4.15. DSC thermogram of DM- β -CD-Cilostazol physical mixture (3:1).

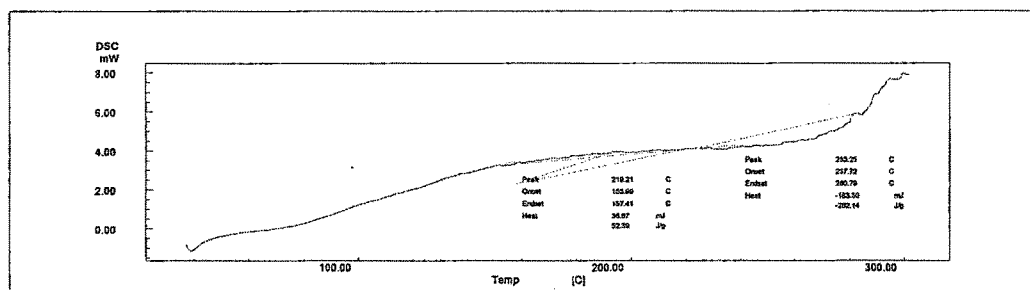


Figure 3.3.2.4.16. DSC thermogram of DM-β-CD-Cilostazol Inclusion complex by co-precipitation method (3:1)

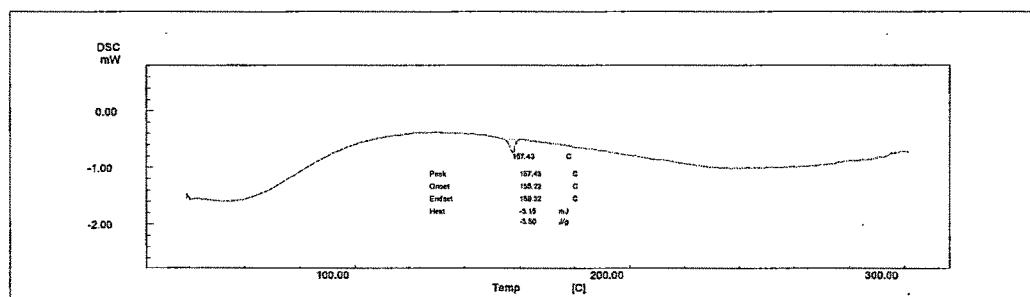
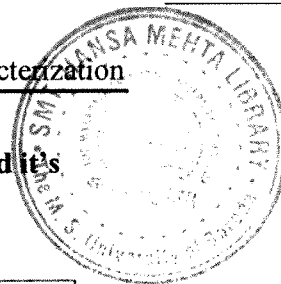


Figure 3.3.2.4.17. DSC thermogram of DM-β-CD-Cilostazol Inclusion complex by kneading method (3:1)



3.3.2.5. X-Ray diffraction pattern of Cilostazol, CDs, its Physical mixtures and its Inclusion complexes.

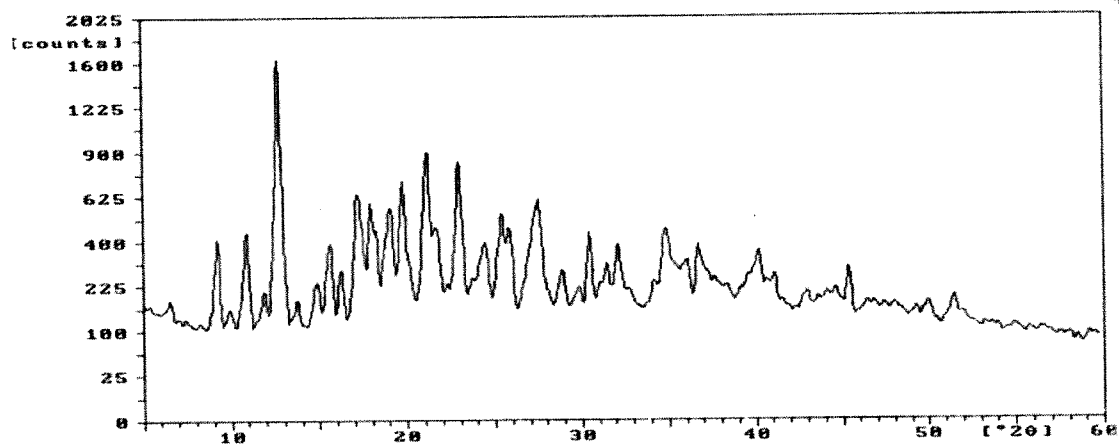


Figure 3.3.2.5.1. X-Ray diffraction pattern of β -CD.

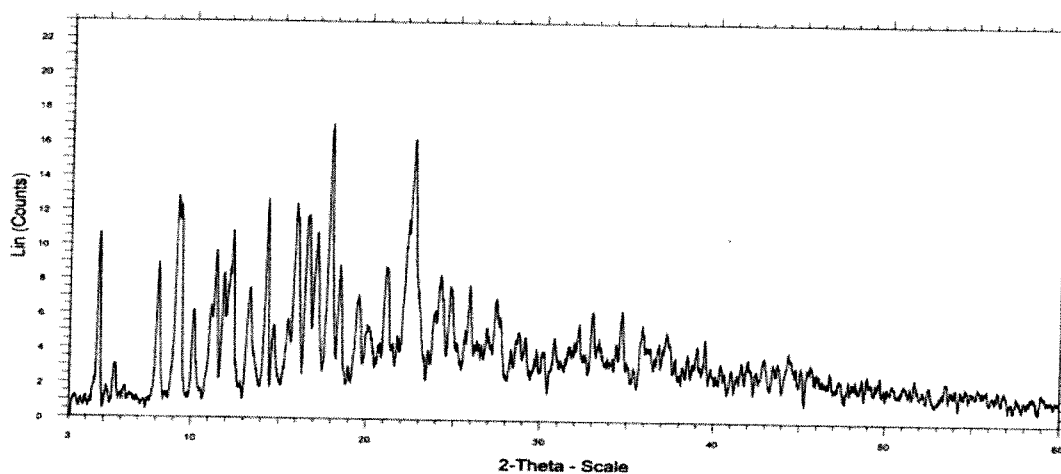


Figure 3.3.2.5.2. X-Ray diffraction pattern of γ -CD.

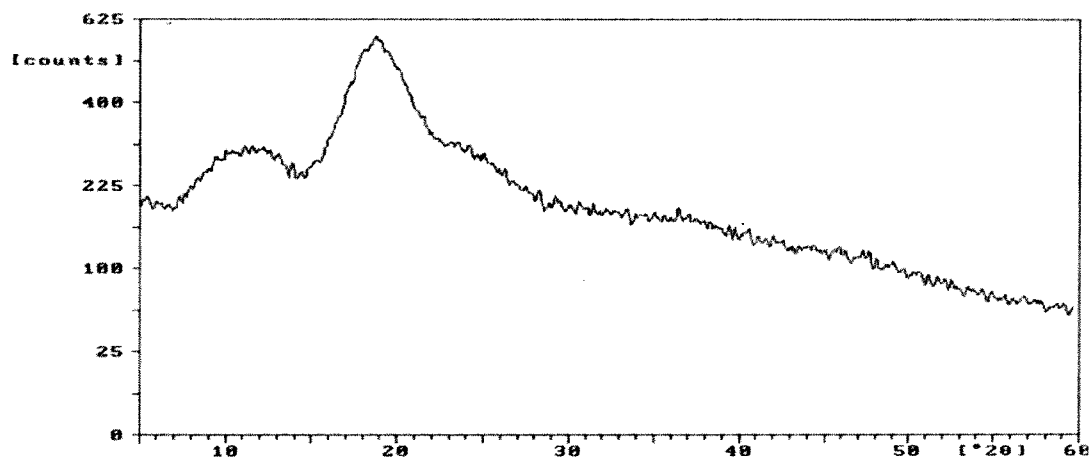


Figure 3.3.2.5.3. X-Ray diffraction pattern of HP- β -CD.

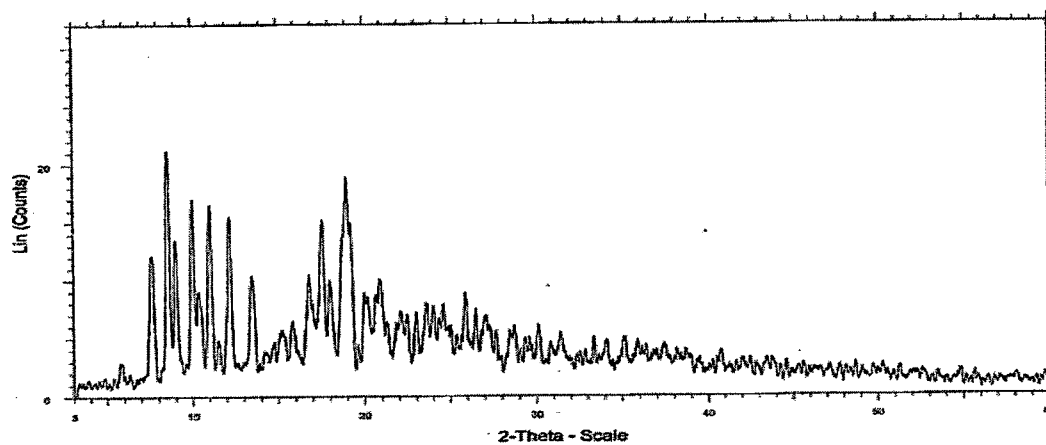


Figure 3.3.2.5.4. X-Ray diffraction pattern of DM-β-CD.

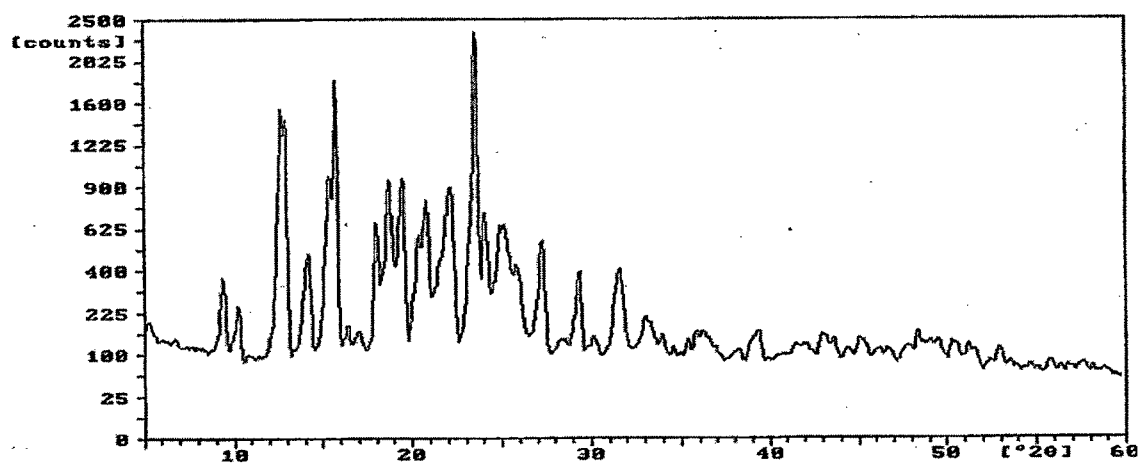


Figure 3.3.2.5.5. X-Ray diffraction pattern of Cilostazol.

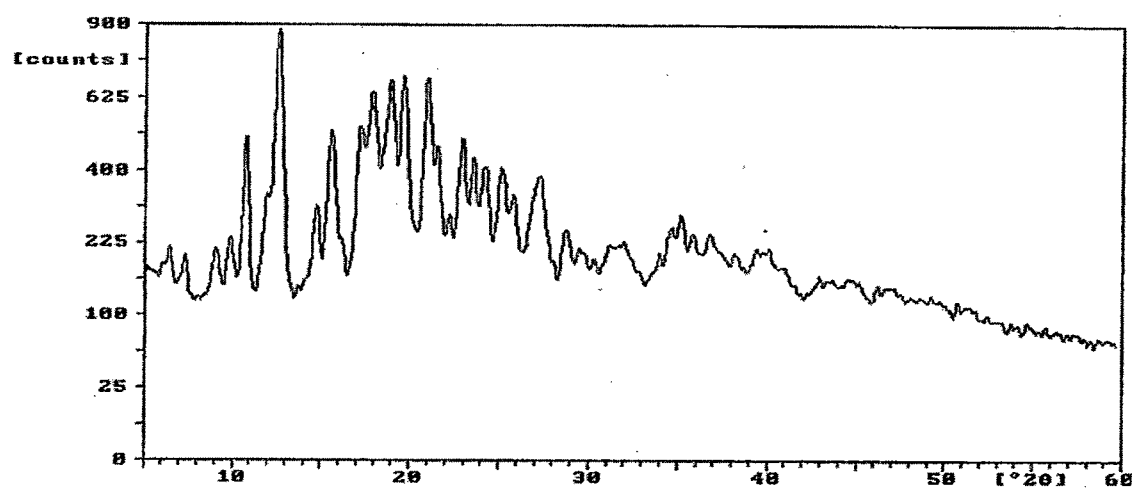


Figure 3.3.2.5.6. X-Ray diffraction pattern of β -CD-Cilostazol Physical mixture(3:1).

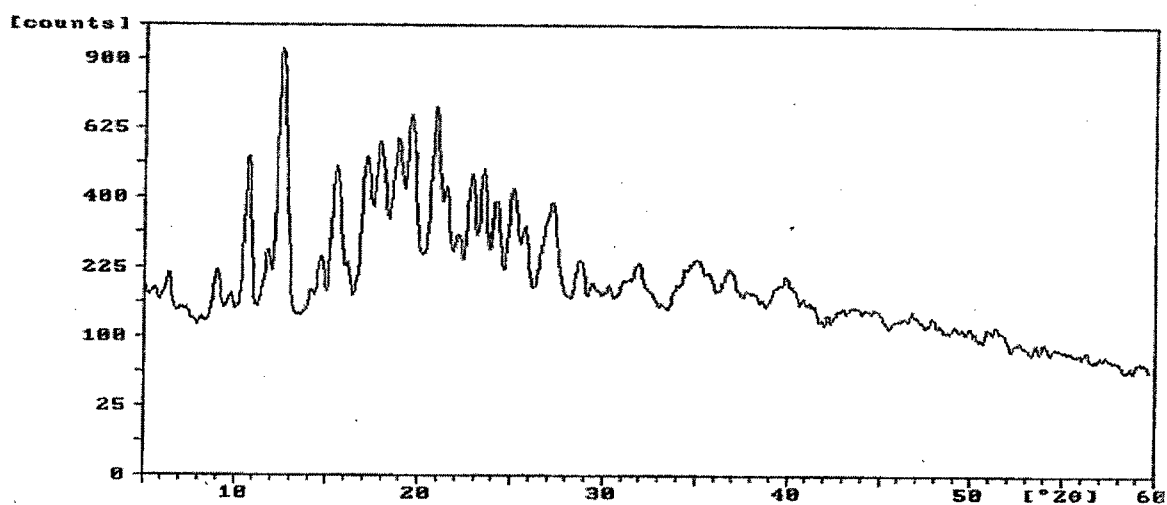


Figure 3.3.2.5.7 X-Ray diffraction pattern of β -CD-Cilostazol Inclusion complex (2:1).

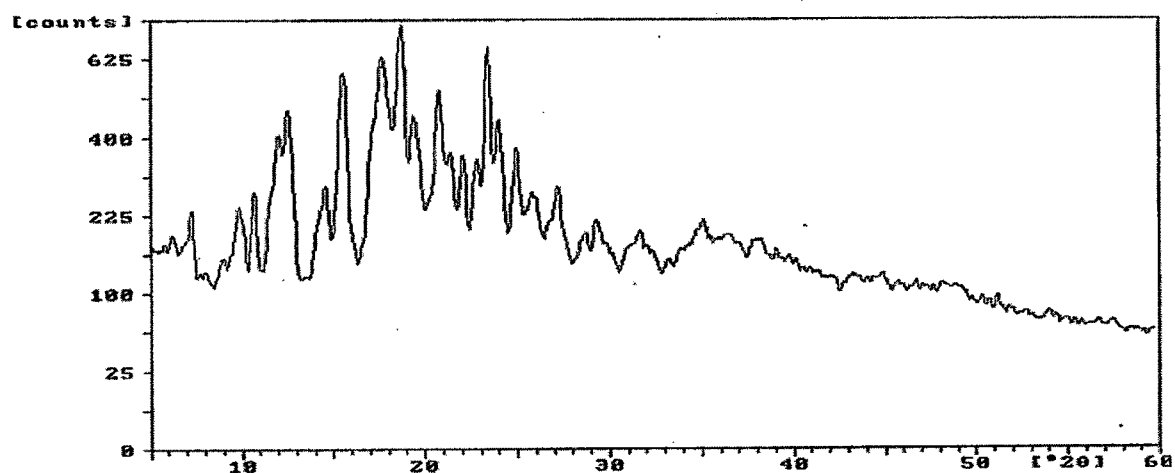


Figure 3.3.2.5.8. X-Ray diffraction pattern of β -CD -Cilostazol Inclusion complex(3:1).

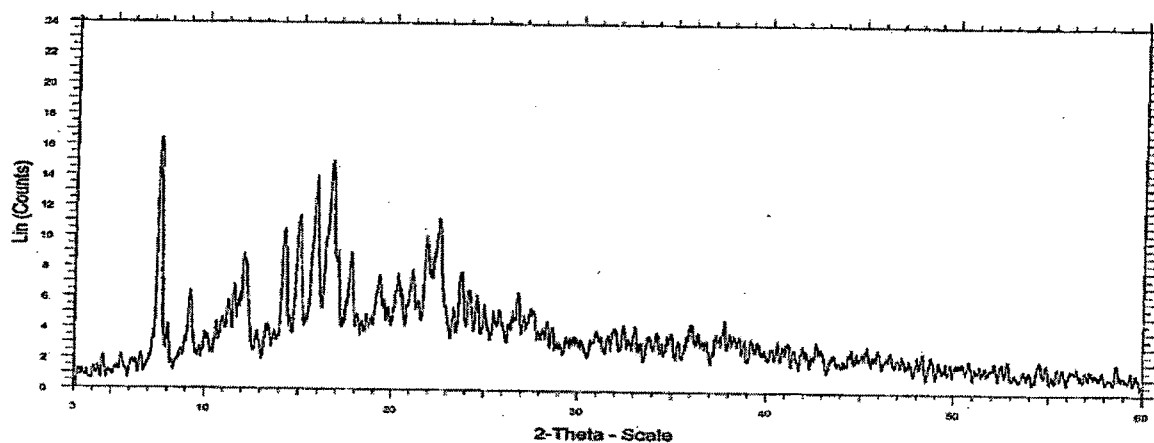


Figure 3.3.2.5.9. X-Ray diffraction pattern of γ -CD -Cilostazol Physical mixture(3:1).

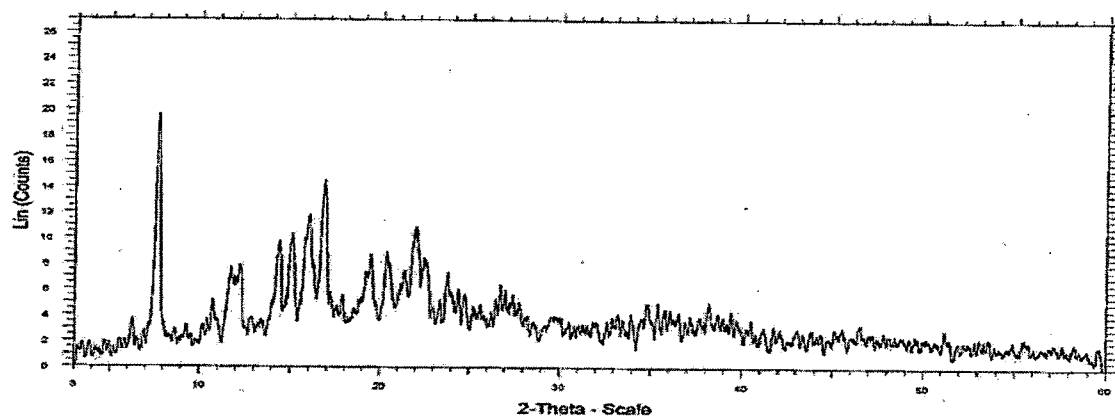


Figure 3.3.2.5.10. X-Ray diffraction pattern of γ -CD - Cilostazol Inclusion complex (2:1).

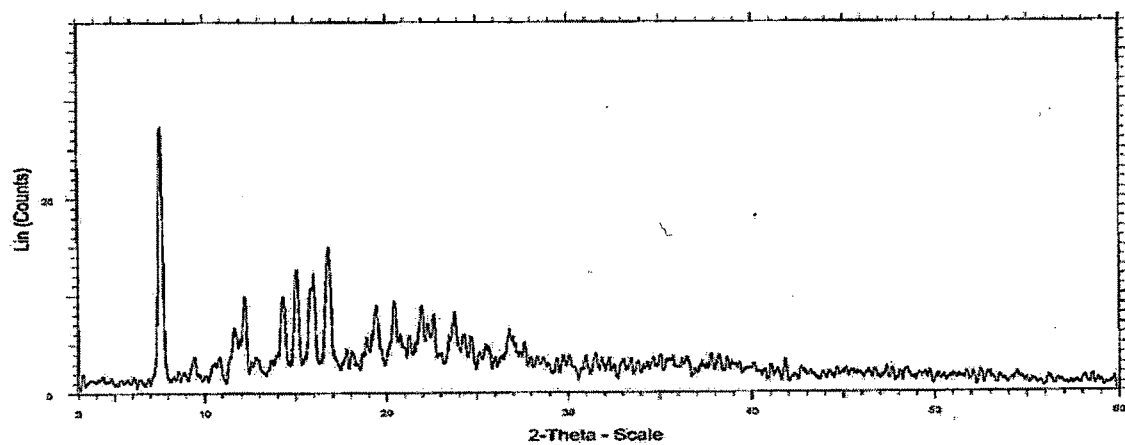


Figure 3.3.2.5.11. X-Ray diffraction pattern of γ -CD -Cilostazol Inclusion complex (3:1).

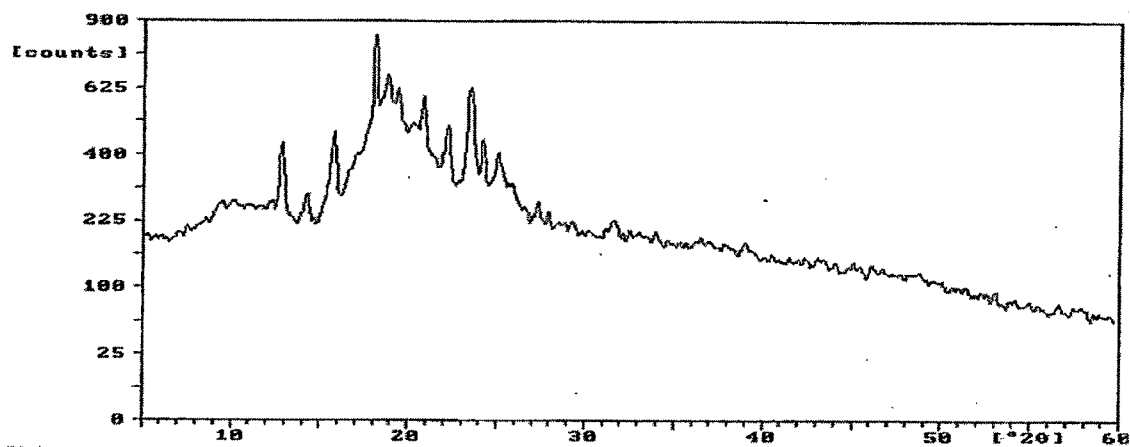


Figure 3.3.2.5.12. X-ray Diffraction pattern of HP- β -CD -Cilostazol physical mixture (3:1).

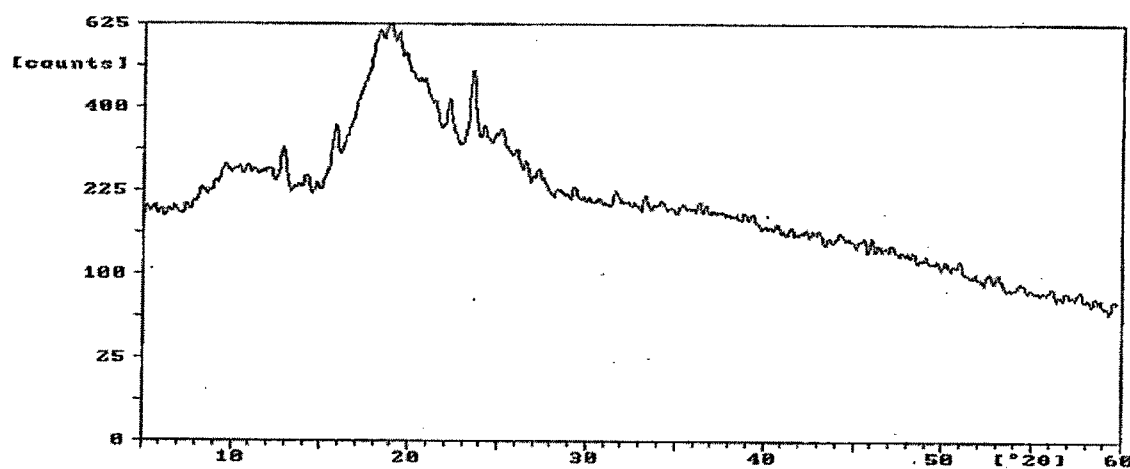


Figure 3.3.2.5.13. X-Ray diffraction pattern of HP- β -CD -Cilostazol Inclusion complex (2:1).

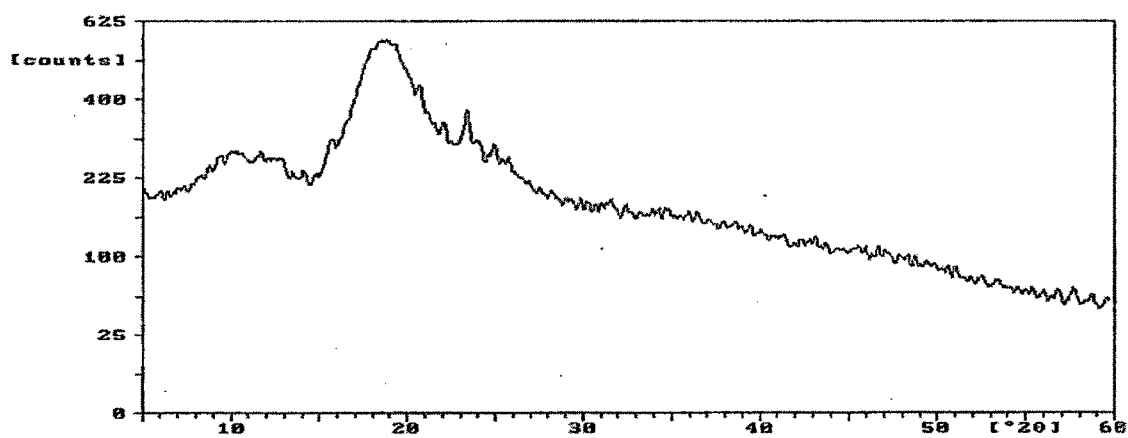


Figure 3.3.2.5.14. X-Ray diffraction pattern of HP- β -CD -Cilostazol Inclusion complex (3:1).

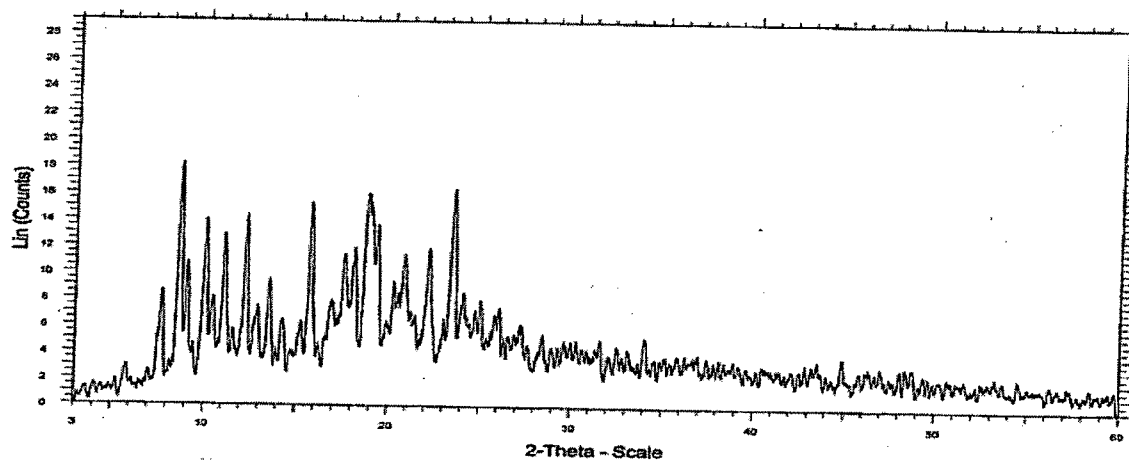


Figure 3.3.2.5.15. X-ray Diffraction pattern of DM- β -CD -Cilostazol physical mixture (3:1).

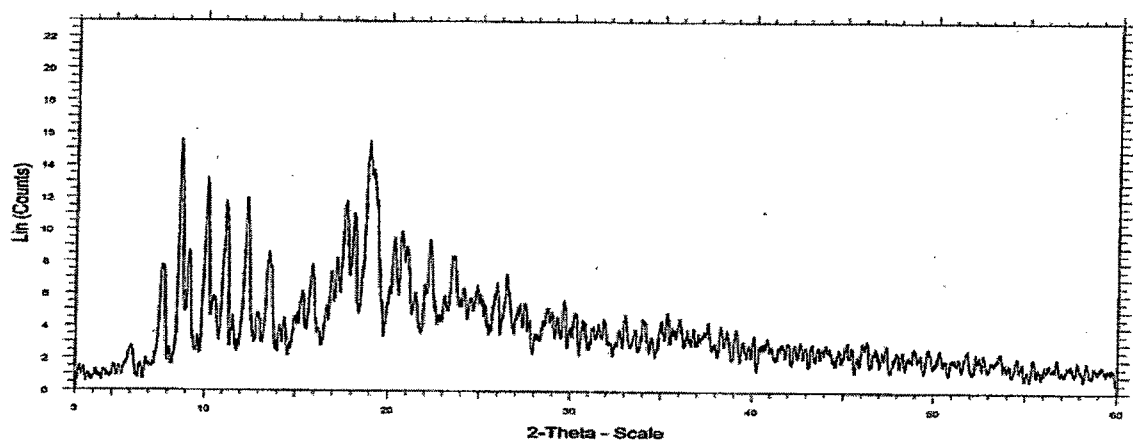


Figure 3.3.2.5.16. X-Ray diffraction pattern of DM- β -CD -Cilostazol Inclusion complex (2:1).

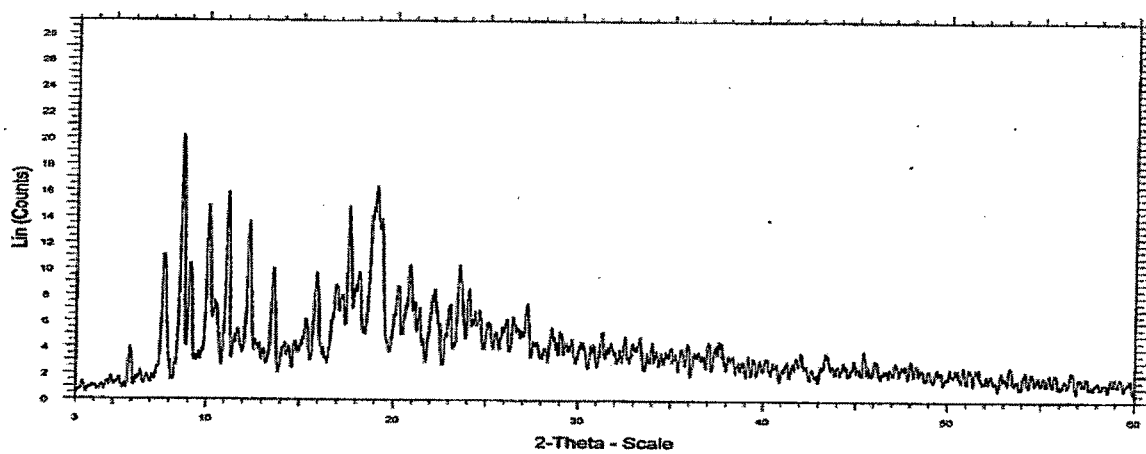


Figure 3.3.2.5.17. X-Ray diffraction pattern of DM- β -CD -Cilostazol Inclusion complex (3:1).

3.3.3. Dissolution Study of Cilostazol-cyclodextrins Inclusion Complexes.

3.3.3.1. Introduction :

The most direct assessment of a drug's release from various Tablet or Capsule formulations is accomplished through *in vivo* bioavailability measurements. The use of *in vivo* studies is restricted, however, for several reasons, i.e. the length of time needed to plan, conduct, and interpret the studies; the highly skilled personnel required for human studies; the low precision and high variability typical of the measurements; the high cost of the studies; the use of human subjects for "nonessential" research; and the necessary assumption that a perfect correlation exists between the patient and a healthy human subject used in the test. Consequently, *in vitro* dissolution test have been expensively studied, developed, and used as an indirect measurement of drug availability, especially in preliminary assessments of formulation factors and manufacturing methods that are likely to influence bioavailability. Since 1970, the United States Pharmacopoeia and the National Formulary have provided procedures for dissolution testing. The determine compliance with the limits on dissolution as specified in the individual monograph for a tablet (or a capsule). The USPXX/NFXV, Supplement 3, specified the either of two apparatus be used for determining dissolution tests¹².

Apparatus 1 :- Basket type apparatus.

Apparatus 2 :- Paddle type apparatus.

Description of a dissolution test in a USP/NF monograph specified the dissolution test medium and volume, the apparatus to be used, the speed (rpm) at which the test is to be performed, the time limit of the test, and the assay procedure. The test tolerance is expressed as a percentage of the labeled amount of drug dissolved in the time limit¹³.

Specified amounts of Drug-CDs Inclusion complexes and its Physical mixtures were filled into a separate hard gelatin capsule according to their active ingredient weight and according to the specified USP/NF monograph the dissolution tests were carried out by following the procedure using USP 1 apparatus. The dissolution results were compared with those of Marketed formulation (Pletoz-50) of the drugs in triplicate and the physicochemical parameters were calculated as mentioned below.

A. Percent Drug Released :

Percent Drug release at predetermined sampling time interval was determined using formula,

$$\% \text{ Drug Released} = \frac{\text{Amount of drug released at time 't'}}{\text{Initial amount of Drug at t=0 time}} \times 100$$

(B) Dissolution Efficiency DE_{120 min.} and Time required for 50% drug dissolved(T_{50%}) :

Khan¹⁴ suggested Dissolution Efficiency (DE) as a suitable parameter for the evaluation of *in vitro* dissolution data. DE is defined as the area under dissolution curve up to a certain time 't' expressed as percentage of the area of the rectangle described by 100% dissolution in the same time. DE_{120min} values were calculated from the dissolution data by using the equation.

$$\text{Dissolution efficiency (DE)} = \frac{\int_0^t Y \cdot dt}{Y_{100 \cdot t}} \times 100$$

Time required for 50 % drug dissolved (T_{50%}) were calculated from the dissolution data by using Khan Equation¹⁴.

(C) Kinetics of Release

In order to investigate the mechanism of drug release from the formulation, the release rates were integrated into each of the following equation and the regression coefficient was investigated from each of the regressed graph¹⁵.

Zero-order equation:

$$Q = K_0 t$$

Where, Q = Amount of drug released at time t

t = Time in hours

K₀ = Zero-order release rate constant

First-order equation:

$$Q = Q_0 e^{-K_1 t}$$

Where, Q = Amount of drug released at time t

t = Time in hours

K₁ = First-order release rate constant

Higuchi's equation:

$$Q = K_H \times \sqrt{t}$$

Where, Q = Amount of drug released at time t

t = Time in hours

K_H = Higuchi's diffusion rate constant

The order of drug release was determined by performing the regression over the mean values of percent drug diffusion vs. t (for Zero-order), log percent drug diffusion vs. t (for First-order) and percent drug diffusion vs. square root of t (for Higuchi).

3.3.3.2. Experimental design :

Dissolution rate studies were performed in a solution containing (HCl buffer pH 1.2, Distilled water or phosphate buffer pH 6.4, 900 ml)¹⁶ at $37 \pm 0.2^\circ\text{C}$, using USP XXIII¹⁷ apparatus (Electrolab, India Programmable tablet dissolution test apparatus USP XXI/XXII, TDT-06P) with a basket rotating (Apparatus I) at 50 rpm but the best results were found in phosphate buffer pH 6.4 Hence, the further study was continued using phosphate buffer pH 6.4 as a dissolution medium. Physical mixtures and Inclusion complexes, each containing 50 mg of Cilostazol were filled into empty hard gelatin capsules shell and subjected to dissolution study. Samples (5mL) were withdrawn at (10.0, 20.0, 30.0, 40.0, 50.0, 60.0, 75.00, 90.00, 105.0 and 120.0 min), filtered through Whatman filter paper No. 41 and assayed spectrophotometrically for drug content at 257.8 nm as mentioned in, Section 3.1.1.4.4. The experiments were repeated thrice and the mean cumulative % drug diffused along with SD was calculated (Table 3.3.3.2. to Table 3.3.3.4, Table 3.3.3.6. to 3.3.3.8., Table 3.3.3.10. to 3.3.3.12 and Table 3.3.3.14. to 3.3.3.16. respectively) for different Cilostazol-CD inclusion complexes. The graphs are shown in Figure 3.3.3.1, 3.3.3.3., 3.3.3.5. and 3.3.3.7 respectively. The % Dissolution Efficiency ($DE_{120 \text{ min.}}$) values based on the dissolution data along with SD were calculated as per Khan method¹⁴ and time taken for 50% drug dissolved ($T_{50\%}$ value) was identified from the dissolution profiles. All this data are shown in Table 3.3.3.5., 3.3.3.9., 3.3.3.13. and 3.3.3.17. Comparison data of $DE_{120 \text{ min.}}$ study and $T_{50\%}$ study are shown in Figure 3.3.3.2., 3.3.3.4., 3.3.3.6., and 3.3.3.8. The release kinetics of diffusion was studied by calculating the regression coefficient for zero order, first order, and Higuchi's equations. The regression coefficients for the different Cilostazol-CDs inclusion complexes, Physical mixtures, Marketed formulation (Pletoz-50) and Cilostazol are recorded in Table 3.3.3.18. Finally the result were compared with the dissolution profile of Marketed formulation (Pletoz-50) (Pletoz - 50, Tablet containing 50 mg of Cilostazol) and Cilostazol (50 mg) (Table 3.3.3.1.)¹⁸⁻²².

Table 3.3.3.1. Dissolution data of Pure Cilostazol and its Marketed formulation (Pletoz-50) in phosphate buffer pH 6.4.

Time in Min.	% Drug release of Pure Cilostazol [#]	% Drug release of Marketed formulation (Pletoz-50) [#]
0	0.0 ± 0.55	0.00 ± 0.55
10	5.25 ± 0.265	3.12 ± 0.67
20	8.31 ± 0.148	8.88 ± 1.32
30	11.55 ± 0.310	13.55 ± 0.89
40	14.32 ± 0.434	18.32 ± 0.69
50	18.23 ± 0.316	25.35 ± 1.55
60	21.36 ± 0.345	33.57 ± 0.91
75	26.45 ± 0.478	40.66 ± 1.56
90	31.32 ± 0.236	42.22 ± 0.38
105	32.58 ± 0.8	45.55 ± 1.98
120	32.98 ± 0.91	46.56 ± 2.1

[#] All values are represented as mean ± SD (±n=3).

Table 3.3.3.2. Dissolution data of Cilostazol – β -CD Physical mixture in phosphate buffer pH 6.4.

Time in Min.	% Drug release of Cilostazol – β -CD Physical mixture (1:1) #	% Drug release of Cilostazol – β -CD Physical mixture (1:2) #	% Drug release of Cilostazol – β -CD Physical mixture (1:3) #
0	0.00 \pm 0.36	0.00 \pm 0.12	0.00 \pm 0.45
10	5.54 \pm 0.55	5.78 \pm 0.33	11.21 \pm 0.85
20	9.8 \pm 1.25	10.11 \pm 0.64	19.57 \pm 0.39
30	14.25 \pm 0.98	15.05 \pm 0.59	31.45 \pm 0.23
40	21.22 \pm 1.35	24.58 \pm 0.88	45.56 \pm 1.85
50	29.97 \pm 1.66	32.22 \pm 0.94	52.72 \pm 1.23
60	35.67 \pm 2.12	39.94 \pm 0.99	56.60 \pm 1.33
75	40.70 \pm 1.77	45.85 \pm 1.01	60.82 \pm 1.28
90	42.55 \pm 1.86	50.86 \pm 1.38	64.04 \pm 1.43
105	43.89 \pm 1.43	53.33 \pm 1.83	67.06 \pm 1.67
120	45.35 \pm 1.59	56.67 \pm 1.93	69.32 \pm 1.75

All values are represented as mean \pm SD ($\pm n=3$).

Table 3.3.3.3. Dissolution data of Cilostazol- β -CD Inclusion complex by CO-PRECIPIATION METHOD in phosphate buffer pH 6.4.

Time in Min.	% Drug release of Cilostazol - β -CD Inclusion complex (1:1) [#]	% Drug release of Cilostazol - β -CD Inclusion complex (1:2) [#]	% Drug release of Cilostazol - β -CD Inclusion complex (1:3) [#]
0	0.00 \pm 0.36	0.00 \pm 0.25	0.00 \pm 0.71
10	3.33 \pm 0.54	12.34 \pm 0.75	17.71 \pm 0.82
20	6.28 \pm 0.67	19.99 \pm 0.64	31.33 \pm 0.21
30	13.63 \pm 0.43	27.37 \pm 0.89	47.88 \pm 0.11
40	20.41 \pm 0.76	39.56 \pm 0.98	56.60 \pm 0.62
50	29.66 \pm 0.93	54.67 \pm 0.72	64.84 \pm 1.11
60	36.76 \pm 0.99	57.77 \pm 0.71	69.32 \pm 1.20
75	41.81 \pm 1.01	60.81 \pm 1.32	71.39 \pm 1.56
90	45.38 \pm 1.32	63.33 \pm 1.45	74.03 \pm 1.34
105	47.57 \pm 0.86	66.83 \pm 1.65	75.55 \pm 1.62
120	52.57 \pm 0.85	68.88 \pm 1.56	76.49 \pm 1.09

[#] All values are represented as mean \pm SD ($\pm n=3$).

Table 3.3.3.4. Dissolution data of Cilostazol- β -CD Inclusion complex by KNEADING METHOD in phosphate buffer pH 6.4.

Time in Min.	% Drug release of Cilostazol - β -CD Inclusion complex (1:1) #	% Drug release of Cilostazol - β -CD Inclusion complex (1:2) #	% Drug release of Cilostazol - β -CD Inclusion complex (1:3) #
0	0.00 \pm 0.41	0.00 \pm 0.43	0.00 \pm 0.13
10	2.22 \pm 0.27	7.27 \pm 0.45	15.33 \pm 2.06
20	7.28 \pm 0.83	14.54 \pm 0.55	24.58 \pm 1.23
30	12.55 \pm 0.48	22.72 \pm 1.45	36.38 \pm 1.98
40	17.89 \pm 0.31	30.4 \pm 1.37	51.06 \pm 2.35
50	25.65 \pm 1.56	37.75 \pm 1.73	63.06 \pm 2.52
60	31.42 \pm 0.91	44.83 \pm 1.93	69.98 \pm 2.11
75	39.48 \pm 1.55	51.55 \pm 1.22	72.44 \pm 1.99
90	43.52 \pm 1.48	56.73 \pm 1.93	75.23 \pm 2.14
105	45.57 \pm 1.23	60.57 \pm 1.53	77.88 \pm 2.01
120	47.83 \pm 1.47	63.76 \pm 1.65	73.28 \pm 1.93

All values are represented as mean \pm SD ($\pm n=3$).

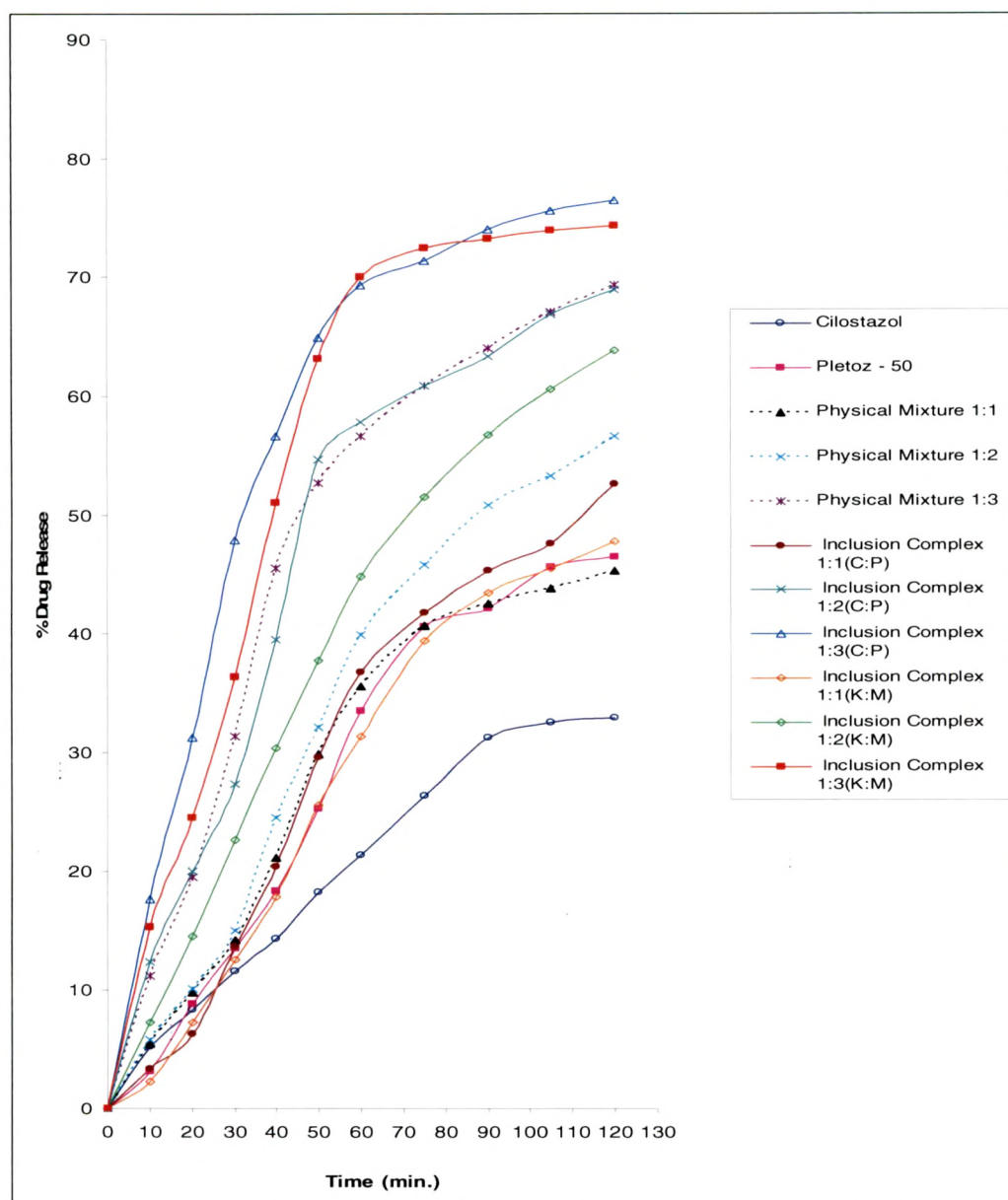


Figure 3.3.3.1. Cumulative % drug released from Cilostazol – β -CD inclusion complexes, Physical mixtures, Marketed formulation (Pletoz-50) and Pure Drug at different time intervals.

Table 3.3.3.5. Dissolution efficiency and time required for 50% drug dissolved ($T_{50\%}$) for Cilostazol, Marketed formulation (Pletoz-50), Cilostazol- β -CD Physical mixtures and Inclusion complexes.

Type	Dissolution efficiency for 120 min (%)		Time required for 50% drug dissolved (Min)	
	Mean \pm SD [#]	%RSD	Mean \pm SD [#]	%RSD
Cilostazol	20.385 \pm 1.02	2.16	181.92 \pm 0.67	2.84
Pletoz-50	28.2339 \pm 0.66	1.17	128.86 \pm 0.49	1.76
Physical Mixture 1:1	29.17 \pm 0.36	0.57	132.3 \pm 0.13	1.71
Physical Mixture 1:2	33.7689 \pm 1.53	2.24	88.47 \pm 1.04	1.04
Physical Mixture 1:3	47.5941 \pm 0.45	0.62	47.55 \pm 0.85	0.88
Inclusion Complex 1:1(C:P)	30.068 \pm 0.13	0.18	114.13 \pm 0.99	1.89
Inclusion Complex 1:2(C:P)	47.02 \pm 1.23	1.94	45.72 \pm 0.76	1.32
Inclusion Complex 1:3(C:P)	57.8193 \pm 0.67	3.36	31.32 \pm 0.97	0.45
Inclusion Complex 1:1(K:M)	27.7993 \pm 0.49	2.64	125.44 \pm 0.68	0.23
Inclusion Complex 1:2(K:M)	39.151 \pm 0.40	3.02	72.74 \pm 0.15	0.87
Inclusion Complex 1:3(K:M)	55.2433 \pm 0.33	1.15	39.16 \pm 1.35	1.67

[#] All values are represented as mean \pm SD ($\pm n=3$).

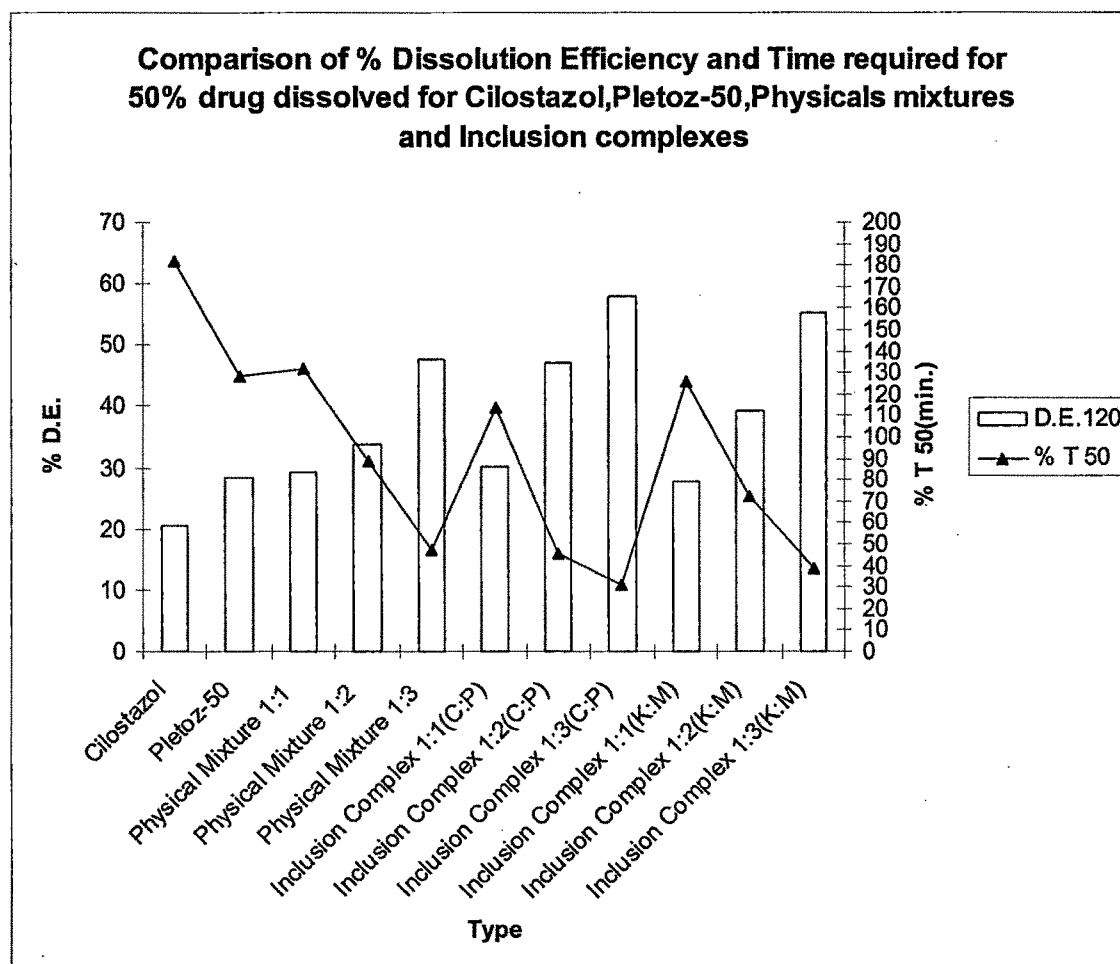


Figure 3.3.3.2. Comparison of % Dissolution efficiency and time required for 50 % drug dissolved for Cilostazol, Marketed formulation (Pletoz-50), Cilostazol- β -CD physical mixtures and inclusion complexes.

Table 3.3.3.6. Dissolution data of Cilostazol – γ -CD Physical mixture in phosphate buffer pH 6.4.

Time in Min.	% Drug release of Cilostazol – γ -CD Physical mixture (1:1) [#]	% Drug release of Cilostazol – γ -CD Physical mixture (1:2) [#]	% Drug release of Cilostazol – γ -CD Physical mixture (1:3) [#]
0	0.00 ± 1.11	0.00 ± 0.94	0.00 ± 0.91
10	36.52 ± 2.31	10.8 ± 2.22	16.64 ± 0.83
20	38.37 ± 2.09	21.9 ± 1.68	24.86 ± 1.22
30	40.58 ± 1.99	34.75 ± 1.34	36.4 ± 1.56
40	42.8 ± 1.53	47.97 ± 1.82	56.46 ± 1.43
50	45.01 ± 1.60	50.92 ± 0.91	62.37 ± 1.71
60	47.6 ± 2.20	52.03 ± 0.87	65.32 ± 1.01
75	49.18 ± 2.83	53.88 ± 0.63	66.4 ± 1.55
90	50.92 ± 1.73	55.72 ± 1.23	68.13 ± 1.83
105	51.18 ± 1.47	56.09 ± 1.55	70.13 ± 2.06
120	51.98 ± 2.62	55.72 ± 1.01	71.13 ± 1.24

[#] All values are represented as mean ± SD ($\pm n=3$).

Table 3.3.3.7. Dissolution data of Cilostazol – γ -CD Inclusion complex by CO-PRECIPIATION METHOD in phosphate buffer pH 6.4.

Time in Min.	% Drug release of Cilostazol – γ -CD Inclusion complex (1:1) #	% Drug release of Cilostazol – γ -CD Inclusion complex (1:2) #	% Drug release of Cilostazol – γ -CD Inclusion complex (1:3) #
0	0.00 \pm 1.01	0.00 \pm 0.59	0.00 \pm 0.33
10	21.68 \pm 0.42	24.52 \pm 0.81	35.60 \pm 0.23
20	43.84 \pm 1.32	45.26 \pm 1.32	56.34 \pm 0.56
30	51.014 \pm 1.82	56.00 \pm 1.67	77.81 \pm 0.65
40	59.23 \pm 1.83	67.47 \pm 1.83	89.29 \pm 0.72
50	62.70 \pm 1.43	71.21 \pm 1.92	90.77 \pm 0.48
60	64.18 \pm 1.92	74.95 \pm 1.90	92.99 \pm 1.82
75	65.66 \pm 2.32	78.95 \pm 2.52	94.46 \pm 1.43
90	67.87 \pm 2.11	79.69 \pm 2.11	95.94 \pm 1.92
105	67.87 \pm 1.99	78.95 \pm 2.62	95.20 \pm 2.04
120	67.87 \pm 1.82	78.95 \pm 1.64	95.20 \pm 2.31

All values are represented as mean \pm SD ($\pm n=3$).

Table 3.3.3.8. Dissolution data of Cilostazol – γ -CD Inclusion complex by KNEADING METHOD in phosphate buffer pH 6.4.

Time in Min.	% Drug release of Cilostazol – γ -CD Inclusion complex (1:1) #	% Drug release of Cilostazol – γ -CD Inclusion complex (1:2) #	% Drug release of Cilostazol – γ -CD Inclusion complex (1:3) #
0	0.00 ± 0.97	0.00 ± 1.45	0.00 ± 0.89
10	12.45 ± 1.13	15.62 ± 2.66	29.35 ± 0.67
20	27.19 ± 1.5	25.84 ± 2.13	40.09 ± 1.27
30	35.62 ± 2.23	31.23 ± 1.15	51.57 ± 1.58
40	43.32 ± 2.34	45.96 ± 0.87	67.47 ± 1.43
50	51.01 ± 1.55	53.44 ± 1.56	73.21 ± 2.15
60	58.27 ± 1.78	60.13 ± 2.23	79.69 ± 1.35
75	61.23 ± 2.58	65.66 ± 1.56	85.6 ± 2.25
90	62.23 ± 1.89	66.4 ± 0.98	85.86 ± 1.55
105	63.09 ± 1.56	65.66 ± 1.51	86.38 ± 0.98
120	63.99 ± 1.04	66.4 ± 2.33	87.08 ± 2.02

All values are represented as mean ± SD ($\pm n=3$).

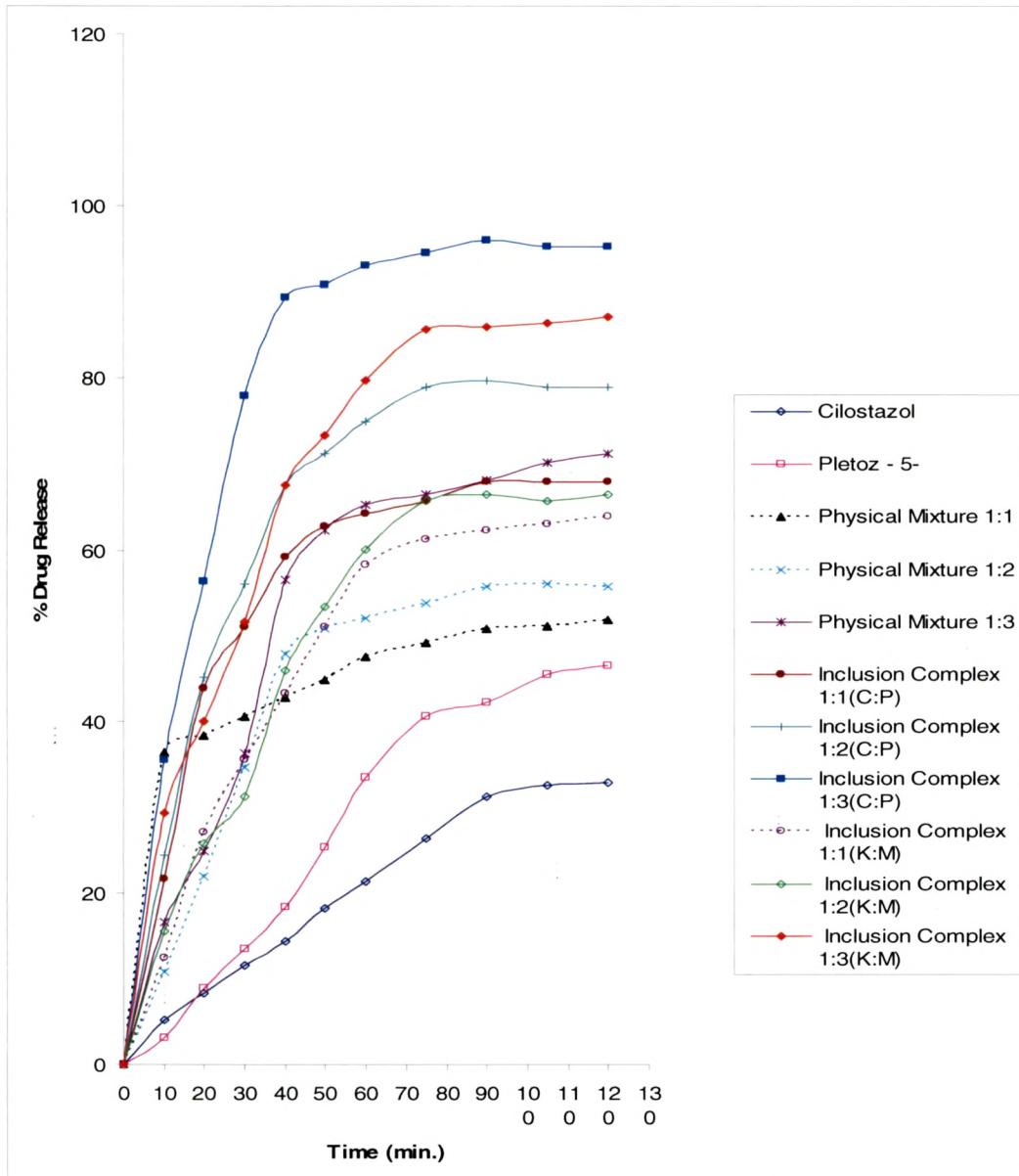


Figure 3.3.3.3. Cumulative % drug released from Cilostazol – γ -CD inclusion complexes, Physical mixtures, Marketed formulation (Pletoz-50) and Pure Drug at different time intervals.

Table 3.3.3.9. Dissolution efficiency and time required for 50% drug dissolved ($T_{50\%}$) for Cilostazol, Marketed formulation (Pletoz-50), Cilostazol- γ -CD Physical mixtures and Inclusion complexes.

Type	Dissolution efficiency for 120 min (%)		Time required for 50% drug dissolved (Min)	
	Mean \pm SD [#]	%RSD	Mean \pm SD [#]	%RSD
Cilostazol	20.385 \pm 1.02	2.16	181.92 \pm 1.44	2.41
Pletoz-50	28.2339 \pm 0.29	0.40	128.86 \pm 0.41	1.14
Physical Mixture 1:1	44.057 \pm 0.31	0.40	76.86 \pm 1.01	0.28
Physical Mixture 1:2	43.47 \pm 0.37	0.45	49.09 \pm 0.52	0.19
Physical Mixture 1:3	52.2264 \pm 0.32	0.38	35.42 \pm 0.68	0.50
Inclusion Complex 1:1(C:P)	55.9742 \pm 0.44	0.52	29.4 \pm 0.11	1.37
Inclusion Complex 1:2(C:P)	64.4787 \pm 0.52	0.60	21.99 \pm 0.14	0.56
Inclusion Complex 1:3(C:P)	80.4872 \pm 0.60	1.08	17.74 \pm 1.23	0.89
Inclusion Complex 1:1(K:M)	47.5204 \pm 0.68	0.82	49 \pm 0.58	1.21
Inclusion Complex 1:2(K:M)	49.4693 \pm 0.53	0.89	46.78 \pm 0.85	1.65
Inclusion Complex 1:3(K:M)	67.78 \pm 1.32	1.83	29.08 \pm 1.57	0.87

[#] All values are represented as mean \pm SD ($\pm n=3$).

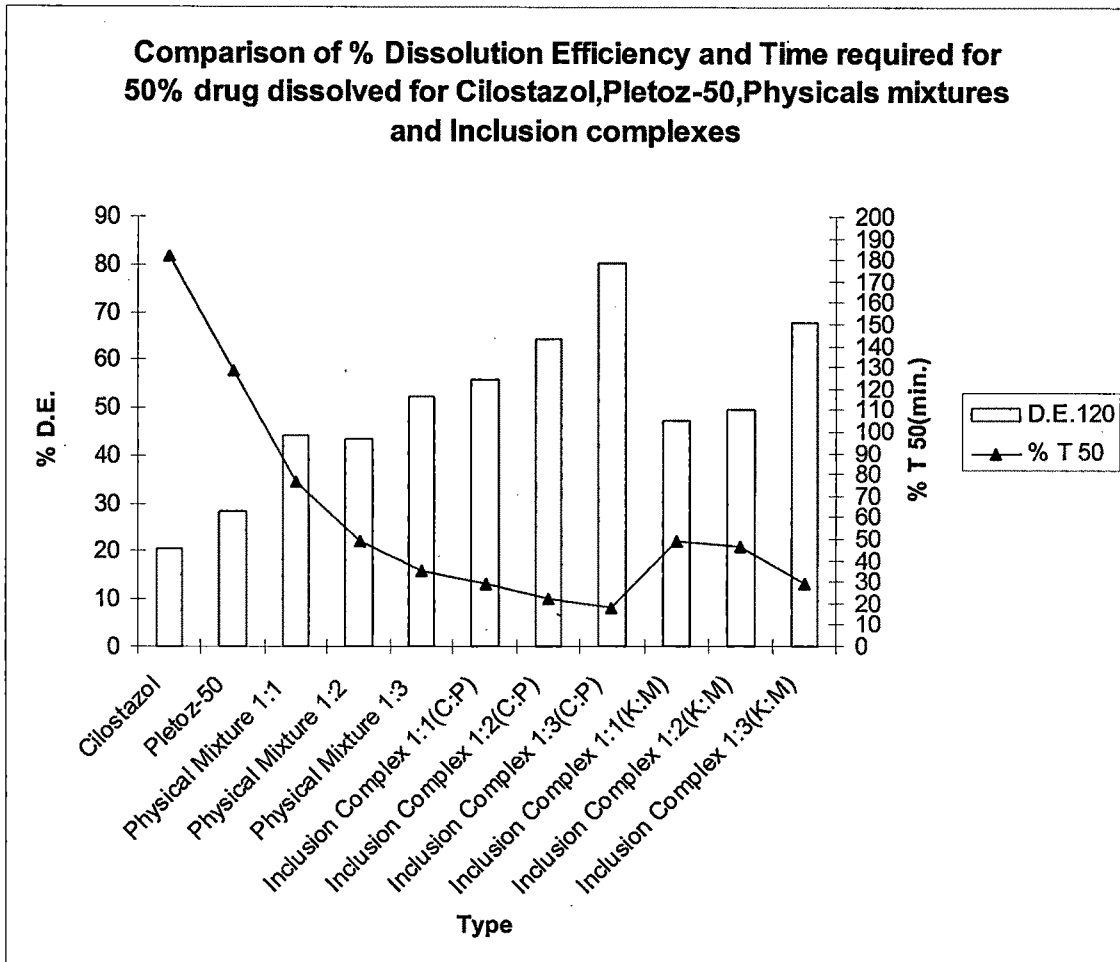


Figure 3.3.3.4. Comparison of % Dissolution efficiency and time required for 50 % drug dissolved for Cilostazol, Marketed formulation (Pletoz-50), Cilostazol- γ -CD physical mixtures and inclusion complexes.

Table 3.3.3.10. Dissolution data of Cilostazol -HP- β -CD Physical mixture in phosphate buffer pH 6.4.

Time in Min.	% Drug release of Cilostazol HP- β -CD Physical mixture (1:1) #	% Drug release of Cilostazol HP- β -CD Physical mixture (1:2) #	% Drug release of Cilostazol HP- β -CD Physical mixture (1:3) #
0	0.00 \pm 2.14	0.00 \pm 1.34	0.00 \pm 0.87
10	6.8 \pm 1.89	8.22 \pm 2.13	10.56 \pm 1.24
20	14.55 \pm 2.13	16.44 \pm 1.69	16.77 \pm 2.34
30	21.44 \pm 2.56	23.34 \pm 2.15	22.34 \pm 1.56
40	30.3 \pm 1.56	35.55 \pm 1.78	31.34 \pm 1.78
50	37.68 \pm 0.89	44.22 \pm 2.18	42.52 \pm 0.79
60	43.43 \pm 0.45	51.64 \pm 0.89	55.57 \pm 2.31
75	50.92 \pm 0.84	57.88 \pm 1.34	63.77 \pm 1.49
90	55.66 \pm 1.26	60.35 \pm 2.35	67.87 \pm 2.56
105	59.21 \pm 2.10	63.33 \pm 1.56	69.31 \pm 1.57
120	61.55 \pm 1.45	66.56 \pm 1.59	72.34 \pm 2.14

All values are represented as mean \pm SD ($\pm n=3$).

Table 3.3.3.11. Dissolution data of Cilostazol – HP- β -CD Inclusion complex by CO-PRECIPIATION METHOD in phosphate buffer pH 6.4.

Time in Min.	% Drug release of Cilostazol HP- β -CD Inclusion complex (1:1) [#]	% Drug release of Cilostazol HP- β -CD Inclusion complex (1:2) [#]	% Drug release of Cilostazol HP- β -CD Inclusion complex (1:3) [#]
0	0.00 \pm 0.33	0.00 \pm 0.49	0.00 \pm 0.56
10	19.43 \pm 1.54	23.55 \pm 1.33	25.45 \pm 0.83
20	31.87 \pm 0.67	37.69 \pm 1.56	41.51 \pm 1.22
30	43.33 \pm 0.89	39.21 \pm 1.69	53.49 \pm 1.56
40	49.00 \pm 1.55	44.89 \pm 1.91	65.56 \pm 1.43
50	58.72 \pm 1.72	67.06 \pm 1.44	70.08 \pm 1.71
60	63.6 \pm 1.34	69.68 \pm 0.84	72.12 \pm 1.01
75	68.82 \pm 1.64	71.68 \pm 0.7	74.54 \pm 1.55
90	71.33 \pm 1.05	75.36 \pm 1.24	76.44 \pm 1.83
105	74.84 \pm 0.98	78.68 \pm 1.11	80.50 \pm 2.06
120	78.32 \pm 0.830	83.72 \pm 1.24	86.72 \pm 1.24

[#] All values are represented as mean \pm SD ($\pm n=3$).

Table 3.3.3.12. Dissolution data of Cilostazol – HP- β -CD Inclusion complex by KNEADING METHOD in phosphate buffer pH 6.4.

Time in Min.	% Drug release of Cilostazol HP- β -CD Inclusion complex (1:1) [#]	% Drug release of Cilostazol HP- β -CD Inclusion complex (1:2) [#]	% Drug release of Cilostazol HP- β -CD Inclusion complex (1:3) [#]
0	0.00 \pm 1.14	0.00 \pm 2.56	0.00 \pm 2.80
10	6.66 \pm 1.45	7.75 \pm 0.78	10.11 \pm 1.34
20	9.89 \pm 1.34	14.44 \pm 0.57	16.66 \pm 1.26
30	14.64 \pm 2.35	21.33 \pm 2.34	29.69 \pm 1.38
40	21.35 \pm 2.45	31.33 \pm 1.56	41.31 \pm 1.58
50	29.57 \pm 0.98	42.24 \pm 1.67	49.75 \pm 2.11
60	38.88 \pm 0.78	52.23 \pm 2.45	61.55 \pm 2.56
75	44.55 \pm 0.56	61.44 \pm 2.75	70.66 \pm 1.96
90	49.73 \pm 1.78	64.88 \pm 2.39	73.33 \pm 1.98
105	53.33 \pm 2.34	68.53 \pm 1.45	76.98 \pm 1.46
120	55.76 \pm 1.85	70.5 \pm 2.67	79.89 \pm 1.24

[#] All values are represented as mean \pm SD ($\pm n=3$).

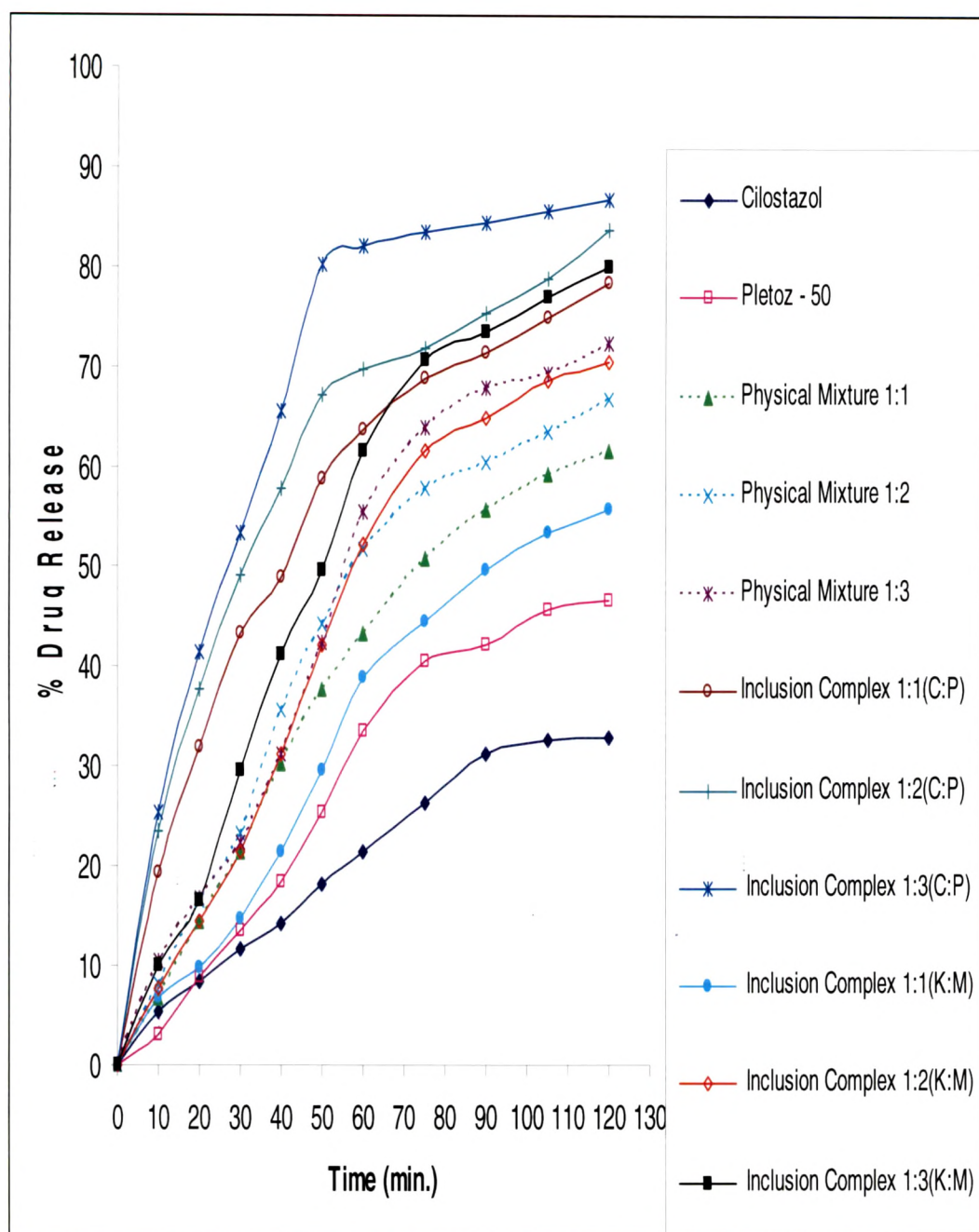


Figure 3.3.3.5. Cumulative % drug released from Cilostazol – HP- β -CD inclusion complexes, Physical mixtures, Marketed formulation (Pletoz-50) and Pure Drug at different time intervals.

Table 3.3.3.13. Dissolution efficiency and time required for 50% drug dissolved ($T_{50\%}$) for Cilostazol, Marketed formulation (Pletoz-50), Cilostazol-HP- β -CD Physical mixtures and Inclusion complexes.

Type	Dissolution efficiency for 120 min (%)		Time required for 50% drug dissolved (Min)	
	Mean \pm SD [#]	%RSD	Mean \pm SD [#]	%RSD
Cilostazol	20.385 \pm 1.82	0.74	181.92 \pm 0.95	0.92
Pletoz-50	28.2339 \pm 0.74	1.88	128.86 \pm 1.39	1.39
Physical Mixture 1:1	38.3254 \pm 2.12	2.16	73.64 \pm 0.79	0.33
Physical Mixture 1:2	42.8816 \pm 2.20	2.27	46.47 \pm 0.89	0.67
Physical Mixture 1:3	45.722 \pm 0.84	2.29	53.98 \pm 0.66	0.46
Inclusion Complex 1:1(C:P)	55.2562 \pm 1.23	0.86	40.81 \pm 0.92	0.81
Inclusion Complex 1:2(C:P)	60.3225 \pm 1.22	1.23	30.48 \pm 1.11	1.01
Inclusion Complex 1:3(C:P)	67.8333 \pm 1.5	1.51	28.04 \pm 0.53	1.60
Inclusion Complex 1:1(K:M)	32.8287 \pm 0.78	1.65	90.48 \pm 0.81	1.44
Inclusion Complex 1:2(K:M)	43.9606 \pm 1.00	1.55	57.43 \pm 0.77	1.95
Inclusion Complex 1:3(K:M)	51.3191 \pm 0.74	1.89	50.25 \pm 1.47	1.52

[#] All values are represented as mean \pm SD ($\pm n=3$).

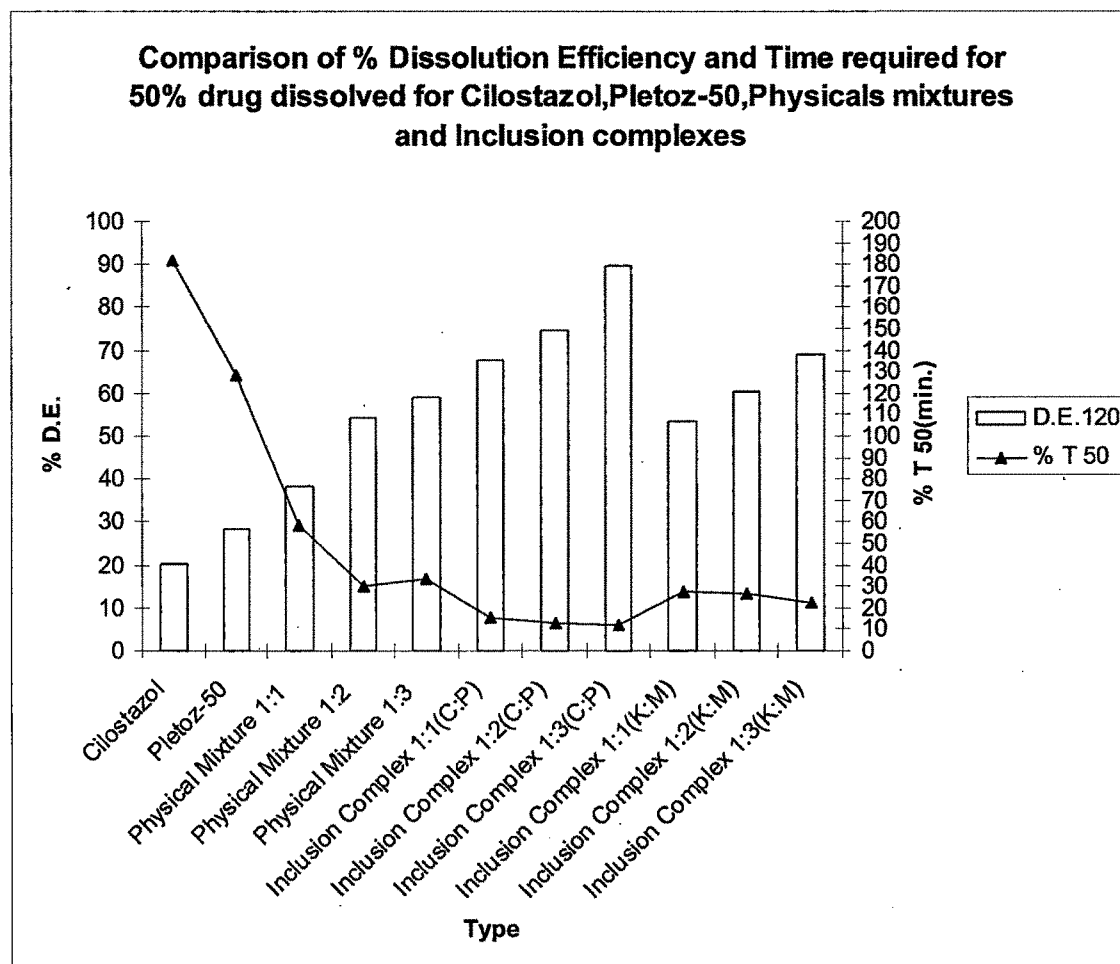


Figure 3.3.3.6. Comparison of % Dissolution efficiency and time required for 50 % drug dissolved for Cilostazol, Marketed formulation (Pletoz-50), Cilostazol-HP- β -CD physical mixtures and inclusion complexes.

Table 3.3.3.14. Dissolution data of Cilostazol-DM- β -CD Physical mixture in phosphate buffer pH 6.4.

Time in Min.	% Drug release of Cilostazol DM- β -CD Physical mixture (1:1) #	% Drug release of Cilostazol DM- β -CD Physical mixture (1:2) #	% Drug release of Cilostazol DM- β -CD Physical mixture (1:3) #
0	0.00 \pm 1.67	0.00 \pm 1.57	0.00 \pm 1.14
10	8.99 \pm 2.34	11.42 \pm 1.34	15.07 \pm 2.34
20	12.39 \pm 1.55	25.26 \pm 2.14	25.75 \pm 1.65
30	22.98 \pm 0.87	49.11 \pm 2.15	41.63 \pm 2.35
40	29.16 \pm 0.65	59.32 \pm 1.56	59.02 \pm 1.85
50	43.74 \pm 1.58	61.80 \pm 1.89	71.19 \pm 2.35
60	51.43 \pm 2.65	66.54 \pm 0.85	73.03 \pm 1.97
75	53.22 \pm 2.83	67.28 \pm 1.67	75.25 \pm 1.56
90	53.22 \pm 1.64	68.76 \pm 0.65	76.25 \pm 2.13
105	53.22 \pm 0.78	69.76 \pm 0.35	78.62 \pm 2.68
120	53.22 \pm 0.13	69.76 \pm 0.25	78.62 \pm 1.78

All values are represented as mean \pm SD (\pm n=3).

Table 3.3.3.15. Dissolution data of Cilostazol-DM- β -CD Inclusion complex by CO-PRECIPIATION METHOD in phosphate buffer pH 6.4.

Time in Min.	% Drug release of Cilostazol DM- β -CD Inclusion complex (1:1) #	% Drug release of Cilostazol DM- β -CD Inclusion complex (1:2) #	% Drug release of Cilostazol DM- β -CD Inclusion complex (1:3) #
0	0.00 \pm 1.45	0.00 \pm 1.89	0.00 \pm 0.59
10	32.70 \pm 0.45	37.87 \pm 2.13	42.32 \pm 0.92
20	64.18 \pm 0.28	69.35 \pm 2.19	56.78 \pm 1.32
30	67.87 \pm 1.48	70.83 \pm 1.14	75.38 \pm 1.78
40	70.83 \pm 2.14	73.78 \pm 1.55	80.05 \pm 1.99
50	72.30 \pm 2.16	78.21 \pm 1.88	85.94 \pm 2.45
60	75.26 \pm 1.45	83.38 \pm 0.77	91.11 \pm 2.21
75	78.21 \pm 1.68	85.60 \pm 0.56	92.99 \pm 1.11
90	78.21 \pm 2.35	88.55 \pm 1.56	94.11 \pm 1.46
105	78.21 \pm 1.78	88.55 \pm 1.66	96.32 \pm 0.32
120	78.21 \pm 2.56	88.55 \pm 2.14	98.16 \pm 2.24

All values are represented as mean \pm SD ($\pm n=3$).

Table 3.3.3.16. Dissolution data of Cilostazol-DM- β -CD Inclusion complex by KNEADING METHOD in phosphate buffer pH 6.4.

Time in Min.	% Drug release of Cilostazol DM- β -CD Inclusion complex (1:1) #	% Drug release of Cilostazol DM- β -CD Inclusion complex (1:2) #	% Drug release of Cilostazol DM- β -CD Inclusion complex (1:3) #
0	0.00 \pm 2.14	0.00 \pm 1.23	0.00 \pm 1.13
10	30.20 \pm 1.18	35.88 \pm 1.56	36.95 \pm 1.23
20	44.91 \pm 2.19	41.58 \pm 0.56	44.69 \pm 2.03
30	54.58 \pm 2.98	55.79 \pm 0.90	55.43 \pm 1.50
40	57.53 \pm 0.46	59.27 \pm 1.67	69.43 \pm 1.54
50	59.01 \pm 0.31	64.75 \pm 1.82	78.64 \pm 2.40
60	59.01 \pm 0.48	68.23 \pm 2.08	80.64 \pm 0.95
75	60.49 \pm 1.44	69.70 \pm 1.04	82.38 \pm 0.44
90	60.49 \pm 2.58	72.66 \pm 1.99	83.38 \pm 1.57
105	61.96 \pm 1.80	73.61 \pm 2.55	84.86 \pm 1.87
120	61.96 \pm 2.85	73.61 \pm 1.33	84.86 \pm 1.23

All values are represented as mean \pm SD ($\pm n=3$).

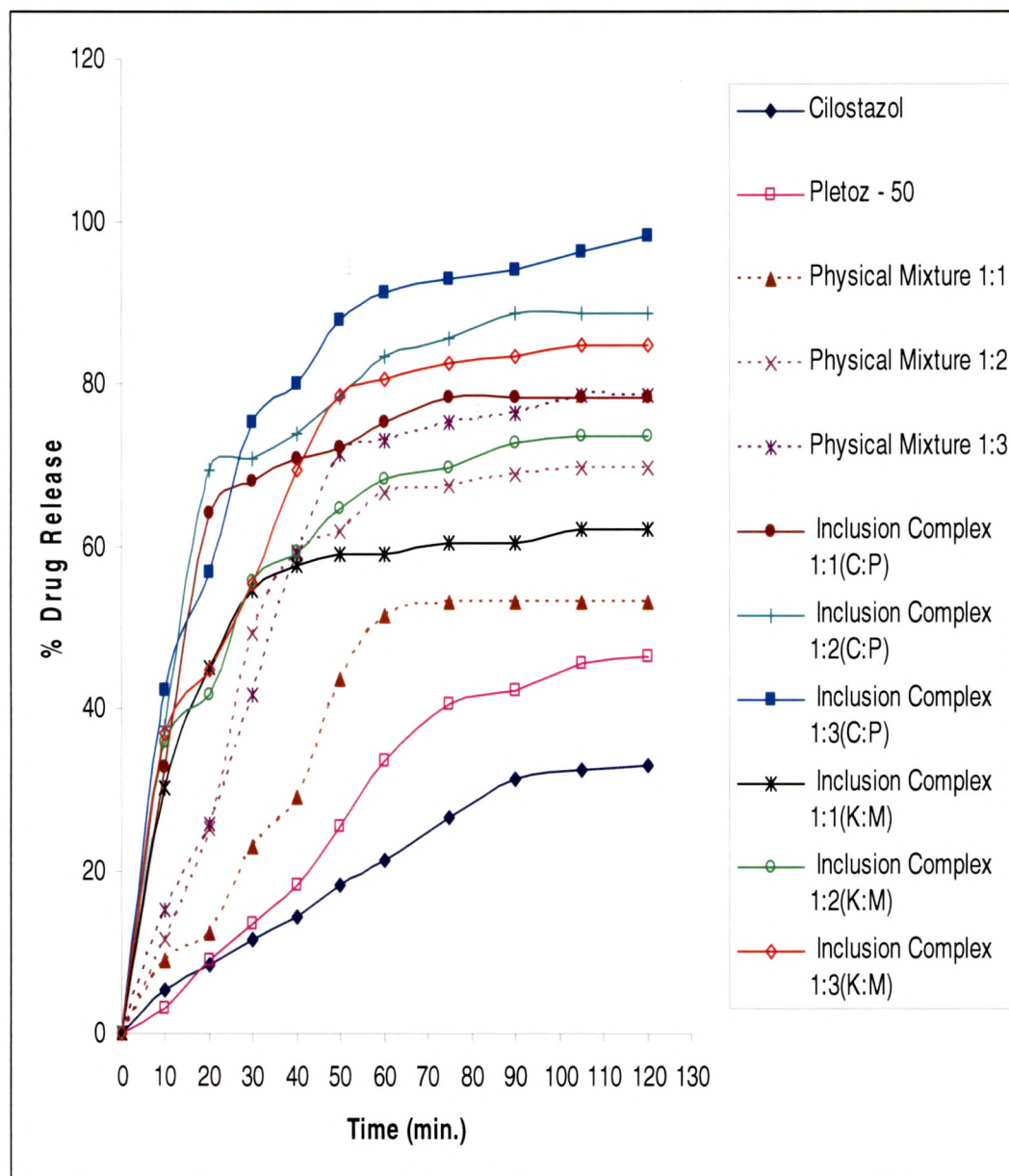


Figure 3.3.3.7. Cumulative % drug released from Cilostazol – DM- β -CD inclusion complexes, Physical mixtures, Marketed formulation (Pletoz-50) and Pure Drug at different time intervals.

Table 3.3.3.17. Dissolution efficiency and time required for 50% drug dissolved ($T_{50\%}$) for Cilostazol, Marketed formulation (Pletoz-50), Cilostazol-DM- β -CD Physical mixtures and Inclusion complexes.

Type	Dissolution efficiency for 120 min (%)		Time required for 50% drug dissolved (Min)	
	Mean \pm SD [#]	%RSD	Mean \pm SD [#]	%RSD
Cilostazol	20.385 \pm 1.89	1.29	181.92 \pm 0.46	1.00
Pletoz-50	28.2339 \pm 1.53	1.24	128.86 \pm 0.70	1.17
Physical Mixture 1:1	38.4127 \pm 1.15	1.12	58.33 \pm 0.35	0.63
Physical Mixture 1:2	54.2587 \pm 1.73	2.34	30.54 \pm 0.37	1.65
Physical Mixture 1:3	59.0077 \pm 1.53	2.26	33.88 \pm 0.79	0.47
Inclusion Complex 1:1(C:P)	67.7131 \pm 1.01	1.61	15.58 \pm 0.99	0.71
Inclusion Complex 1:2(C:P)	74.5606 \pm 0.89	1.18	13.2 \pm 0.70	0.36
Inclusion Complex 1:3(C:P)	89.5922 \pm 0.98	2.09	11.81 \pm 0.90	1.65
Inclusion Complex 1:1(K:M)	53.406 \pm 1.17	1.78	27.48 \pm 0.89	1.97
Inclusion Complex 1:2(K:M)	60.1433 \pm 0.62	1.20	26.88 \pm 0.44	1.70
Inclusion Complex 1:3(K:M)	68.7929 \pm 1.64	1.55	22.37 \pm 0.65	1.75

[#] All values are represented as mean \pm SD ($\pm n=3$).

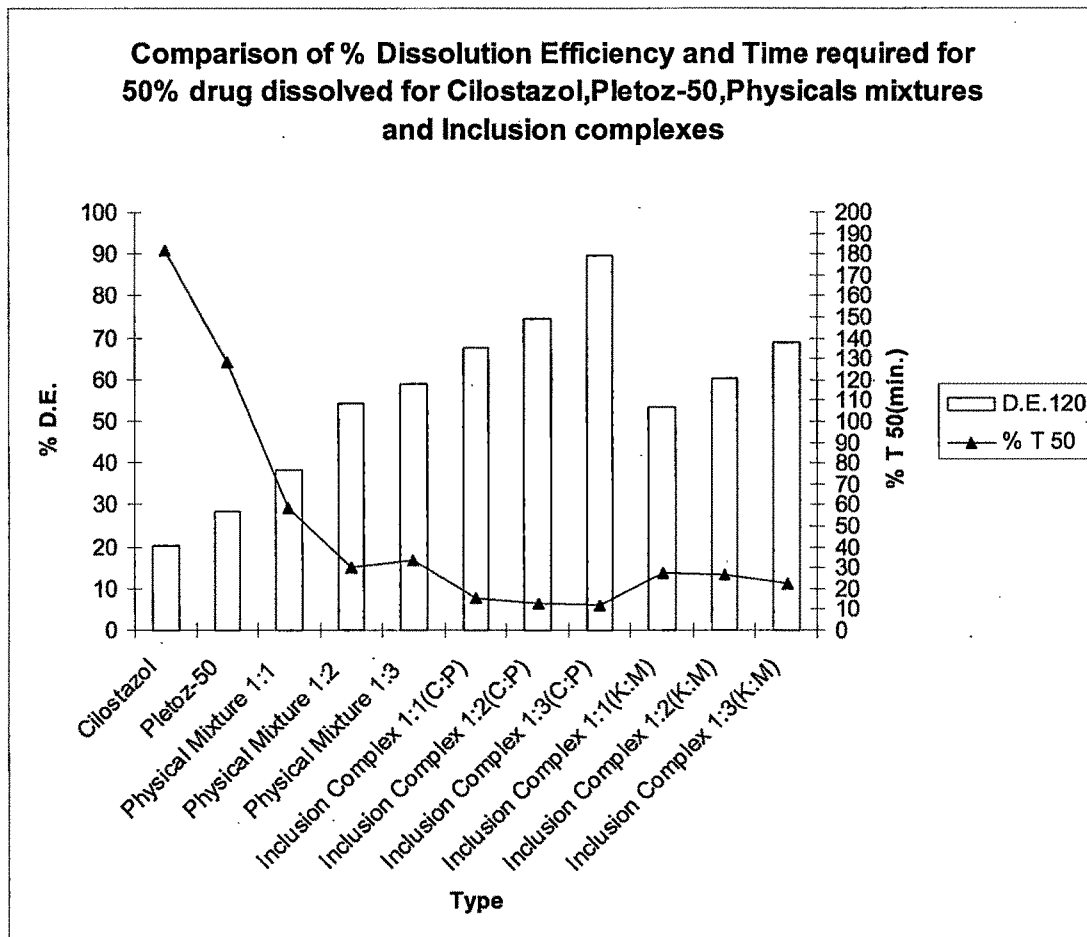


Figure 3.3.3.8. Comparison of % Dissolution efficiency and time required for 50 % drug dissolved for Cilostazol, Marketed formulation (Pletoz-50), Cilostazol-DM- β -CD physical mixtures and inclusion complexes.

Table 3.3.3.18. Regression coefficients of Cilostazol-CDs inclusion complexes, Physical mixtures, Marketed formulation (Pletoz-50) and Pure Drug

Formulations		Zero-order equation	First-order equation	Higuchi's equation
		r^2	r^2	r^2
Cilostazol		0.9692	0.7556	0.943
Pletoz – 50		0.9503	0.7468	0.9094
Cilostazol – β -CD Physical mixture	1:1	0.9208	0.6959	0.9199
	1:2	0.9569	0.7217	0.9245
	1:3	0.8701	0.5334	0.9524
Cilostazol – β -CD Inclusion complex (Co-precipitation)	1:1	0.9527	0.7609	0.9005
	1:2	0.8748	0.5707	0.9431
	1:3	0.7863	0.4656	0.9531
Cilostazol – β -CD Inclusion complex (Kneading method)	1:1	0.9625	0.7676	0.9012
	1:2	0.9567	0.6610	0.9084
	1:3	0.8118	0.5182	0.9592
Cilostazol – γ -CD Physical mixture	1:1	0.5464	0.2975	0.8157
	1:2	0.734	0.4907	0.9168
	1:3	0.7792	0.49	0.9278
Cilostazol – γ -CD Inclusion complex (Co-precipitation)	1:1	0.654	0.3804	0.8866
	1:2	0.6949	0.395	0.9084
	1:3	0.6124	0.3523	0.9333
Cilostazol – γ -CD Inclusion complex (Kneading method)	1:1	0.8196	0.5046	0.9568
	1:2	0.8277	0.5087	0.9615
	1:3	0.7771	0.421	0.9643
Cilostazol –HP- β -CD	1:1	0.9512	0.6631	0.925

3.3.3. Dissolution Study

Physical mixture	1:2	0.9203	0.6328	0.9448
	1:3	0.9368	0.6513	0.9505
Cilostazol – HP- β -CD	1:1	0.8624	0.4786	0.9423
Inclusion complex (Co-precipitation)	1:2	0.8143	0.4383	0.9686
	1:3	0.7454	0.4229	0.9839
Cilostazol – HP- β -CD	1:1	0.9651	0.731	0.9118
Inclusion complex (Kneading method)	1:2	0.9433	0.6789	0.9254
	1:3	0.9275	0.6314	0.9411
Cilostazol – DM- β -CD Physical mixture	1:1	0.8293	0.6078	0.8998
	1:2	0.718	0.4848	0.9083
	1:3	0.7816	0.5056	0.9252
Cilostazol – DM- β -CD Inclusion complex (Co-precipitation)	1:1	0.5368	0.3193	0.8321
	1:2	0.6028	0.3282	0.8766
	1:3	0.6707	0.3488	0.9198
Cilostazol – DM- β -CD Inclusion complex (Kneading method)	1:1	0.5404	0.3173	0.8402
	1:2	0.6855	0.3543	0.933
	1:3	0.7072	0.3737	0.9395

It can be concluded from the above studies that Cilostazol-DM- β -CD inclusion complex having a ratio 1:3 prepared by co-precipitation method showed maximum incorporation of Cilostazol. This fact was supported by its FTIR, DSC and XRD study. Hence, it was selected further for chemical stability study.

3.3.4. Chemical Stability of Cilostazol-cyclodextrin Inclusion complex.

Cilostazol-DM- β -CD Inclusion complex having a ratio 1:3 prepared by co-precipitation method was subjected to accelerated temperature and stress conditions (<http://www.nihs.go.jp/dig/ich/quality/q1e/Q1E>). The Inclusion complex was analyzed for chemical stability. Approximately 5 gms. of the formulation was filled in USP type III glass vial and sealed using VP6 crimp on spray pump fitted with 10 μ m actuator.

The accelerated stability was performed at 30° C \pm 2° C / 65% \pm 5% relative humidity (RH) and 40° C \pm 2° C / 75% \pm 5% RH as per ICH guideline (Photostability testing for new drug substances and products- Q1A (R2)). The duration of stability was 6 months and samples were withdrawn at predetermined time intervals after 1 month, 2 months, 3 months and 6 months consider as a test samples. The method is well described in ICH guideline Q1A (R2). Withdrawn samples were frequently compared with *in vitro* dissolution profiles of a test product before and after stability study as per the SUPAC IR guidelines which helps in assures similarity in the product performance and bioequivalence. The similarity factor f_2 was calculated using the equation proposed by various scientist^{23,24}, in which initial dissolution data considered as a reference values.

$$f_2 = 50 \text{LOG} \left\{ \left[1 + \frac{1}{n} \sum_{t=1}^n n(R_t - T_t)^2 \right]^{-0.5} \times 100 \right\}$$

Where R_t and T_t are the percentage of drug dissolved for Reference and Test samples at each time point. An f_2 value between 50 and 100 suggests the dissolution profiles are consider as similar.

Table 3.3.4.1. Dissolution data for stability study of Cilostazol –DM- β-CD Inclusion complex(1:3) by CO-PRECIPIATION method in phosphate buffer pH 6.4.

Time in Min.	% Drug release of Cilostazol-DM- β-CD Inclusion complex (1:3) [#] (Reference)	% Drug release of Cilostazol-DM- β-CD Inclusion complex (1:3) [#] after 1 month stability	% Drug release of Cilostazol –DM- β-CD Inclusion complex (1:3) [#] after 2 months stability	% Drug release of Cilostazol –DM-β-CD Inclusion complex (1:3) [#] after 4 months stability	% Drug release of Cilostazol –DM- β-CD Inclusion complex (1:3) [#] after 6 months stability
0	0.00 ± 0.59	0.00 ± 2.13	0.00 ± 2.56	0.00 ± 1.23	0.00 ± 0.91
10	42.32 ± 0.92	41.11 ± 3.45	39.85 ± 3.57	35.27 ± 2.45	34.88 ± 1.46
20	56.78 ± 1.32	53.27 ± 1.11	50.56 ± 2.46	47.87 ± 3.74	44.18 ± 3.58
30	75.38 ± 1.78	74.24 ± 4.58	72.72 ± 3.58	69.29 ± 4.75	66.11 ± 2.82
40	80.05 ± 1.99	78.38 ± 5.27	76.29 ± 4.92	73.33 ± 3.27	71.92 ± 3.74
50	85.94 ± 2.45	82.27 ± 3.84	79.45 ± 3.84	77.27 ± 5.48	75.27 ± 2.53
60	91.11 ± 2.21	90.29 ± 4.26	87.92 ± 2.58	85.54 ± 6.72	83.87 ± 4.84
75	92.99 ± 1.11	91.26 ± 5.83	89.29 ± 5.74	88.32 ± 7.02	86.27 ± 5.47
90	94.11 ± 1.46	93.26 ± 6.57	92.72 ± 3.95	90.26 ± 6.49	88.25 ± 3.48
105	96.32 ± 0.32	95.85 ± 3.45	93.82 ± 2.84	92.56 ± 3.55	90.19 ± 5.31
120	98.16 ± 2.24	97.55 ± 5.75	96.16 ± 6.76	94.22 ± 4.27	93.67 ± 3.77

[#] All values are represented as mean ± SD (±n=3).

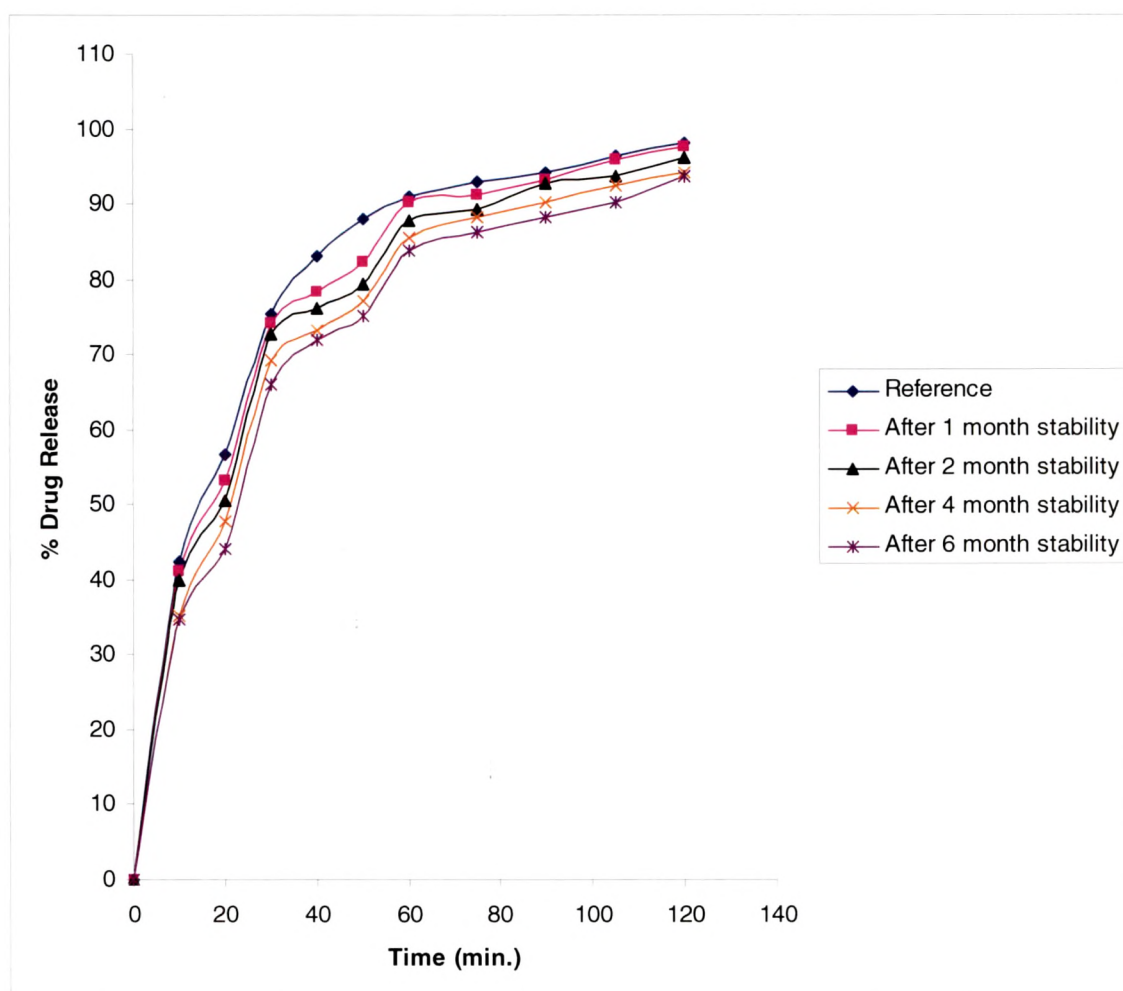


Figure:3.3.4.1. Cumulative % drug released from Cilostazol-DM- β -CD inclusion complex (1:3) by Co-precipitation method for Stability study at different time intervals.

Table :3.3.4.2. Similarity factor (f_2) and Student's T-test values for the stability profile of Cilostazol- β -CD inclusion complex(1:3) by Co-precipitation method for 6 months.

Batch	f_2	T stat	T cri
Reference batch compared with After 6 month storage batch	66.85	0.5990	2.0859

3.3.5. Results and Discussion.

Cilostazol-CDs Inclusion complexes were successfully prepared using kneading and co-precipitation methods. The complexing agents selected were β -CD, γ -CD, HP- β -CD and DM- β -CD according to their suitability for oral administration.

Solubility study is the preliminary study to identify the interaction between drug and CD in solution because it gives not only the solubilizing ability of the host molecules but also the stability constant of the complexes by analysis of the solubility curve.

The phase solubility profiles for the complex formation between Cilostazol and CDs in aqueous solution (HCl buffer pH 1.2, water and Phosphate buffer pH 6.8) at 37° C are shown in figure 3.3.2.1.1, 3.3.2.1.2 and 3.3.2.1.3.²⁵ Initial studies indicated that Cilostazol is chemically stable in water for at least 7 days at 37° C. The extremely low solubility of Cilostazol (0.101 ± 0.004 $\mu\text{g/mL}$ in water at 37° C) was increased in a concentration depending manner linearly with the increase in CDs concentration, giving rise to A_L - type solubility diagrams with strictly linear ascent having a regression values(r^2) $>0.99^6$. This linear Cilostazol-CDs correlation, suggested the formation of a 1:1 (mol/mol) Cilostazol-CDs inclusion complexes at the different pH values. The calculated stability constant values are shown in Table 3.3.2.1.1. These results indicated that Cilostazol-CD complexes (1:1 molar ratio) were sufficiently stable in phosphate buffer pH 6.8 and the values of stability constant were more than 100 M^{-1} . Values of stability constant were less than 100 M^{-1} in water and HCl buffer pH 1.2 indicating that the inclusion complexes of Cilostazol-CDs were not stable in these solutions. The complexes having the stability constant values in the range of 100 M^{-1} to 1000 M^{-1} were always stable as these are considered ideal values²⁶. Actually smaller values of K_C (less than 100 M^{-1}) indicate a too weak interaction between drug and CD, while larger values (more than 1000 M^{-1}) are symptomatic of an incompatible drug release from the inclusion complex. As per results shown in Table 3.3.2.1.1., highest solubility (393.52 ± 4 $\mu\text{g/mL}$) of Cilostazol and stability constant ($390.071 \pm 35 \text{ M}^{-1}$) of Cilostazol-DM- β -CD inclusion complex (1:1 molar ratio) were found in phosphate buffer solution pH 6.8. This may be due to the contribution of DM- β -CD on the increased solubility of Cilostazol, which was almost completely un-ionized at this pH.

According to the solubility studies data, suitable ratios 1:1, 2:1 and 3:1 of CDs along with Cilostazol were selected to form inclusion complexes.

The inclusion efficiency data of Cilostazol-CDs complexes are recorded in Table 3.3.2.2.1., 3.3.2.2.2, 3.3.2.2.3. and 3.3.2.2.4. The % inclusion efficiency of 1:3 Cilostazol-

CDs inclusion complexes were more than $98.5 \pm 1.50\%$ compared with the another inclusion complexes and all physical mixtures having a values in the range of 49.2 ± 1.53 to 89.4 ± 1.33 which indicated that Cilostazol was uniformly distributed in all 1:3 inclusion complex whereas, the other ratios used for inclusion complexes and physical mixtures did not show satisfactory drug incorporation.

The prepared physical mixtures, inclusion complexes, pure Cilostazol and excipients were subjected to FTIR, DSC and XRD study for their characterization.

FTIR spectra of Cilostazol, Physical mixture and Inclusion complexes were obtained and interpreted in following manner (Table 3.3.5.1.and Table 3.3.5.2.)

Table 3.3.5.1. Important peaks of FTIR spectra of pure Cilostazol, β -CD, γ -CD, HP- β -CD and DM- β -CD.

	Important Peaks
Pure Cilostazol	- aromatic and aliphatic C-H stretching peaks - 2867 to 3315 cm^{-1} - N-H stretching band of quinolinone - 3315 cm^{-1} - C=O stretching band - 1822.61 cm^{-1} - C=N stretching peak of tetrazole - 1757 cm^{-1} - N=N stretching peak of tetrazole - 1687 cm^{-1} - aromatic C=C stretching band - 1506 cm^{-1}
Pure β -CD	- intense bands at $3465 - 3247\text{ cm}^{-1}$ corresponding to absorption by hydrogen bonded OH groups. - C-H and $-\text{CH}_2$ stretching bands - $3000 - 2800\text{ cm}^{-1}$
Pure γ -CD	
Pure HP- β -CD	
Pure DM- β -CD	

Table 3.3.5.2. Important peaks of prepared Cilostazol-CDs physical mixtures and inclusion complexes.

Cilostazol-CDs (molar ratios)	Physical Mixture Important Peaks	Inclusion Complex Important Peaks
Cilostazol- β -CD (1:3 ratio)	-peaks of both the Cilostazol and β -CD were observed. - reduction in the peak intensity of Cilostazol. - right shift of OH stretching peak from	- (right shift of OH stretching peak from 3290 to 3261 cm^{-1})* - left shift of CH stretching peak of β -CD from 2923.88 to 2931.60 cm^{-1}

	3352.05 to 3315 cm^{-1} - right shift of CH stretching peak for β -CD from 2923.88 to 2908.45 cm^{-1}	
Cilostazol- γ -CD (1:3 ratio)	- peaks of both the Cilostazol and γ -CD were observed. - reduction in the peak intensity of Cilostazol. -right shift of OH stretching peak from 3380 to 3340 cm^{-1} -right shift of CH stretching peak of γ -CD from 2880 to 2929.67 cm^{-1}	- (right shift of OH stretching peak from 3340 to 3300 cm^{-1})* - left shift of CH stretching peak of γ -CD from 2929.67 to 2950 cm^{-1}
Cilostazol- HP- β -CD (1:3 ratio)	- peaks of both the Cilostazol and HP- β -CD were observed. - reduction in the peak intensity of Cilostazol. - right shift of OH stretching peak from 3380.98 to 3313 cm^{-1} - right shift of CH stretching peak of HP- β -CD from 2927.74 to 2929.67 cm^{-1}	- (right shift of OH stretching peak from 3407.98 to 3398.34 cm^{-1})* - left shift of CH stretching peak of HP- β -CD from 2925.81 to 2927.74 cm^{-1}
Cilostazol- DM- β -CD (1:3 ratio)	- peaks of both the Cilostazol and DM- β -CD were observed. - reduction in the peak intensity of Cilostazol. - right shift of OH stretching peak from 3465.84 to 3461.99 cm^{-1} - right shift of CH stretching peak of DM- β -CD from 2923.88 to 2931.60 cm^{-1}	- (right shift of OH stretching peak from 3421.48 to 3400 cm^{-1})* - left shift of CH stretching peak of DM- β -CD from 2923.88 to 2950 cm^{-1}

* results suggested that some of the existing bonds formed between the OH groups were disturbed after the formation of inclusion complexes.

The DSC thermogram of Cilostazol (Figure 3.3.2.4.5) showed sharp endothermic peak at 165.13 $^{\circ}\text{C}$ (ΔH value -433.02 mJ and -139.68J/g, respectively) corresponding to its melting point. The DSC thermogram of β -CD (Figure 3.3.2.4.1.) has large broad endothermic

peak between 130.00 °C to 160.00 °C (148.59 °C) that was related to the loss of hydration water of the starting material. β -CD decomposes at about 300.00 °C, so there was no trace of melting peak of β -CD in the chosen temperature range, while any endothermic peak was not observed in γ -CD, HP- β -CD and DM- β -CD (Figure 3.3.2.4.2, 3.3.2.4.3. and 3.3.2.4.4.).

Physical mixture of Cilostazol- β -CD (Figure 3.3.2.4.6) showed small and sharp endothermic peak at 149.69 corresponding to the β -CD and another peak at 162.14 °C corresponding to the Cilostazol while an inclusion complex of Cilostazol- β -CD prepared by kneading method showed minute peak at 162.5°C (Figure 3.3.2.4.8).The DSC thermogram of Cilostazol- β -CD inclusion complex prepared by co-precipitation method(Figure 3.3.2.4.7.) did not show any endothermic peak indicating the total entrapment of the Cilostazol as the inclusion complex.

Physical mixture of Cilostazol- γ -CD (Figure 3.3.2.4.9.) showed a sharp endothermic peak at 159.38 °C corresponding to the Cilostazol (165.13 °C). The inclusion complexes of Cilostazol- γ -CD) prepared by co-precipitation and kneading method (Figure 3.3.2.4.10 and 3.3.2.4.11.) showed minute peak at 159.31°C and 159.12°C respectively.

Physical mixture of Cilostazol-HP- β -CD showed (Figure 3.3.2.4.12) a sharp endothermic peak at 162.53 °C corresponding to the Cilostazol while the inclusion complexes of Cilostazol-HP- β -CD prepared by kneading method showed minute peak at 159.31 °C (Figure 3.3.2.4.14).The DSC thermogram of Cilostazol-HP- β -CD inclusion complex prepared by co-precipitation method (Figure 3.3.2.4.13.) did not show any endothermic peak, indicating the formation of inclusion complexes. Shifting of the peak temperature in physical mixtures and inclusion complexes might be attributed to the amorphous form of the drug in complex formation.

Physical mixture of Cilostazol-DM- β -CD (Figure 3.3.2.4.15.) showed a sharp endothermic peak at 158.30 °C (165.13 °C, ΔH value -120.44 mJ and -50.18J/g for pure Cilostazol) corresponding to the Cilostazol (ΔH value -433.02 mJ and -139.68J/g) while the inclusion complexes of Cilostazol-DM- β -CD showed minute peak at (157.43 °C ΔH value -3.15 mJ and -3.35 J/g) by kneading method (Figure 3.3.2.4.17.). **The DSC thermogram of Cilostazol-DM- β -CD inclusion complex prepared by co-precipitation method (Figure 3.3.2.4.16.) did not show any endothermic peak, which indicated that co-precipitation method was suitable method for formation of inclusion complex of Cilostazol.**

Powder XRD study was used to measure the crystallinity of the formed inclusion complexes. The peak position (angle of diffraction) is an identification tool of a crystal structure, where as the number of peaks is a measure of samples crystallinity in a

diffraction²⁸. The formation of an amorphous state proves that the drug was dispersed in a molecular state with CD. It was shown by various researchers that the formation of a diffused diffraction pattern, appearance of new peaks, and disappearance of a characteristic peaks of the guest as evidence for the formation of inclusion complexes of a drug with CDs^{29,30,31,32}.

The powder X-ray diffraction patterns of pure Cilostazol are represented in Figure 3.3.2.5.5. The diffraction pattern of Cilostazol exhibited a series of intense peaks at 12.67, 12.98, 15.35, 15.76, 17.98, 18.71, 19.52, 22.19 and 22.58° which were indicative of their crystallinity. β -CD (Figure 3.3.2.5.1) exhibited characteristic peaks at 12.74, 21.18 and 22.96 due to its crystalline nature. γ -CD (Figure 3.3.2.5.2) exhibited characteristic peaks at 4.61, 8.01, 9.09, 14.22, 17.81 and 22.56. The diffraction peaks were not observed in the spectrum of HP- β -CD (Figure 3.3.2.5.3) indicating that HP- β -CD was an amorphous compound. DM- β -CD (Figure 3.3.2.5.4) exhibited characteristic peaks at 7.57, 8.51, 10.99, 12.16, 13.43, 17.53, and 18.98.

Most of the principle peaks of Cilostazol and β -CD were present in the diffraction patterns of physical mixture shown in Figure 3.3.2.5.6. This indicated that there was no interaction between the pure components in the case of physical mixture. The diffraction pattern corresponding to the inclusion complexes (Figure 3.3.2.5.7. and 3.3.2.5.8.) showed that the intensity of the diffraction peaks as well as the number of peaks were lower than pure components and the physical mixture. This indicated that the crystallinity of Cilostazol was decreased when the proportion of β -CD in inclusion complex was increased.

The powder X-ray diffraction pattern of pure Cilostazol- γ -CD physical mixture was represented in Figure 3.3.2.5.9. According to the data obtained, most of the peaks of physical mixture were superimposed on peaks of Cilostazol and γ -CD. Partial peaks of Cilostazol declined and disappeared, showing the slight complexation may have occurred in the process of mixing, whereas X-ray diffraction patterns of Cilostazol- γ -CD inclusion complexes (Figure 3.3.2.5.10. and 3.3.2.5.11.) were having a less intense as well as less numbers of peaks compared with pure components and the physical mixture demonstrating a different diffused pattern.

The X-ray diffraction pattern of the physical mixture of Cilostazol- HP- β -CD (Figure 3.3.2.5.12) was approximately superposition of the patterns of the pure Cilostazol and HP- β -CD. The number of peaks and the peak intensity were also decreased. In contrast to the data observed, inclusion complex of Cilostazol-HP- β -CD complexes (Figure 3.3.2.5.13. and 3.3.2.5.14.) showed a halo pattern, with the disappearance of all the peaks corresponding to

the both Cilostazol and HP- β -CD, which was indicated that Cilostazol was completely incorporated in to the cavity of HP- β -CD.

In the case of Cilostazol DM- β -CD physical mixture (Figure 3.3.2.5.15.), intensity of the peaks was reduced compared with pure Cilostazol and DM- β -CD, while in the case of inclusion complexes of Cilostazol- DM- β -CD (Figure 3.3.2.5.16. and 3.3.2.5.17.) diffraction pattern of inclusion complex was similar with the diffraction pattern of DM- β -CD indicating complete incorporation of Cilostazol into the cavity of DM- β -CD.

It can be concluded from the XRD study that, Drug-CDs inclusion complexes having a ratio of 1:3 showed less numbers of peaks having low intensity. The diffraction pattern for the inclusion complexes of Cilostazol-DM- β -CD and Cilostazol-HP- β -CD was changed altogether. These positive effects might be involved in enhancement of dissolution characteristic of Cilostazol.

In vitro dissolution studies were performed to evaluate relative solubility behavior of different formulations of Cilostazol. From the phase solubility study, phosphate buffer pH 6.4 was found to be suitable dissolution medium as it showed maximum drug release. Dissolution study were carried for all Cilostazol-CDs physical mixtures in different ratios (1:1, 1:2 and 1:3) as well as Cilostazol-CDs inclusion complexes were prepared in different ratios (1:1, 1:2 and 1:3) by using co-precipitation and kneading methods and the maximum mean cumulative % drug dissolved \pm SD are shown in Table 3.3.5.3.

Table 3.3.5.3.: Maximum % cumulative drug release of all physical mixtures, inclusion complexes, Pletoz-50 and pure Cilostazol.

Method	Cilostazol- CDs ratios	Maximum % cumulative drug release \pm SD			
		Cilostazol- B -CD	Cilostazol- γ -CD	Cilostazol- HP- β -CD	Cilostazol- DM- β -CD
Physical Mixture	1:1	45.35 \pm 1.59	51.98 \pm 2.62	61.55 \pm 1.45	53.22 \pm 0.13
	1:2	56.67 \pm 1.93	56.09 \pm 1.55	66.56 \pm 1.59	69.76 \pm 0.25
	1:3	69.32 \pm 1.75	71.13 \pm 1.24	72.34 \pm 2.14	78.62 \pm 1.78
Co- precipitation Method	1:1	69.32 \pm 1.75	67.87 \pm 1.82	78.32 \pm 0.830	78.21 \pm 2.56
	1:2	68.88 \pm 1.56	78.95 \pm 1.64	83.72 \pm 1.24	88.55 \pm 2.14
	1:3	76.49 \pm 1.09	95.20 \pm 2.31	83.72 \pm 1.24	98.16 \pm 2.24
Kneading Method	1:1	47.83 \pm 1.47	63.99 \pm 1.04	55.76 \pm 1.85	61.96 \pm 2.85
	1:2	63.76 \pm 1.65	66.4 \pm 2.33	70.5 \pm 2.67	73.61 \pm 1.33
	1:3	73.28 \pm 1.93	87.08 \pm 2.02	79.89 \pm 1.24	84.86 \pm 1.23

PLETOZ 50	46.56 ± 2.1
Pure Cilostazol	32.98 ± 0.91

These are graphically represented in Figures 3.3.3.1, 3.3.3.3., 3.3.3.5. and 3.3.3.7 respectively. It is evident from the data that optimized Cilostazol-CDs inclusion complexes prepared by co-precipitation method showed better drug release than other inclusion complexes, physical mixtures, marketed formulation (Pletoz-50) and drug solution.

Cilostazol- β -CD inclusion complex (1:3 ratio) showed 1.64-fold higher drug release compared to Pletoz-50 and 2.31-fold higher diffusion compared to Cilostazol solution, Cilostazol- γ -CD inclusion complex (1:3 ratio) showed 2.04-fold higher drug release compared to Pletoz-50 and 2.88-fold higher drug release compared to Cilostazol solution. While Cilostazol-HP- β -CD inclusion complex(1:3 ratio) showed 1.86-fold higher drug release compared to Pletoz-50 and 2.62-fold higher diffusion compared to Cilostazol solution and Cilostazol-DM- β -CD inclusion complex(1:3 ratio) showed 2.10-fold higher diffusion compared to Pletoz-50 and 2.97-fold higher drug release compared to Cilostazol solution.(All above complexes are prepared by Co-precipitation method).

The regression study was carried out for all inclusion complexes, physical mixtures, Pletoz-50 and pure Cilostazol. The graphs of percent drug dissolved vs. time were found to be non-linear, suggesting that the dissolution pattern did not follow zero order kinetics. However, the correlation coefficients indicated that Higuchi's model was found to be the best-fit curve compared with zero order and first order kinetic for all the tested formulations.

The values of DE_{120min} and T_{50} study for all Cilostazol-CDs physical mixtures, inclusion complexes, Cilostazol and Pletoz – 50 are shown in Table 3.3.3.5., 3.3.3.9., 3.3.3.13. and 3.3.3.17. These are graphically represented in Figures 3.3.3.2., 3.3.3.4., 3.3.3.6. and 3.3.3.8. **All these results indicated that inclusion complex of Cilostazol-DM- β -CD in the ratio of 1:3, prepared by co-precipitation method was having highest dissolution efficiency (89.59%) among the all inclusion complexes. Reduction in the time taken for 50 % dissolution (T_{50} value-11.81 min.) indicated that the inclusion complex was having a rapid and higher dissolution rate.** The increase in dissolution of Cilostazol from the inclusion complexes might be attributed to the factors such as a reduction in particle size of the drug in the presence of CDs, increase in the surface area, reduced crystallinity and increase in the solubility of the drug in presence of CDs. As the inclusion complex of Cilostazol-DM- β -CD in the ratio of 1:3, prepared by co-precipitation method was having rapid dissolution rate (less dissolution time) was further selected for stability study.

Stability study was carried out as per ICH Q1A (R2) and SUPAC IR guidelines. The sample was stored at $30^{\circ}\text{C} \pm 2^{\circ}\text{C}$ / $65\% \pm 5\%$ relative humidity (RH) and $40^{\circ}\text{C} \pm 2^{\circ}\text{C}$ / $75\% \pm 5\%$ RH for 6 months time duration. The samples were withdrawn at predetermined time intervals upto 6 months and assessed for *in vitro* dissolution study. The dissolution data are mention in Table 3.3.4.1. and graphically it is represented in Figure 3.3.4.1. As per the results obtained, change of cumulative percentage of drug release after of 6 months was from 4.0 % to 12.0%. The dissolution curve (Fig. 3.3.4.1) also showed similar changes in dissolution patterns indicating that Cilostazol was stable in the inclusion complex. The results of student's t-test and similarity factor (f_2) show insignificant difference between the dissolution profiles (Table 3.3.4.2). The calculated f_2 values for the batches are higher than 50. Hence, it can be concluded that the there is insignificant change in the formulated product on storage.

It can be concluded from the above studies that Cilostazol-DM- β -CD inclusion complex having a ratio 1:3 prepared by co-precipitation method showed maximum incorporation of Cilostazol. This fact was supported by its FTIR, DSC and XRD study. It also showed higher dissolution rate compared to all other formulations. The dissolution rate and DE_{120} values were increased as the proportion DM- β -CD in inclusion complexes were increased. So it was selected for further *in-vivo* pharmacokinetic study.

3.3.6. References

1. D. Duchene, New trends in cyclodextrins and derivatives. Paris: Edition de Sante,1992,351-407.
2. K. H. Formming, J. Szejtli,Cyclodextrins in pharmacy,Topics in inclusion science. Dordrecht, The Netherlands,Kulwer Academic Publishers,1994.
3. D.O. Thompson,Cyclodextrins-enabling excipients:their present and future use in pharmaceuticals. *Crit. Rev. Ther.Drug Carrier Syst.* 1997,14,1-104.
4. M. Masson, T.Loftson, G. Masson,E.S. Steffanson, Cyclodextrin as permeation enhancer some theoretical evaluation and in vitro testing. *J. Coontrol Release*, 1999,59,81-99.
5. Rawat S. Jain S., K.:Roficoxib-beta Cyclodextrin Inclusion Complex for Solubility Enhancement, *Pharmazie*, 2003, 58(9), 639-641.
6. T. Higuchi and K.A. Connors, Phase solubility techniques, *Adv. Anal. Chem. Instrum*, 1965,4, 207-212.
7. Attama A. A.,Ndibe O. N.and Nnamani P. O. Studies on Diclofenac β -cyclodextrin inclusion complexes. *J. of Pharm. Research.*, 2004,3(3),47-49.
8. Liu X., et.al. : Inclusion of Acitrein Cyclodextrins:Phase Solubility, Photostability, and Physicochemical Characterization. *J. Pharm. Sci.*, 2003,92(12),2449-2457.
9. H. Arima, K. Yunomae,K. Miyake, T. Irie, F. Hiriyama and K. Uekama, Comperative studies of the enhancing effect of cyclodextrins on the solubility and oral bioavailability of tacrolimus rats. *J. Pharm. Sci.*, 2001,90(6),690-701.
10. M. L. Manca, M. Zaru, D. Valinte, C. Sinico, G Loy and A. M. Fadda, Diclofenac- β -cyclodextrin binary systems: Physical characterization and In vitro dissolution and diffusion studies, *AAPS Pharm. Sci.,Tech.*,2005,6(3), E464-E472.
11. J. A. C. Harmida, H. G. couso, M.E.Ares-mazas, M.M.Gonazalez-bedia, N. Castaneda-Cancio, F. J. Othero-Espinder and J. Blanco-mendez, Anticryptosporidal activity of furan derivative G1 and its inclusion complex with beta-cyclodextrin, *J. Pharm., Sci.*,2004,93(1),197-206.
12. *United States Pharmacopoeia XX/National Formulary XV*. Supplement 3. U.S. Pharmacopeial Convection, Rockville, MD, 1982,310-311.
13. The Theory and Practice of Industrial Pharmacy by L. Lechman, H. A. Lieberman and J.

-
- L. Kaing, Third edition, Vargish publication Bombay, 1991, 302-303.
14. K.A. Khan, C.T. Rhodes, Concept of dissolution efficiency, *J. Pharm. Pharmacol.* 27 (1975) 48-49.
 15. P. Costa, J. manuel, S. Lobo, Modeling and comparison of dissolution profiles, *Eur. J. of Pharm. Sci.* 2001, 13, 123-133.
 16. Rawat S.; Jain S., K.: Rofecoxib-beta Cyclodextrin Inclusion Complex for Solubility Enhancement, *Pharmazie*, 2003, 58(9), 639-641.
 17. Dissolution study, *United State Pharmacopoeia, XXIII, NF XVIII*, The USP convention, Inc, Rockville, MD (1995) 1791-1799.
 18. H. Arima, K. Yunomae, K. Miyake, T. Irie, F. Hirayama and K. Uekama, Comparative studies of the enhancing effect of cyclodextrins on the solubility and oral bioavailability of tacrolimus rats. *J. Pharm. Sci.*, 2001, 90(6), 690-701.
 19. J. A. Castillo, J. P. Canales, J. J. Gracia, J.L. Lastres, F. Bolas and J.J. Torrado, Preparation and Characterization of Albendazole β -cyclodextrin Complex. *Drug Dev. And Ind. Pharm.* 1999, 25(12), 1241-1248.
 20. H. G. Choi, D.D. Kim, H. W. Jun, B. Yoo and C. Yong, Improvement of Dissolution and Bioavailability of Nitrendipine by Inclusion in Hydroxypropyl- β -cyclodextrin, *Drug Dev. And Ind. Pharm.* 2003, 29(10), 1094-2003.
 21. S. M. Ahmed, Improvement of solubility and dissolution of 19-Norprogesterone via Inclusion complex, *J. of Inclusion Sci. and Mol. Recognition in Chem.* 1998, 30, 111-125.
 22. B. N. nalluri, K.P.R.chowdhry, K. V. R. Murthy, V. Satyanarayana, A. R. Yahman and G. Backet, Inclusion complexation and Dissolution properties of Nimesulide and Meloxicam-hydroxypropyl- β -cyclodextrin Binary Systems. *J. of Inclusion Sci. and Macro. Chem.* 2005, 53, 103-110.
 23. J.W. Moore, H.H. Flanner, Mathematical comparison of dissolution profiles, *Pharm. Technol.* 20 (1996) 64-74.
 24. V. P. Shah, Yi Tsong, p. Sathe and J. P. Lue, In Vitro dissolution profile comparison – Statistics and analysis of the similarity factor (f_2), *Pharm. Res.* 1998, 15(6), 889-896.
 25. K. Okkimoto, R. A. Rajawaski, K. Uekama, J. A. Jona and V. J. Stella, The interaction of charged and uncharged drugs with neutral (HP- β -CD) and unionically charged (SBE7- β -CD) β -cyclodextrins. *Pharm Res.* 1996, 13:256-264.
-

26. A. P. Mukne and M. S. Nagarsankar, Triamterene- β -cyclodextrin Systems: Preparation, Characterization and In vivo Evaluation. *AAPS Pharm. Sci. Tech.* **2004**, 5:E19.
27. M. Wulff and M. Alden, Solid state studies of drug-cyclodextrin inclusion complexes in PEG 6000 prepared by a new method, *Eur. J. Pharm. Sci.*,**1999**,8 269-281.
28. M.D. Veiga, P.J. Diaz and F. Ashan, Intrections of griseofulvin with cyclodextrins in solid binary systems. *J. Pharm. Sci.* **1998**,87,891-900.
29. Y. Nakai, A.E.S. Aboutaleb, K. Yamamoto, K. Saleh and M.O. Ahmed, Study of the interaction of clobazam with cyclodextrins in solution and in the solid state. *Chem. Pharm. Bull.* **1990**,38,728-732.
30. M. Guyot, F. Fawaz, J. Bildet, F. Binini and A.M.Lagueny, Physicochemical characterization and dissolution of norfloxacin/CD inclusion compounds and PEG solid dispersions. *Int.J. Pharm.* **1995**,123,53-63.
31. M.D. Veiga and F. Ashan, Study of Tolbutamide-hydroxypropile- γ -cyclodextrin interaction in the solution and solid state. *Chem. Pharm. Bull.* **2000**,48,793-797.
32. C. M. Fernandes, M.T.Vieira and F.J.B. Viaga, Physicochemical characterization and in-vitro dissolution behavior nicardipine-cyclodextrin inclusion compounds. *Eur. J. Pharm. Sci.*,**2002**,15 79-88.